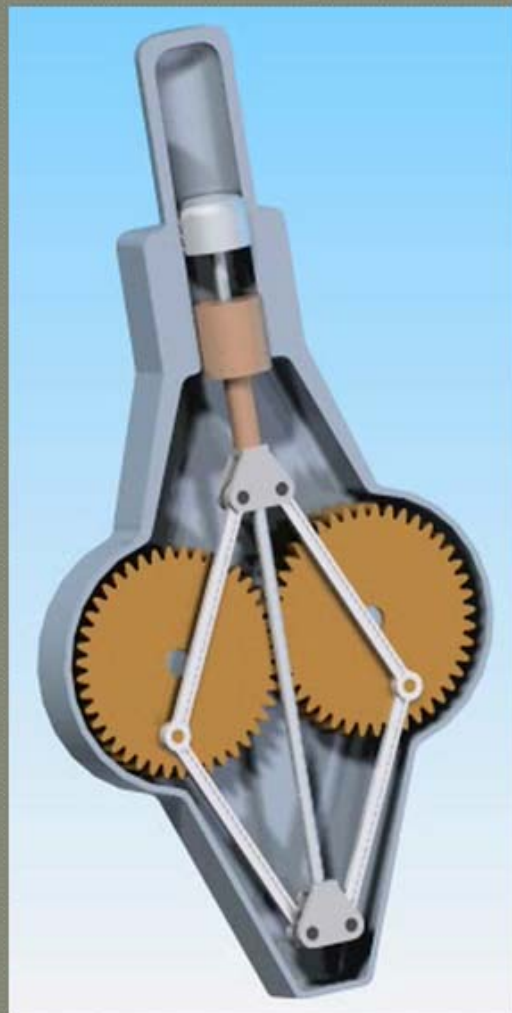


Bob Williams

Mechanism Kinematics & Dynamics



on-line NotesBook Supplement

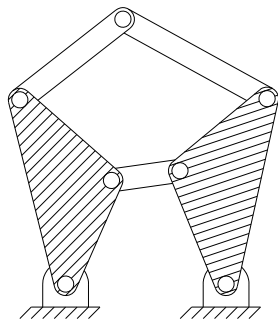
Mechanism Kinematics & Dynamics

Dr. Robert L. Williams II
Mechanical Engineering, Ohio University

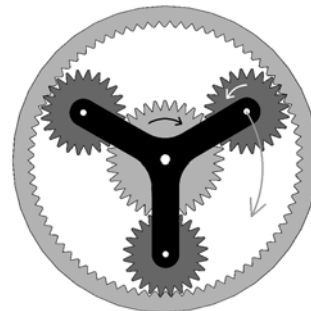
NotesBook Supplement for
ME 3011 Kinematics & Dynamics of Machines
© 2021 Dr. Bob Productions

williar4@ohio.edu

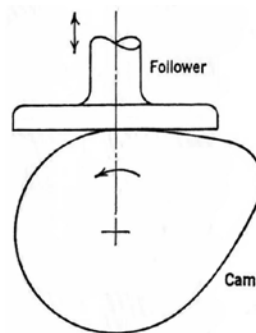
ohio.edu/mechanical-faculty/williams



Stephenson I Six-Bar Mechanism



Planetary Gear Train



Cam/Follower Mechanism

This document presents supplemental notes to accompany the ME 3011 NotesBook. The outline given in the Table of Contents dovetails with and augments the ME 3011 NotesBook outline and hence is incomplete here.

ME 3011 Supplement Table of Contents

1. INTRODUCTION	4
1.3 VECTORS: CARTESIAN RE-IM REPRESENTATION (PHASORS).....	4
2. POSITION KINEMATICS ANALYSIS	6
2.1 FOUR-BAR MECHANISM POSITION ANALYSIS	6
2.1.1 <i>Tangent Half-Angle Substitution Derivation and Alternate Solution Method</i>	6
2.1.3 <i>Four-Bar Mechanism Solution Irregularities</i>	13
2.1.4 <i>Grashof's Law and Four-Bar Mechanism Joint Limits</i>	14
2.2 SLIDER-CRANK MECHANISM IRREGULAR DESIGNS	23
2.3 INVERTED SLIDER-CRANK MECHANISM POSITION ANALYSIS	28
2.4 MULTI-LOOP MECHANISM POSITION ANALYSIS	36
3. VELOCITY KINEMATICS ANALYSIS	40
3.1 VELOCITY ANALYSIS INTRODUCTION.....	40
<i>Cyclist Zig-Zagging Uphill</i>	42
3.5 INVERTED SLIDER-CRANK MECHANISM VELOCITY ANALYSIS	47
3.6 MULTI-LOOP MECHANISM VELOCITY ANALYSIS	51
4. ACCELERATION KINEMATICS ANALYSIS	55
4.2 FIVE-PART ACCELERATION FORMULA.....	55
4.5 INVERTED SLIDER-CRANK MECHANISM ACCELERATION ANALYSIS.....	56
4.6 MULTI-LOOP MECHANISM ACCELERATION ANALYSIS	62
5. OTHER KINEMATICS TOPICS.....	66
5.4 BRANCH SYMMETRY IN KINEMATICS ANALYSIS	66
5.4.1 <i>Four-Bar Mechanism</i>	66
5.4.2 <i>Slider-Crank Mechanism</i>	68
6. INVERSE DYNAMICS ANALYSIS	70
6.1 DYNAMICS INTRODUCTION	70
6.4 FOUR-BAR MECHANISM INVERSE DYNAMICS ANALYSIS	71
6.5 SLIDER-CRANK MECHANISM INVERSE DYNAMICS ANALYSIS	73
6.6 INVERTED SLIDER-CRANK MECHANISM INVERSE DYNAMICS ANALYSIS.....	75
6.7 MULTI-LOOP MECHANISM INVERSE DYNAMICS ANALYSIS	83
6.8 DYNAMIC BALANCING OF ROTATING SHAFTS	88
7. GEARS AND CAMS	92
7.1 GEARS	92
7.1.3 <i>Gear Trains</i>	92
7.1.4 <i>Involute Spur Gear Standardization</i>	94
7.1.5 <i>Planetary Gear Trains</i>	103
7.2 CAMS	112
7.2.3 <i>Analytical Cam Synthesis</i>	112

1. Introduction

1.3 Vectors: Cartesian Re-Im Representation (Phasors)

Here is an alternate vector representation.

$$\underline{P} = P e^{i\theta}$$

The phasor $P e^{i\theta}$ is a polar representation for vectors, where P is the length of vector \underline{P} , e is the natural logarithm base, $i = \sqrt{-1}$ is the imaginary operator, and θ is the angle of vector \underline{P} . $e^{i\theta}$ gives the direction of the length P , according to Euler's identity.

$$e^{i\theta} = \cos \theta + i \sin \theta$$

$e^{i\theta}$ is a unit vector in the direction of vector \underline{P} .

Phasor *Re-Im* representation of a vector is equivalent to Cartesian *XY* representation, where the real (*Re*) axis is along *X* (or \hat{i}) and the imaginary (*Im*) axis is along *Y* (or \hat{j}).

$$\underline{P} = P(\cos \theta + i \sin \theta) = \begin{Bmatrix} P_{Re} \\ P_{Im} \end{Bmatrix} = \begin{Bmatrix} P \cos \theta \\ P \sin \theta \end{Bmatrix} = P e^{i\theta}$$

$$\underline{P} = P(\cos \theta \hat{i} + \sin \theta \hat{j}) = \begin{Bmatrix} P_X \\ P_Y \end{Bmatrix} = \begin{Bmatrix} P \cos \theta \\ P \sin \theta \end{Bmatrix}$$

A strength of Cartesian *Re-Im* representation using phasors is in taking time derivatives of vectors – the derivative of the exponential is easy ($d/ds(e^s) = e^s$).

$$\frac{d^2 \underline{P}}{dt^2} = \frac{d^2 P e^{i\theta}}{dt^2}$$

$$\frac{d^2 \underline{P}}{dt^2} = \frac{d}{dt} (\dot{P} e^{i\theta} + i P \dot{\theta} e^{i\theta})$$

$$\frac{d^2 \underline{P}}{dt^2} = \ddot{P} e^{i\theta} + i \dot{P} \dot{\theta} e^{i\theta} + i \dot{P} \dot{\theta} e^{i\theta} + i P \ddot{\theta} e^{i\theta} + i^2 P \dot{\theta}^2 e^{i\theta}$$

$$\frac{d^2 \underline{P}}{dt^2} = \ddot{P} e^{i\theta} + 2i \dot{P} \dot{\theta} e^{i\theta} + i P \ddot{\theta} e^{i\theta} - P \dot{\theta}^2 e^{i\theta}$$

$$\frac{d^2 \underline{P}}{dt^2} = \begin{Bmatrix} \ddot{P} \cos \theta - 2\dot{P} \dot{\theta} \sin \theta - P \ddot{\theta} \sin \theta - P \dot{\theta}^2 \cos \theta \\ \ddot{P} \sin \theta + 2\dot{P} \dot{\theta} \cos \theta + P \ddot{\theta} \cos \theta - P \dot{\theta}^2 \sin \theta \end{Bmatrix}$$

Where we had to use extensions of Euler's identity

$$\begin{aligned}
 e^{i\theta} &= \cos \theta + i \sin \theta \\
 ie^{i\theta} &= i \cos \theta + i^2 \sin \theta = -\sin \theta + i \cos \theta \\
 i^2 e^{i\theta} &= -i \sin \theta + i^2 \cos \theta = -\cos \theta - i \sin \theta
 \end{aligned}$$

Compare this double-time-derivative with the *XY* approach.

$$\frac{d^2 P}{dt^2} = \frac{d^2}{dt^2} \begin{Bmatrix} P \cos \theta \\ P \sin \theta \end{Bmatrix}$$

$$\frac{d^2 P}{dt^2} = \frac{d}{dt} \begin{Bmatrix} \dot{P} \cos \theta - P \dot{\theta} \sin \theta \\ \dot{P} \sin \theta + P \dot{\theta} \cos \theta \end{Bmatrix}$$

$$\frac{d^2 P}{dt^2} = \begin{Bmatrix} \ddot{P} \cos \theta - \dot{P} \dot{\theta} \sin \theta - \dot{P} \dot{\theta} \sin \theta - P \ddot{\theta} \sin \theta - P \dot{\theta}^2 \cos \theta \\ \ddot{P} \sin \theta + \dot{P} \dot{\theta} \cos \theta + \dot{P} \dot{\theta} \cos \theta + P \ddot{\theta} \cos \theta - P \dot{\theta}^2 \sin \theta \end{Bmatrix}$$

$$\frac{d^2 P}{dt^2} = \begin{Bmatrix} \ddot{P} \cos \theta - 2\dot{P} \dot{\theta} \sin \theta - P \ddot{\theta} \sin \theta - P \dot{\theta}^2 \cos \theta \\ \ddot{P} \sin \theta + 2\dot{P} \dot{\theta} \cos \theta + P \ddot{\theta} \cos \theta - P \dot{\theta}^2 \sin \theta \end{Bmatrix}$$

We obtain the same result, but the *Re-Im* phasor time differentiation is made in compact vector notation along the way.

Above we used the **product** and **chain rules** of time differentiation.

product rule $\frac{d}{dt}(P(t)e^{i\theta(t)}) = \frac{dP(t)}{dt}e^{i\theta(t)} + P(t)\frac{de^{i\theta(t)}}{dt} = \dot{P}(t)e^{i\theta(t)} + P(t)\frac{de^{i\theta(t)}}{dt}$

chain rule $\frac{de^{i\theta(t)}}{dt} = \frac{de^{i\theta(t)}}{d\theta(t)} \frac{d\theta(t)}{dt} = ie^{i\theta(t)} \dot{\theta}(t)$

The result for this example is

$$\frac{d}{dt}(P(t)e^{i\theta(t)}) = \dot{P}(t)e^{i\theta(t)} + P(t)ie^{i\theta(t)}\dot{\theta}(t)$$

2. Position Kinematics Analysis

2.1 Four-Bar Mechanism Position Analysis

2.1.1 Tangent Half-Angle Substitution Derivation and Alternate Solution Method

Tangent half-angle substitution derivation

In this subsection we first derive the tangent half-angle substitution using an analytical/trigonometric method. Defining parameter t to be

$$t = \tan\left(\frac{\phi}{2}\right)$$

i.e. the tangent of half of the unknown angle ϕ , we need to derive $\cos\phi$ and $\sin\phi$ as functions of parameter t . This derivation requires the trigonometric sum of angles formulae.

$$\cos(a \pm b) = \cos a \cos b \mp \sin a \sin b$$

$$\sin(a \pm b) = \sin a \cos b \pm \cos a \sin b$$

To derive the $\cos\phi$ term as a function of t , we start with

$$\cos\phi = \cos\left(\frac{\phi}{2} + \frac{\phi}{2}\right)$$

The cosine sum of angles formula yields

$$\cos\phi = \cos^2\left(\frac{\phi}{2}\right) - \sin^2\left(\frac{\phi}{2}\right)$$

Multiplying by a '1', i.e. $\cos^2\left(\frac{\phi}{2}\right)$ over itself yields

$$\cos\phi = \frac{\cos^2\left(\frac{\phi}{2}\right) - \sin^2\left(\frac{\phi}{2}\right)}{\cos^2\left(\frac{\phi}{2}\right)} \cos^2\left(\frac{\phi}{2}\right) = \left[1 - \tan^2\left(\frac{\phi}{2}\right)\right] \cos^2\left(\frac{\phi}{2}\right)$$

The cosine squared term can be divided by another '1', i.e. $\cos^2\left(\frac{\phi}{2}\right) + \sin^2\left(\frac{\phi}{2}\right) = 1$.

$$\cos \phi = \left[1 - \tan^2 \left(\frac{\phi}{2} \right) \right] \left[\frac{\cos^2 \left(\frac{\phi}{2} \right)}{\cos^2 \left(\frac{\phi}{2} \right) + \sin^2 \left(\frac{\phi}{2} \right)} \right]$$

Dividing top and bottom by $\cos^2 \left(\frac{\phi}{2} \right)$ yields

$$\cos \phi = \left[1 - \tan^2 \left(\frac{\phi}{2} \right) \right] \left[\frac{1}{1 + \tan^2 \left(\frac{\phi}{2} \right)} \right]$$

Remembering the earlier definition for t , this result is the first derivation we need, i.e.

$$\cos \phi = \frac{1-t^2}{1+t^2}$$

To derive the $\sin \phi$ term as a function of t , we start with

$$\sin \phi = \sin \left(\frac{\phi}{2} + \frac{\phi}{2} \right)$$

The sine sum of angles formula yields

$$\sin \phi = \sin \left(\frac{\phi}{2} \right) \cos \left(\frac{\phi}{2} \right) + \cos \left(\frac{\phi}{2} \right) \sin \left(\frac{\phi}{2} \right) = 2 \sin \left(\frac{\phi}{2} \right) \cos \left(\frac{\phi}{2} \right)$$

Multiplying top and bottom by cosine yields

$$\sin \phi = 2 \frac{\sin \left(\frac{\phi}{2} \right)}{\cos \left(\frac{\phi}{2} \right)} \cos^2 \left(\frac{\phi}{2} \right) = 2 \tan \left(\frac{\phi}{2} \right) \cos^2 \left(\frac{\phi}{2} \right)$$

From the first derivation we learned

$$\cos^2 \left(\frac{\phi}{2} \right) = \frac{1}{1 + \tan^2 \left(\frac{\phi}{2} \right)}$$

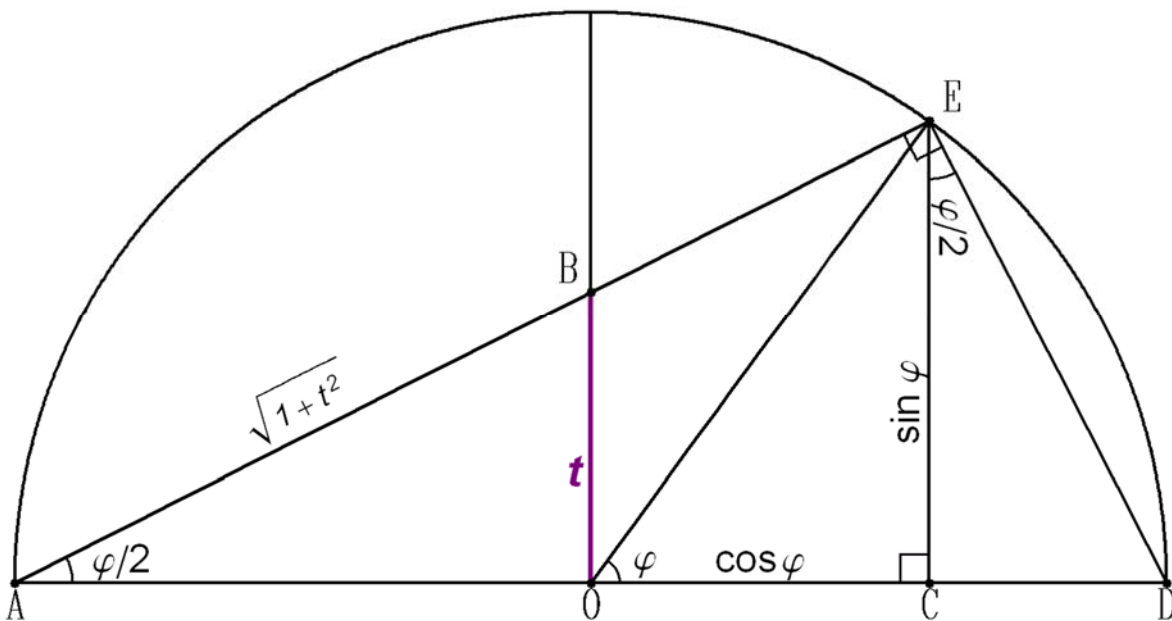
Substituting this term yields

$$\sin \phi = 2 \tan\left(\frac{\phi}{2}\right) \left[\frac{1}{1 + \tan^2\left(\frac{\phi}{2}\right)} \right]$$

Remembering the earlier definition for t , this result is the second derivation we need, i.e.

$$\sin \phi = \frac{2t}{1+t^2}$$

The tangent half-angle substitution can also be derived using a graphical method as in the figure below.



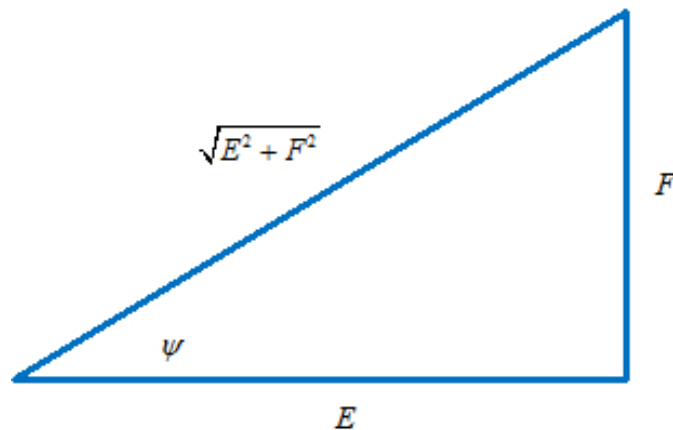
Alternate solution method

The equation form

$$E \cos \theta + F \sin \theta + G = 0$$

arises often in the position solutions for mechanisms and robots. It appeared in the θ_4 solution for the four-bar mechanism in the ME 3011 NotesBook and was solved using the tangent half-angle substitution.

Next we present an alternative and simpler solution to this equation. We make two simple trigonometric substitutions based on the figure below.



Clearly from this figure we have

$$\cos \psi = \frac{E}{\sqrt{E^2 + F^2}} \quad \sin \psi = \frac{F}{\sqrt{E^2 + F^2}}$$

In the original equation we divide by $\sqrt{E^2 + F^2}$ and rearrange.

$$\frac{E}{\sqrt{E^2 + F^2}} \cos \theta + \frac{F}{\sqrt{E^2 + F^2}} \sin \theta = \frac{-G}{\sqrt{E^2 + F^2}}$$

The two simple trigonometric substitutions yield

$$\cos \theta \cos \psi + \sin \theta \sin \psi = \frac{-G}{\sqrt{E^2 + F^2}}$$

Applying the sum-of-angles formula $\cos(a \pm b) = \cos a \cos b \mp \sin a \sin b$ yields

$$\cos(\theta - \psi) = \frac{-G}{\sqrt{E^2 + F^2}}$$

And so the solution for θ is

$$\theta_{1,2} = \psi \pm \cos^{-1} \left[\frac{-G}{\sqrt{E^2 + F^2}} \right]$$

where

$$\psi = \tan^{-1} \left[\frac{F}{E} \right]$$

and the quadrant-specific inverse tangent function **atan2** must be used in the above expression for ψ .

There are two solutions for θ , indicated by the subscripts 1,2, since the inverse cosine function is double-valued. Both solutions are correct. We expected these two solutions from the tangent-half-angle substitution approach. They correspond to the open- and crossed-branch solutions (the engineer must determine which is which) to the four-bar mechanism position analysis problem.

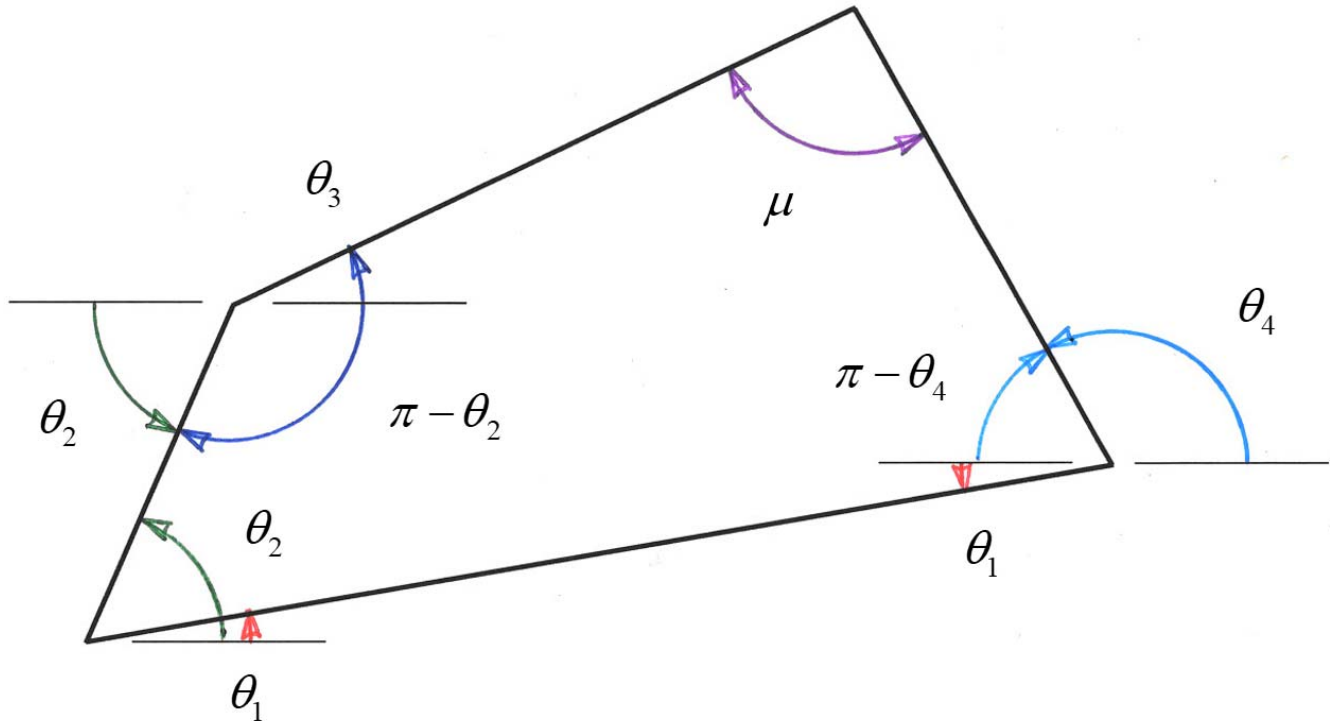
For real solutions for θ to exist, we must have

$$-1 \leq \frac{-G}{\sqrt{E^2 + F^2}} \leq 1 \quad \text{or} \quad 1 \geq \frac{G}{\sqrt{E^2 + F^2}} \geq -1$$

If this condition is violated for the four-bar mechanism, this means that the given input angle θ_2 is beyond its reachable limits (see Grashof's Law).

Alternate Four-Bar Mechanism Transmission Angle Derivation

Rather than using the Vertical Angles Theorem as in the ME 3011 NotesBook, an alternate approach to deriving the Four-Bar Mechanism Transmission Angle μ is presented here, using the fact that the sum of the interior angles for any quadrilateral must be 360° (2π rad).



Alternate Method Figure to Derive μ

As seen in the figure above, the four interior angles of the four-bar mechanism quadrilateral are, in radians:

$$\theta_2 - \theta_1 \qquad \pi - \theta_2 + \theta_3 \qquad \mu \qquad \pi - \theta_4 + \theta_1$$

These four angles must sum to 2π :

$$(\theta_2 - \theta_1) + (\pi - \theta_2 + \theta_3) + (\mu) + (\pi - \theta_4 + \theta_1) = 2\pi$$

Rearranging,

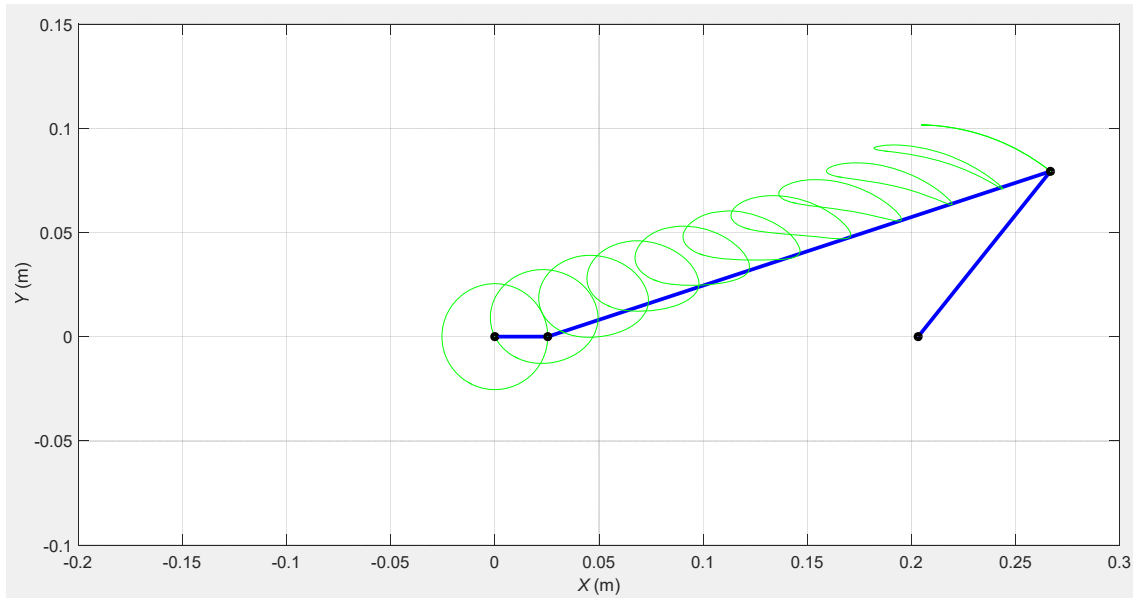
$$\begin{aligned} \theta_2 - \theta_2 + \theta_1 - \theta_1 + \pi + \pi + \theta_3 + \mu - \theta_4 &= 2\pi \\ 2\pi + \theta_3 + \mu - \theta_4 &= 2\pi \\ \mu &= \theta_4 - \theta_3 \end{aligned}$$

Remembering that only the magnitude of this angle is important (not caring the direction), we have $\mu = |\theta_4 - \theta_3|$, identical to the transmission angle result derived in the ME 3011 NotesBook.

Four-Bar Mechanism Coupler Curve Families

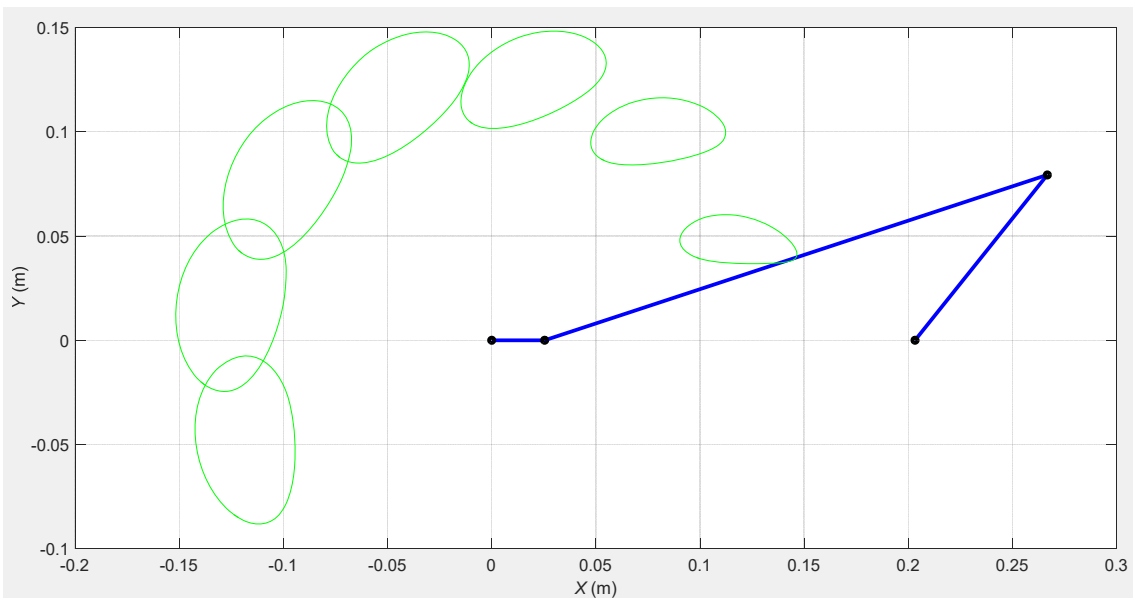
It is difficult to express the coupler curve of a four-bar mechanism analytically. Recall the coupler curve is the trace of point C (the vertex of the coupler triangle for link 3) in the plane. It can be an important design consideration to shape the coupler curve according to specific needs in the task. This subsection presents an example of different coupler curves for the same four-bar mechanism.

First we present the different coupler curves for different lengths along r_3 . Then we present the different coupler curves for different angles δ_3 .



Coupler Curve Family for Different Lengths along r_3

$$r_{CA} = [0 \ 0.1 \ 0.2 \ 0.3 \ 0.4 \ 0.5 \ 0.6 \ 0.7 \ 0.8 \ 0.9 \ 1] r_3 \quad \delta_3 = 0$$



Coupler Curve Family for Different Angles δ_3

$$r_{CA} = 0.5 r_3 \quad \delta_3 = [0^\circ \ 30^\circ \ 60^\circ \ 90^\circ \ 120^\circ \ 150^\circ \ 180^\circ]$$

2.1.3 Four-Bar Mechanism Solution Irregularities

Four-bar mechanism position singularity $G-E=0$

$$E = 2r_4(r_1c_1 - r_2c_2)$$

$$G = r_1^2 + r_2^2 - r_3^2 + r_4^2 - 2r_1r_2 \cos(\theta_1 - \theta_2)$$

For simplicity, let $\theta_1 = 0$ (just rotate the entire four-bar mechanism model for zero ground link angle).

$$G - E = r_1^2 + r_2^2 - r_3^2 + r_4^2 - 2r_1r_4 + 2r_2(r_4 - r_1)c_2 = 0$$

I have encountered two example four-bar mechanisms with this $G-E=0$ singularity.

Case 1

When $r_1 = r_4$ and $r_2 = r_3$, $G - E = r_1^2 + r_2^2 - r_2^2 + r_1^2 - 2r_1^2 + 2r_2(r_1 - r_1)c_2 = 0$ ALWAYS, regardless of θ .

Example

Given $r_1 = 10, r_2 = 6, r_3 = 6, r_4 = 10$; this mechanism is ALWAYS singular. To fix this let $r_1 = 10, r_2 = 5.9999, r_3 = 6.0001, r_4 = 10$ and MATLAB will be able to calculate the position analysis reliably at every input angle.

Case 2

When $r_1 = 2r_3$ and $r_4 = 2r_2$, and furthermore $3r_3 = 5r_2$,

$$\begin{aligned} G - E &= 4r_3^2 + r_2^2 - r_3^2 + 4r_2^2 - 8r_2r_3 + 4r_2(r_2 - r_3)c_2 \\ &= \frac{100}{9}r_2^2 + r_2^2 - \frac{25}{9}r_2^2 + 4r_2^2 - \frac{40}{3}r_2^2 - \frac{8}{3}r_2^2 c_2 \\ &= -\frac{8}{3}r_2^2 c_2 \end{aligned}$$

This $G-E=0$ occurs only when $\theta_2 = \pm 90^\circ$. Case 2 is much less general than case 1.

Example

Given $r_1 = 10, r_2 = 3, r_3 = 5, r_4 = 6$; this mechanism is singular when $\theta_2 = \pm 90^\circ$. To fix this ignore $\theta_2 = \pm 90^\circ$ or set your θ array to avoid these values.

2.1.4 Grashof's Law and Four-Bar Mechanism Joint Limits

Grashof's Law

Grashof's Law was presented in the ME 3011 NotesBook to determine the input and output link rotatability in a four-bar mechanism. Applying Grashof's Law we determine if the input and output links are a crank (**C**) or a rocker (**R**). A crank enjoys full 360 degree rotation while a rocker has a rotation that is a subset of this full rotation. This section presents more information on Grashof's Law and then the next subsection presents four-bar mechanism joint limits.

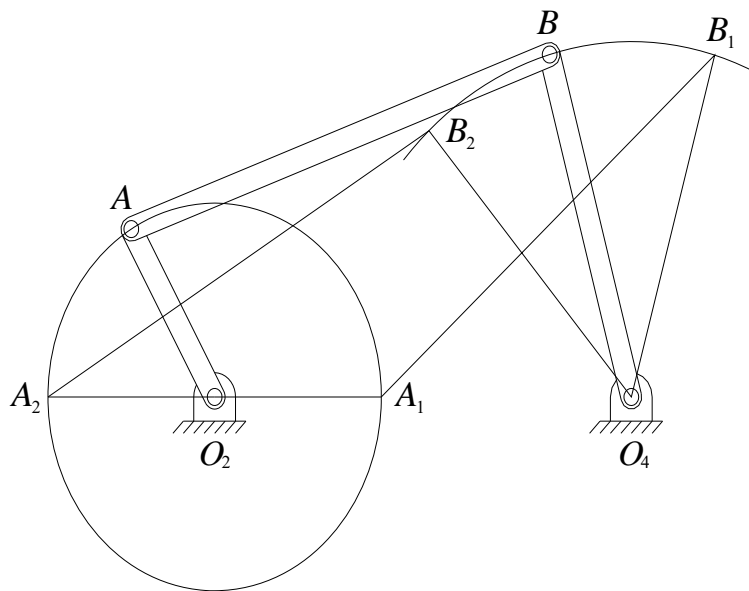
Grashof's condition states "For a four-bar mechanism, the sum of the shortest and longest link lengths should not be greater than the sum of two remaining link lengths". With a given four-bar mechanism, the Grashof Condition is satisfied if $L + S < P + Q$ where S and L are the lengths of the shortest and longest links, and P and Q are the lengths of the other two intermediate-sized links. If the Grashof condition is satisfied, at least one link will be fully rotatable, i.e. can rotate 360 degrees.

For a four-bar mechanism, the following inequalities must be satisfied to avoid locking of the mechanism for all motion.

$$r_2 - r_1 + r_3 > r_4$$

$$r_4 - r_1 + r_2 > r_3$$

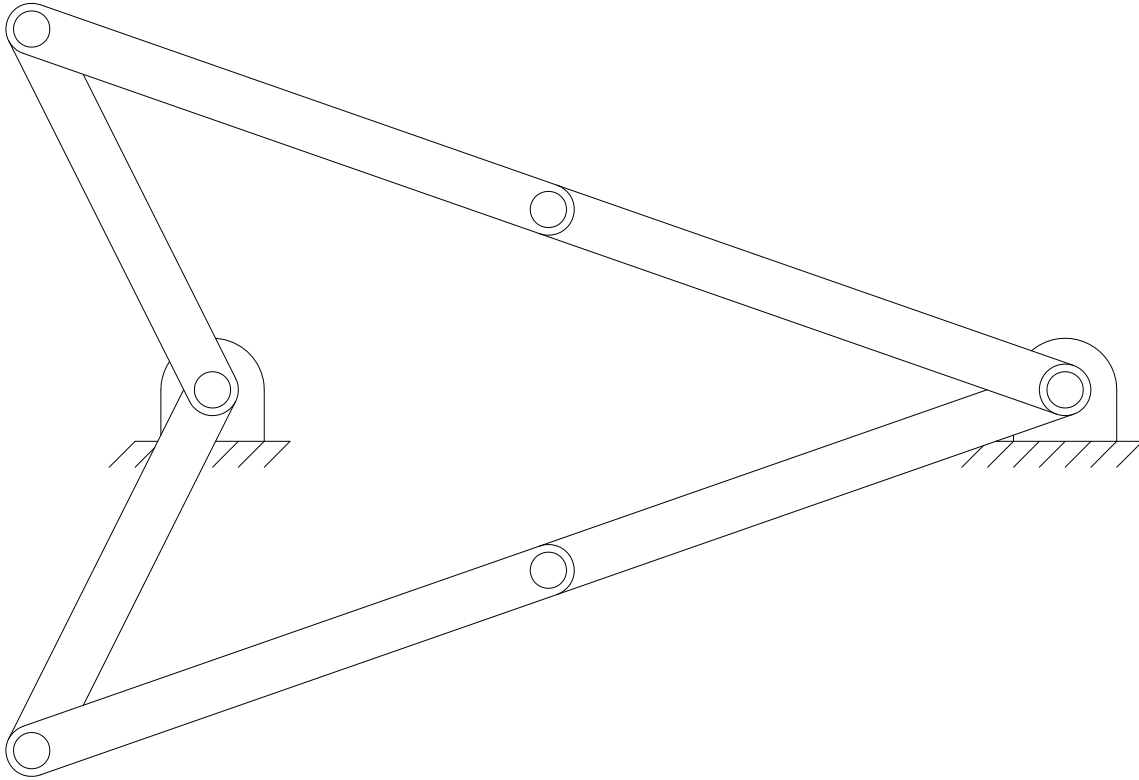
With reference to the figure below, these inequalities are derived from the fact that the sum of two sides of a triangle must be greater than the third side, for triangles $O_4A_1B_1$ and $O_2A_2B_2$, respectively. Note from our standard notation, $r_1 \equiv O_2O_4$, $r_2 \equiv O_2A$, $r_3 \equiv AB$, and $r_4 \equiv O_4B$.



Four-Bar Mechanism Joint Limits

Input Angle Joint Limits

If **Grashof's Law** predicts that the input link is a rocker, there will be rotation limits on the input link. These joint limits occur when links 3 and 4 are aligned. As shown in the figure below, there will be two joint limits, symmetric about the ground link.



To calculate the input joint limits, when they exist, we use the **law of cosines**.

$$(r_3 + r_4)^2 = r_1^2 + r_2^2 - 2r_1r_2 \cos \theta_{2L}$$

$$\theta_{2L} = \pm \cos^{-1} \left[\frac{r_1^2 + r_2^2 - (r_3 + r_4)^2}{2r_1r_2} \right]$$

\pm with symmetry about r_1 .

Joint Limit Example 1

$$\text{Given } r_1 = 10, r_2 = 6, r_3 = 8, r_4 = 7$$

$$L + S > P + Q \quad (10 + 6 > 8 + 7)$$

so we predict only double rockers from this **Non-Grashof Mechanism**.

$$\theta_{2L} = \pm \cos^{-1} \left[\frac{10^2 + 6^2 - (8 + 7)^2}{2(10)(6)} \right] = \pm \cos^{-1} [-0.742] = \pm 137.9^\circ$$

This method can also be used to find angular limits on link 4 when it is a rocker. In this case links 2 and 3 align.

$$\phi = \pm \cos^{-1} \left[\frac{10^2 + 7^2 - (6 + 8)^2}{2(10)(7)} \right] = \pm \cos^{-1} [-0.336] = \pm 109.6^\circ$$

$$\theta_{4L} = 180^\circ - \phi = \pm 70.4^\circ$$

In this example, the allowable input and output angle ranges are:

$$-137.9^\circ \leq \theta_2 \leq 137.9^\circ \qquad 70.4^\circ \leq \theta_4 \leq 289.6^\circ$$

This example is shown graphically in the ME 3011 NotesBook, in the Grashof's Law section (2. Non-Grashof double rocker, first inversion).

Caution

The figure on the previous page does not apply in all joint limit cases. For **Grashof Mechanisms** with a rocker input link, one link 2 limit occurs when links 3 and 4 fold upon each other and the other link 2 limit occurs when links 3 and 4 stretch out in a straight line. See Example 4 (and Example 3 for a similar situation with the output link 4 limits).

Joint Limit Example 2

$$\text{Given } r_1 = 10, r_2 = 4, r_3 = 8, r_4 = 7$$

$$L + S < P + Q \quad (10 + 4 < 8 + 7)$$

Since the S link is adjacent to the fixed link, we predict this **Grashof Mechanism** is a crank-rocker. Therefore, there are no θ_2 joint limits.

$$\theta_{2L} = \pm \cos^{-1} \left[\frac{10^2 + 4^2 - (8+7)^2}{2(10)(4)} \right] = \pm \cos^{-1} [-1.3625]$$

which is undefined, thus confirming there are no θ_2 joint limits.

There are limits on link 4 since it is a rocker. For $\theta_{4\min}$, links 2 and 3 are stretched in a straight line (their absolute angles are identical).

$$\phi = + \cos^{-1} \left[\frac{10^2 + 7^2 - (4+8)^2}{2(10)(7)} \right] = \cos^{-1} [0.036] = 88.0^\circ$$

$$\theta_{4\min} = 180^\circ - \phi = 92.0^\circ$$

For $\theta_{4\max}$, links 2 and 3 are instead folded upon each other (their absolute angles are different by π).

$$\phi = + \cos^{-1} \left[\frac{10^2 + 7^2 - (-4+8)^2}{2(10)(7)} \right] = \cos^{-1} [0.95] = 18.2^\circ$$

$$\theta_{4\max} = 180^\circ - \phi = 161.8^\circ$$

In this example, the output angle range is

$$92.0^\circ \leq \theta_4 \leq 161.8^\circ$$

and θ_2 is not limited. This example is shown graphically in the ME 3011 NotesBook, in the Grashof's Law section (1a. Grashof crank-rocker).

Joint Limit Example 3

Given $r_1 = 11.18, r_2 = 3, r_3 = 8, r_4 = 7$ (in) and $\theta_1 = 10.3^\circ$

$$L + S < P + Q \quad (11.18 + 3 < 8 + 7)$$

This is the four-bar mechanism from Term Example 1 and it is a four-bar crank-rocker **Grashof Mechanism**. There are no limits on θ_2 since link 2 is a crank.

The θ_4 limits are

$$\theta_{4L} = 120.1^\circ \text{ (links 2 and 3 stretched in a line)}$$

$$\theta_{4L} = 172.5^\circ \text{ (links 2 and 3 folded upon each other in a line)}$$

The output angle range is

$$120.1^\circ \leq \theta_4 \leq 172.5^\circ$$

and θ_2 is not limited. This example is NOT shown graphically in the ME 3011 NotesBook Grashof's Law section. However, these θ_4 limits are clearly seen in the F.R.O.M. plot for angle θ_4 in Term Example 1 in the ME 3011 NotesBook.

Joint Limit Example 4

$$\text{Given } r_1 = 10, r_2 = 8, r_3 = 4, r_4 = 7$$

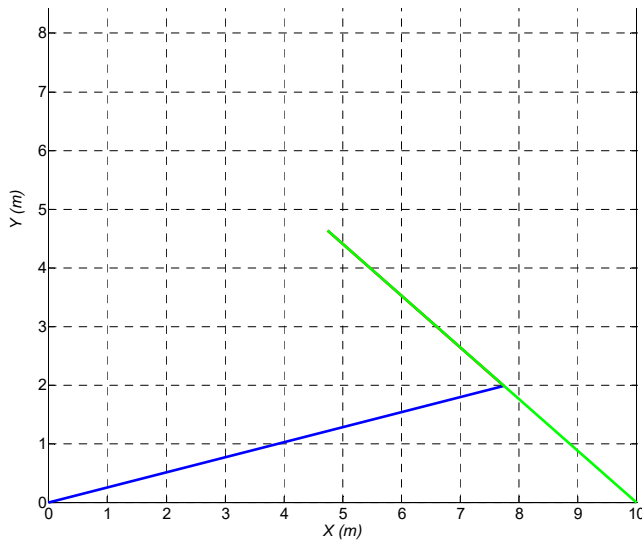
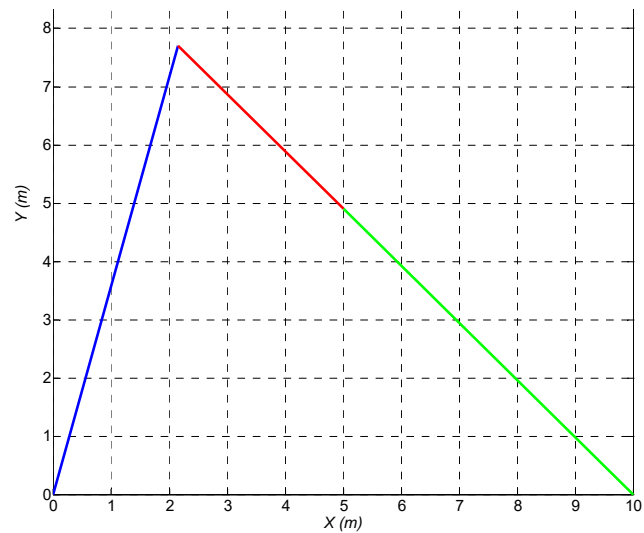
$$L + S < P + Q \quad (10 + 4 < 8 + 7)$$

so we predict this **Grashof Mechanism** is a double-rocker (S opposite fixed link). The θ_2 joint limits are no longer symmetric about the ground link, as was the case in the **Non-Grashof Mechanism** double rocker (Example 1). For $\theta_{2\min}$, links 3 and 4 are folded upon each other (their absolute angles are identical).

$$\theta_{2\min} = +\cos^{-1} \left[\frac{10^2 + 8^2 - (7-4)^2}{2(10)(8)} \right] = \cos^{-1} [0.969] = 14.4^\circ$$

For $\theta_{2\max}$, links 3 and 4 are instead stretched in a straight line (their absolute angles are different by π as in Example 1).

$$\theta_{2\max} = +\cos^{-1} \left[\frac{10^2 + 8^2 - (7+4)^2}{2(10)(8)} \right] = \cos^{-1} [0.269] = 74.4^\circ$$

 $\theta_{2\min}$ Diagram $\theta_{2\max}$ Diagram

This behavior reverses for the θ_4 joint limits. For $\theta_{4\min}$, links 2 and 3 are stretched in a straight line (their absolute angles are identical).

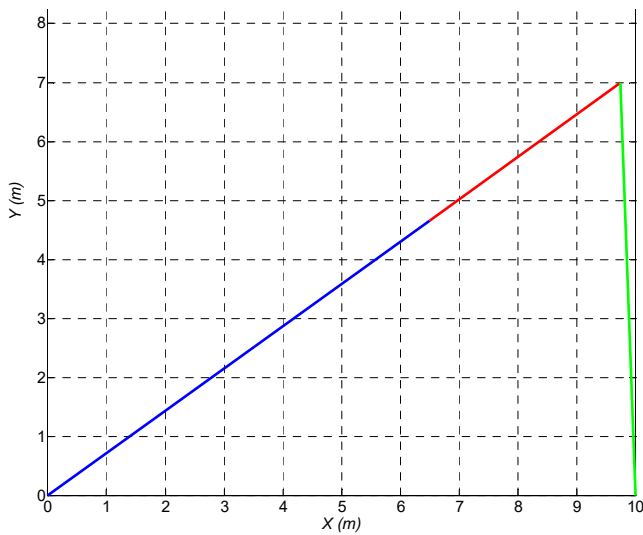
$$\phi = +\cos^{-1}\left[\frac{10^2 + 7^2 - (8+4)^2}{2(10)(7)}\right] = \cos^{-1}[0.036] = 88.0^\circ$$

$$\theta_{4\min} = 180^\circ - \phi = 92.0^\circ$$

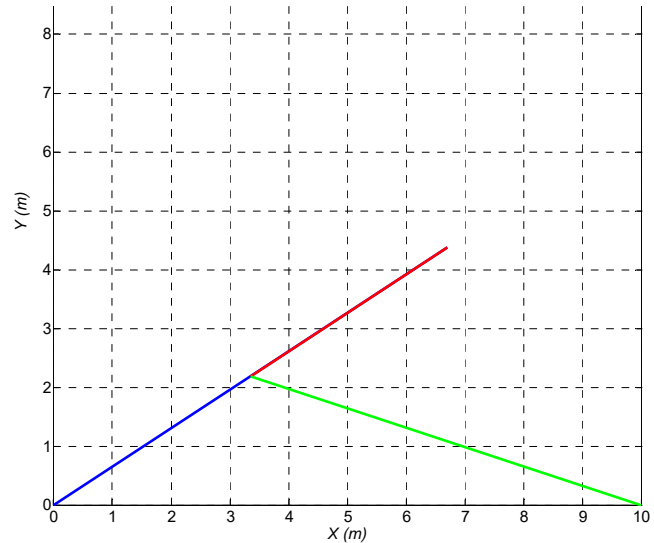
For $\theta_{4\max}$, links 2 and 3 are instead folded upon each other (their absolute angles are different by π).

$$\phi = +\cos^{-1}\left[\frac{10^2 + 7^2 - (8-4)^2}{2(10)(7)}\right] = \cos^{-1}[0.95] = 18.2^\circ$$

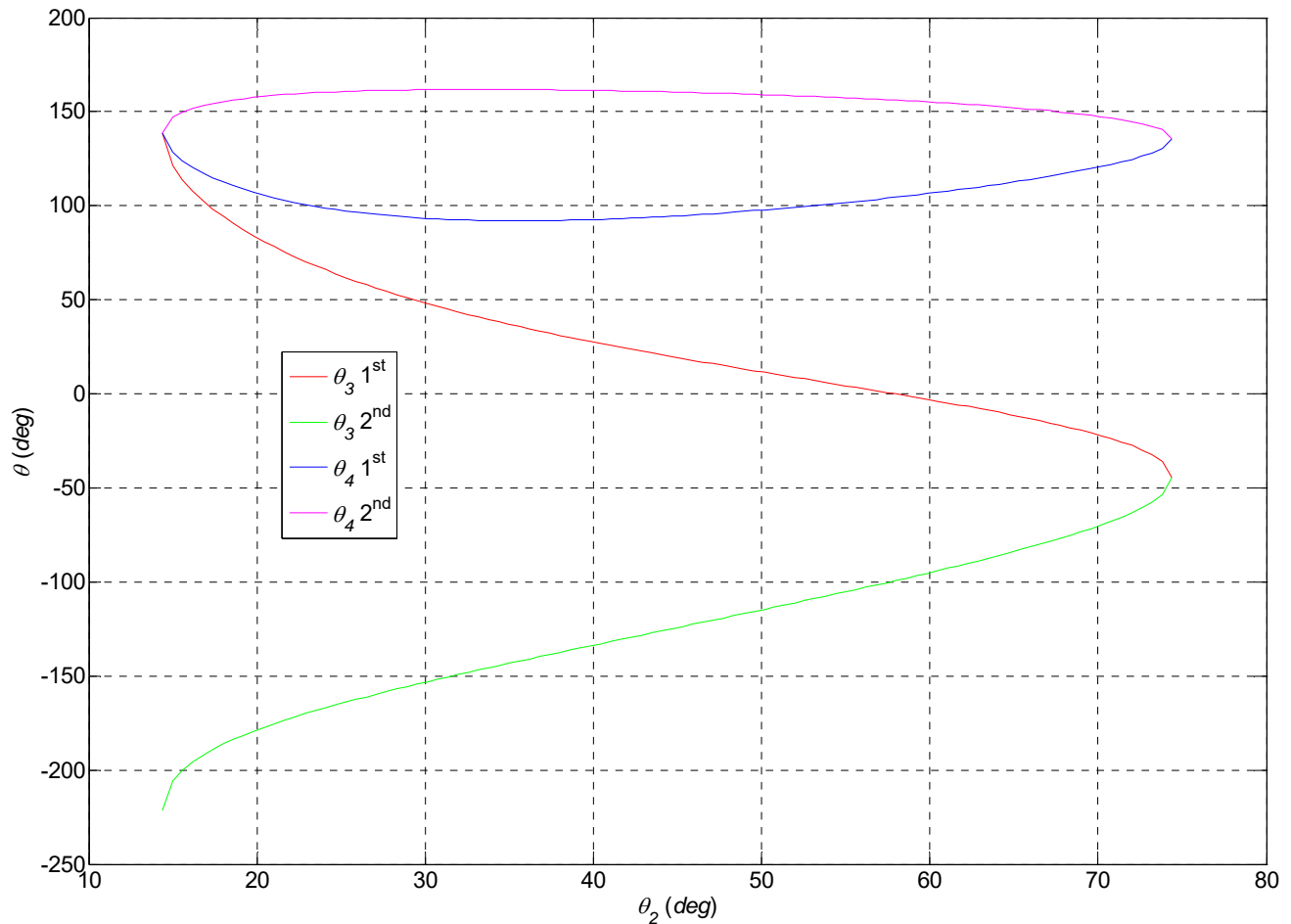
$$\theta_{4\min} = 180^\circ - \phi = 161.8^\circ$$



$\theta_{4\min}$ Diagram



$\theta_{4\max}$ Diagram



In this plot we can see the minimum and maximum values we just calculated for links 2 and 4.

Note at $\theta_{2_{\min}} = 14.4^\circ$, $\theta_3 = 138.6^\circ$ and $\theta_3 = -221.4^\circ$ are the same angle.

Again, this example is NOT shown graphically in the ME 3011 NotesBook Grashof's Law section. However, a similar case with the same dimensions, in different order, is shown in the ME 3011 NotesBook ($r_1 = 7, r_2 = 10, r_3 = 4, r_4 = 8$, 1d. Grashof double rocker).

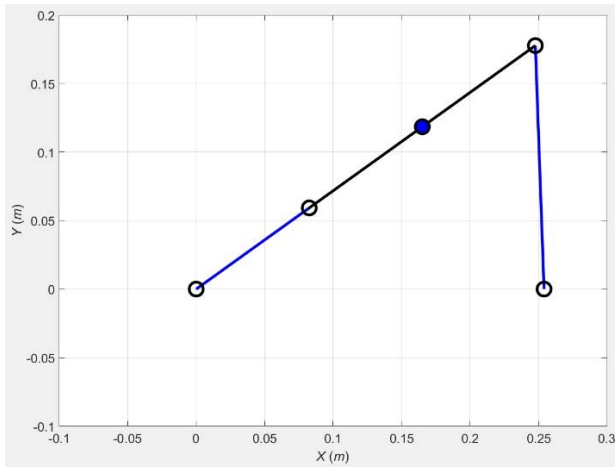
Grashof's Law only predicts the rotatability of the input and output links; it says nothing about the rotatability of the coupler link 3 – in this case, what is the rotatability of the coupler link? (In this case the coupler link S rotates fully, proving that the relative motion is the same amongst all four-bar mechanism inversions, though the absolute motion with respect to the possible 4 ground links is very different.)

For more information, see:

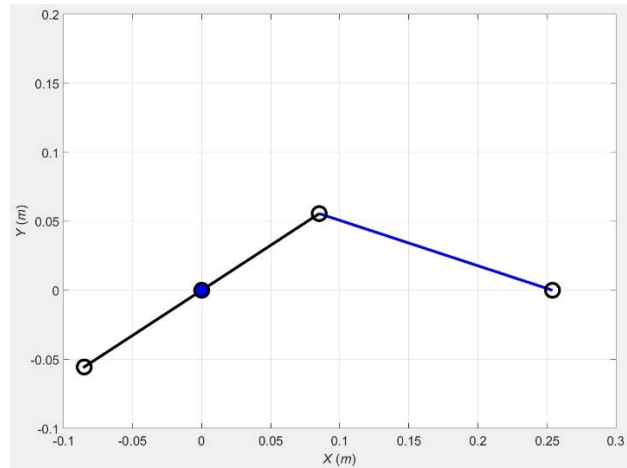
R.L. Williams II and C.F. Reinholtz, 1987, "Mechanism Link Rotatability and Limit Position Analysis Using Polynomial Discriminants", **Journal of Mechanisms, Transmissions, and Automation in Design**, Transactions of the ASME, 109(2): 178-182.

Output Angle Joint Limits

If **Grashof's Law** predicts that the output link is a rocker, there will be rotation limits on the output link. These joint limits occur when links 2 and 3 are aligned. As shown in the figures below, there will be two joint limits. When links 2 and 3 are straight out, this leads to the minimum output joint condition. When links 2 and 3 are folded upon each other, this leads to the maximum output joint condition. Note that the input link is not limited in these cases, but may continue to rotate freely in either direction.



Minimum Output Joint Condition



Maximum Output Joint Condition

To calculate the output joint limits, when they exist, we again use the **law of cosines**. We also need the **law of sines**. Angle a is the interior angle between r_1 and the line of (r_2, r_3) . Angle c is the interior angle between r_4 and the line of (r_2, r_3) .

$$c_{MIN} = \cos^{-1} \left[\frac{(r_2 + r_3)^2 + r_4^2 - r_1^2}{2(r_2 + r_3)r_4} \right]$$

$$c_{MAX} = \cos^{-1} \left[\frac{(r_3 - r_2)^2 + r_4^2 - r_1^2}{2(r_3 - r_2)r_4} \right]$$

$$a_{MIN} = \sin^{-1} \left[\frac{r_4}{r_1} \sin c_{MIN} \right]$$

$$a_{MAX} = \sin^{-1} \left[\frac{r_4}{r_1} \sin c_{MAX} \right]$$

$$\theta_{2MIN} = a_{MIN} + \theta_1$$

$$\theta_{2MAX} = a_{MAX} + \theta_1 + \pi$$

$$\theta_{4MIN} = c_{MIN} + \theta_{2MIN}$$

$$\theta_{4MAX} = c_{MAX} + \theta_{2MAX} - \pi$$

Again, note that the input link is not limited in these cases; the notation θ_{2MIN} and θ_{2MAX} simply means those input angles that correspond to the limited output angles θ_{4MIN} and θ_{4MAX} .

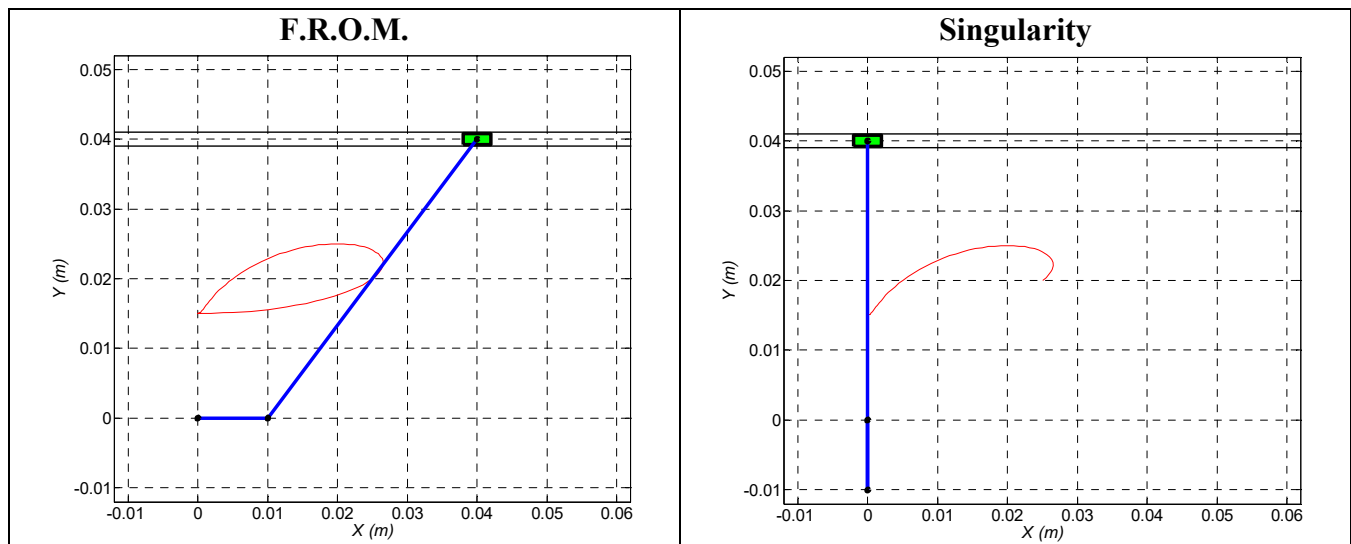
2.2 Slider-Crank Mechanism Irregular Designs

Some alert ME 3011 students posed the question, “For the slider-crank mechanism, what happens if $h = r_3 - r_2$?” This section answers that question and presents three other irregular slider-crank mechanisms and their particular problems. All four design irregularity cases below are for the Inversion 1 Slider-Crank mechanism.

$$\underline{h = r_3 - r_2}$$

In this case, the slider-crank mechanism has a singularity at $\theta_2 = \frac{3\pi}{2}$. The position variables' slopes are discontinuous, and thus the accelerations infinite at this singularity. At the singularity, r_3 is vertical up and r_2 vertical down, and the position variable $x = 0$, as shown below.

In this example, $r_2 = 1, r_3 = 5, h = 4$, and $r_{CA} = 2.5$ cm.



For this situation with $h = r_3 - r_2$, the maximum slider displacement x_{\max} and associated input angle θ_2^* are calculated as follows:

$$\text{for } \theta_2^* = \sin^{-1}\left(\frac{h}{r_2 + r_3}\right) \qquad x_{\max} = (r_2 + r_3) \cos(\theta_2^*)$$

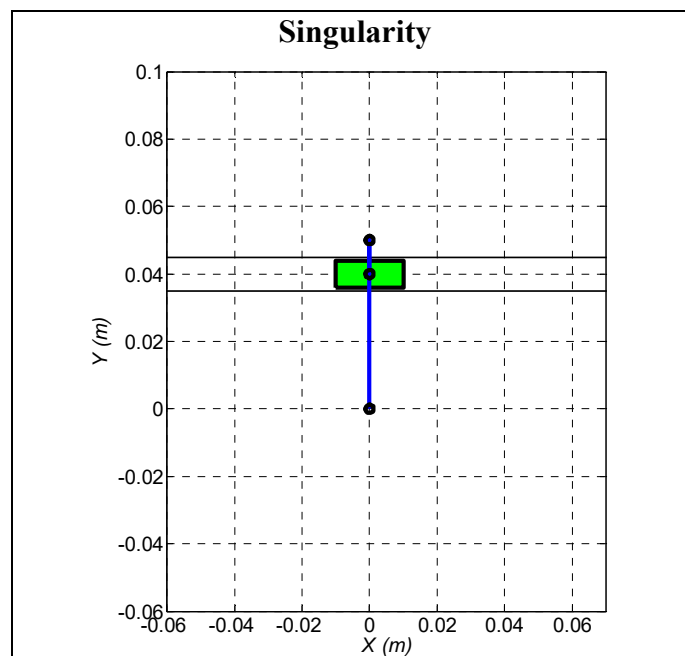
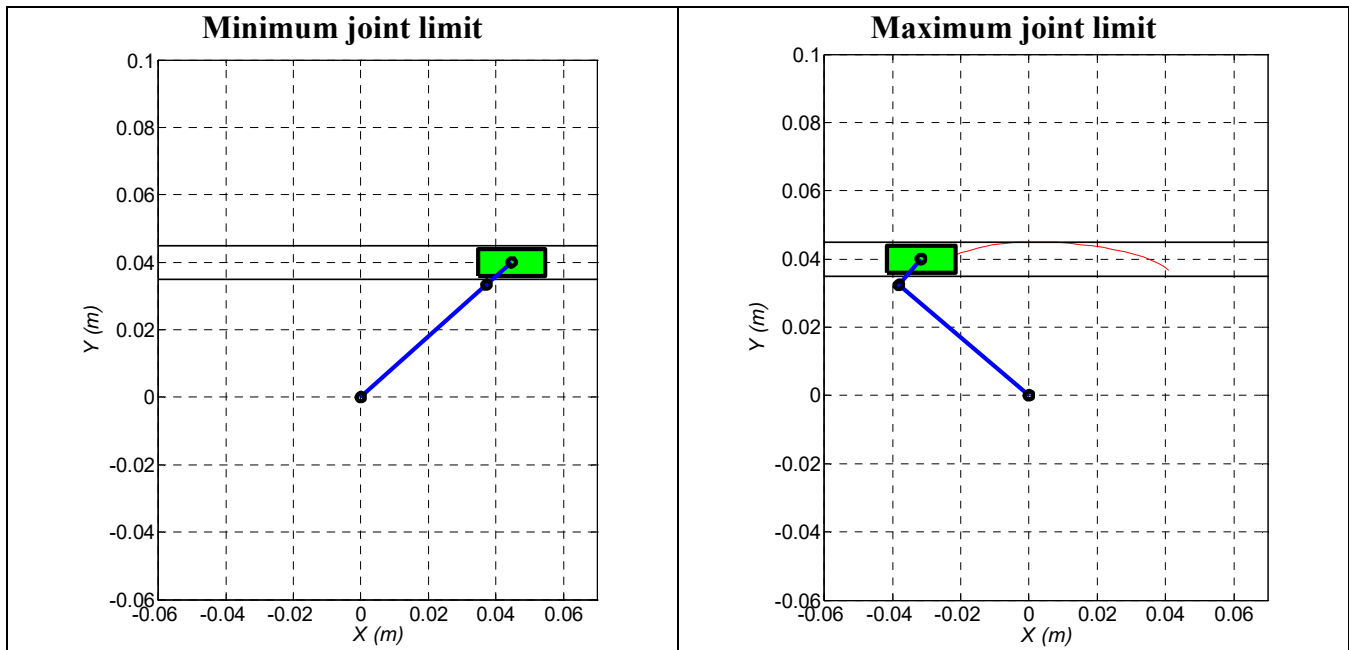
These equations are easily derived by drawing the limiting cases, drawing the applicable right triangles, and using geometry and trigonometry relationships.

In this example, the minimum slider displacement is $x_{\min} = 0$ m, which occurs at input angle $\theta_2 = 270^\circ$, and the maximum slider displacement is $x_{\max} = 0.045$ m, which occurs at input angle $\theta_2 = 41.8^\circ$.

$$h = r_2 - r_3$$

In this case, the slider-crank mechanism has a singularity at $\theta_2 = \frac{\pi}{2}$. At the singularity, r_3 is vertical down and r_2 is vertical up, and the position variable $x = 0$, as shown below. Also, the input angle is limited (i.e. the ‘crank’ is not a crank). Further, unlike standard slider-crank mechanisms, this case has the possibility of branch-jumping (at the singularity), depending on mechanism links’ inertia. The condition for minimum input angle is when r_2 and r_3 are extended in a straight line. If the slider-crank mechanism remains in the right branch, the condition for maximum input angle is when r_2 and r_3 are perpendicular. The limit equations for this case are presented below.

In this example, $r_2 = 5, r_3 = 1, h = 4$, and $r_{CA} = 0.5$ cm.



For this situation with $h = r_2 - r_3$, the maximum slider displacement is associated with the minimum input angle joint limit:

$$\theta_{2\min} = \sin^{-1}\left(\frac{h}{r_2 + r_3}\right) \quad x_{\max} = (r_2 + r_3)\cos(\theta_{2\min})$$

Also, the minimum slider displacement is associated with the maximum input angle joint limit:

$$\theta_{2\max} = \frac{\pi}{2} + \cos^{-1}\left(\frac{h}{\sqrt{r_2^2 + r_3^2}}\right) + \cos^{-1}\left(\frac{r_2}{\sqrt{r_2^2 + r_3^2}}\right) \quad x_{\min} = -h \tan\left(\cos^{-1}\left(\frac{h}{\sqrt{r_2^2 + r_3^2}}\right)\right)$$

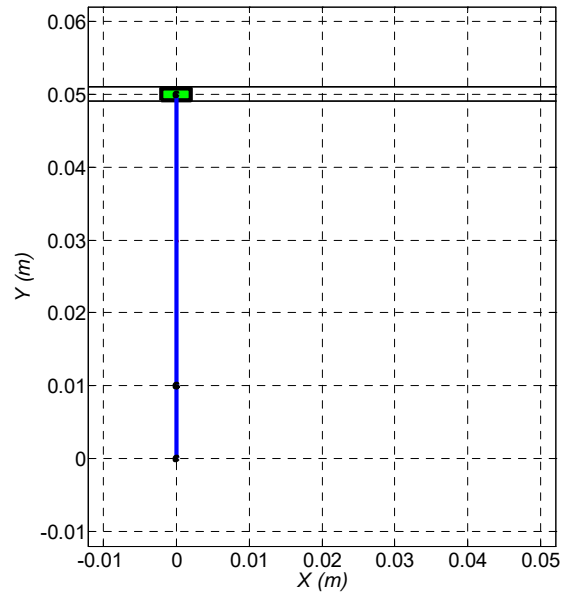
These equations are easily derived by drawing the limiting cases, drawing the applicable right triangles, and using geometry and trigonometry relationships.

In this example, the minimum slider displacement is $x_{\min} = -0.032$ m, which occurs at the maximum input angle joint limit $\theta_{2\max} = 139.6^\circ$, and the maximum slider displacement is $x_{\max} = 0.045$ m, which occurs at the minimum input angle joint limit $\theta_{2\min} = 41.8^\circ$. Note that x_{\max} and its corresponding input angle is identical to the previous example, as derived in the general equations.

$$\underline{h = r_2 + r_3}$$

This case yields a degenerate slider-crank mechanism as shown below, i.e. it is a structure with no motion that can only assemble at $\theta_2 = \frac{\pi}{2}$. Zero motion is allowed for the input link and the slider.

In this example, $r_2 = 1, r_3 = 4, h = 5$ cm.



$$\underline{r_2 = r_3}$$

Also, $h = 0$. At first this case appears to behave as a standard slider-crank mechanism, with:

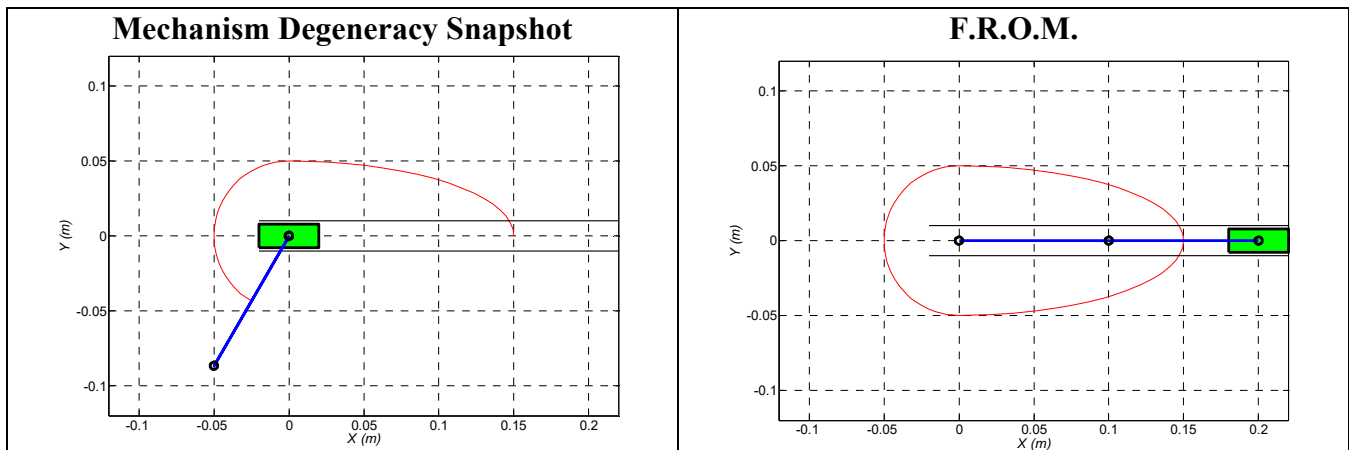
$$x_{\max} = r_2 + r_3 \quad \text{at} \quad \theta_2 = 0$$

However, the minimum slider displacement is 0, which occurs for a large range of input angle:

$$x_{\min} = 0 \quad \text{for} \quad 90^\circ \leq \theta_2 \leq 270^\circ$$

That is, we have a degenerate slider-crank mechanism for half the input angle range, $90^\circ \leq \theta_2 \leq 270^\circ$, where links 2 and 3 align completely as shown in a sample snapshot on the left below.

In this example, $r_2 = r_3 = 10$, $h = 0$, and $r_{CA} = 5$ cm.



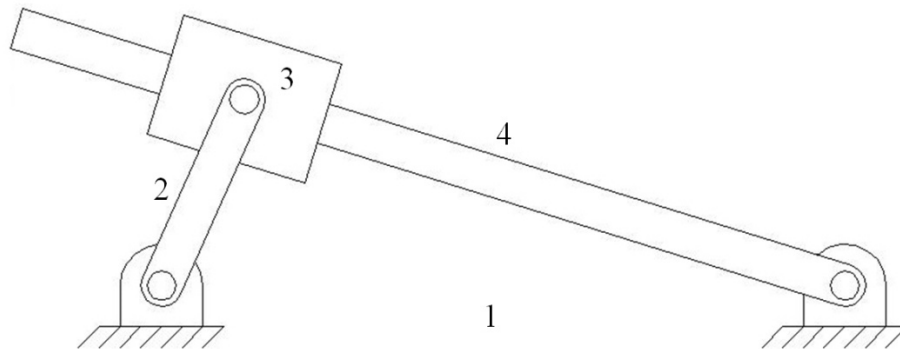
Slider-Crank Mechanism design irregularities summary

In general, the engineer should avoid all these four strange and fascinating cases in design for high-speed slider-crank mechanisms. Possible exceptions: toys or statics-dominated mechanisms such as window-closing mechanisms.

2.3 Inverted Slider-Crank Mechanism Position Analysis

This slider-crank mechanism inversion 2 is an inversion of the standard zero-offset slider-crank mechanism where the sliding direction is no longer the ground link, but along the rotating link 4. Ground link length r_1 and input link length r_2 are fixed; r_4 is a variable. The slider link 3 is attached to the end of link 2 via an R joint and slides relative to link 4 via a P joint. This mechanism converts rotary input to linear motion and rotary motion output. Practical applications include certain doors/windows opening/damping mechanisms. The inverted slider-crank is also part of quick-return mechanisms.

Step 1. Draw the Kinematic Diagram



r_1 constant ground link length
 r_2 constant input link length
 r_4 variable output link length

θ_2 variable input angle
 θ_4 variable output angle
 L_4 constant total output link length

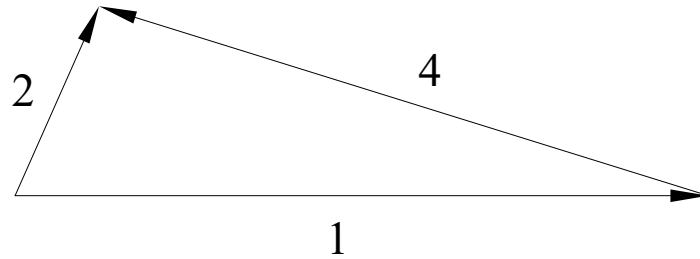
Link 1 is the fixed ground link. Without loss of generality we may force the ground link to be horizontal. If it is not so in the real world, merely rotate the entire inverted slider-crank mechanism so it is horizontal. Both angles θ_2 and θ_4 are measured in a right-hand sense from the horizontal to the link.

Step 2. State the Problem

Given $r_1, \theta_1 = 0, r_2$; plus 1-dof position input θ_2

Find r_4 and θ_4

Step 3. Draw the **Vector Diagram**. Define all angles in a positive sense, measured with the right hand from the right horizontal to the link vector (tail-to-head; your right-hand thumb is located at the vector tail).



Step 4. Derive the **Vector-Loop-Closure Equation**. Starting at one point, add vectors tail-to-head until you reach a second point. Write the VLCE by starting and ending at the same points, but choosing a different path.

$$r_2 = r_1 + r_4$$

Step 5. Write the **XY Components** for the Vector-Loop-Closure Equation. Separate the one vector equation into its two X and Y scalar components.

$$\begin{aligned} r_2 c_2 &= r_1 + r_4 c_4 \\ r_2 s_2 &= r_4 s_4 \end{aligned}$$

Step 6. Solve for the Unknowns from the XY equations. There are two coupled nonlinear equations in the two unknowns r_4 , θ_4 . Unlike the standard slider-crank mechanism, there is no decoupling of X and Y . However, unlike the four-bar mechanism, there is only one unknown angle so the solution is easier than the four-bar mechanism. First rewrite the above XY equations to isolate the unknowns on one side.

$$\begin{aligned} r_4 c_4 &= r_2 c_2 - r_1 \\ r_4 s_4 &= r_2 s_2 \end{aligned}$$

A ratio of the Y to X equations will cancel r_4 and solve for θ_4 .

$$\frac{r_4 s_4}{r_4 c_4} = \frac{r_2 s_2}{r_2 c_2 - r_1}$$

$$\theta_4 = \text{atan2}(r_2 s_2, r_2 c_2 - r_1)$$

Then square and add the XY equations to eliminate θ_4 and solve for r_4 .

$$r_4 = +\sqrt{r_1^2 + r_2^2 - 2r_1 r_2 c_2}$$

Note the same r_4 formula results from the **cosine law**. Alternatively, the same r_4 can be solved from either the X or Y equations after θ_4 is known.

$$X) \quad r_4 = \frac{r_2 c_2 - r_1}{c_4} \qquad Y) \quad r_4 = \frac{r_2 s_2}{s_4}$$

Both of these r_4 alternatives are valid; however, each is subject to a different artificial mathematical singularity ($\theta_4 = \pm 90^\circ$ and $\theta_4 = 0, 180^\circ$, respectively), so only the former square-root formula should be used for r_4 , which has no artificial singularity. The X algorithmic singularity $\theta_4 = \pm 90^\circ$ never occurs unless $r_2 > r_1$, which is to be avoided (see below), but the Y algorithmic singularity occurs twice per full range of motion.

Technically there are two solution sets – the one above and $r_4 = -\sqrt{r_1^2 + r_2^2 - 2r_1 r_2 c_2}$, $\theta_4 + \pi$. However, the negative r_4 is not practical and so only the one solution set (branch) exists, unlike most planar mechanisms with two or more branches.

Full-rotation condition

For the inverted slider-crank mechanism to rotate fully, the fixed length of link 4, L_4 , must be greater than the maximum value of the variable r_4 .

Slider Limits

The slider reaches its minimum and maximum displacements when $\theta_2 = 0$ and π , respectively. Therefore, the slider limits are $r_1 - r_2 \leq r_4 \leq r_1 + r_2$. Thus, the fixed length L_4 must be greater than $r_1 + r_2$. In addition we require $r_1 > r_2$ for full rotation.

Graphical Solution

The Inverted Slider-Crank mechanism position analysis may be solved *graphically*, by drawing the mechanism, determining the mechanism closure, and measuring the unknowns. This is an excellent method to validate your computer results at a given snapshot.

- Draw the known ground link (points O_2 and O_4 separated by r_1 at the fixed angle $\theta_1 = 0$).
- Draw the given input link length r_2 at the given angle θ_2 (this defines point A).
- Draw a line from O_4 to point A .
- Measure the unknown values of r_4 and θ_4 .

Inverted Slider-Crank Mechanism Position Analysis: Term Example 3

Given:

$$r_1 = 0.20$$

$$r_2 = 0.10$$

$$L_4 = 0.32 \text{ m}$$

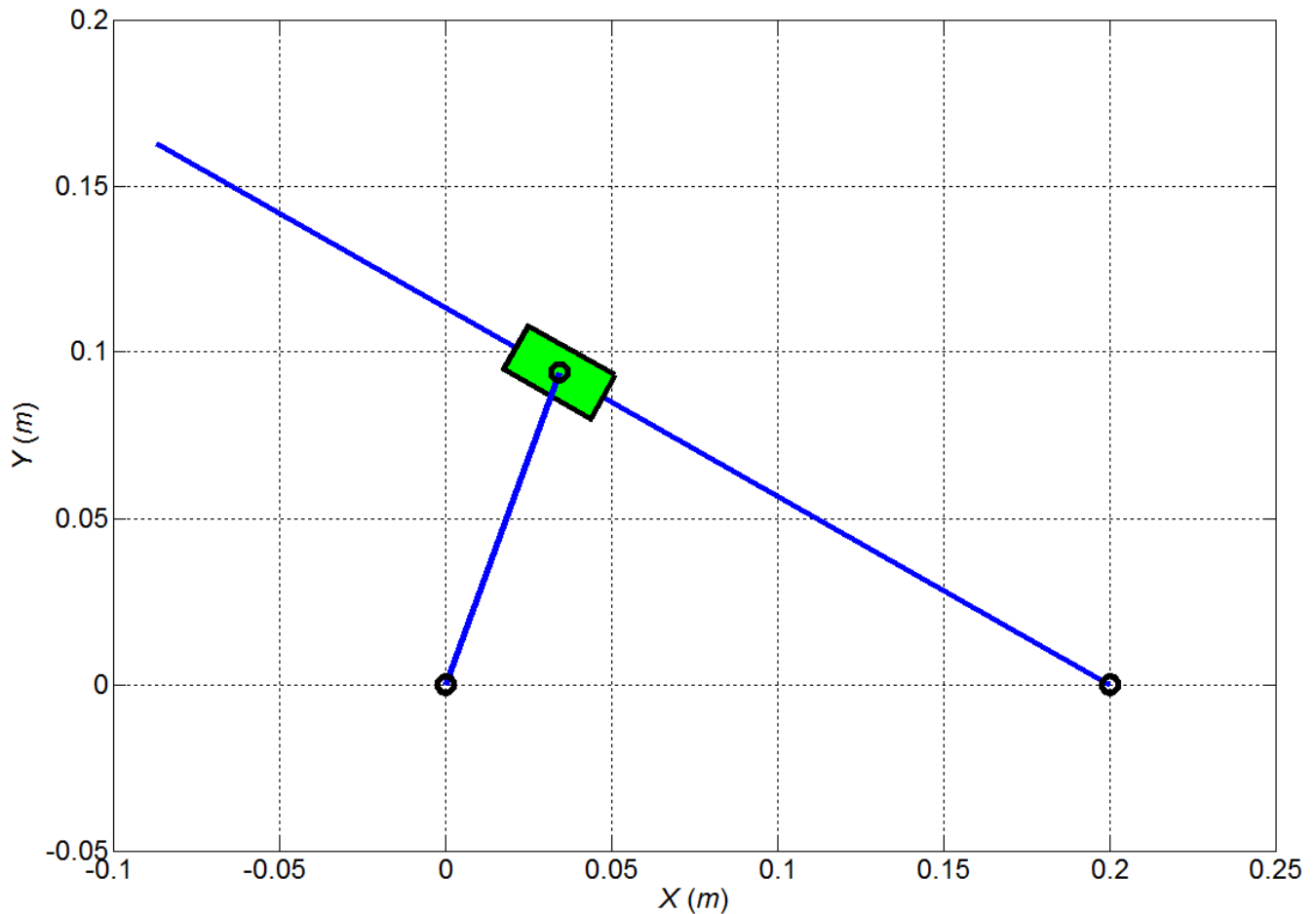
$$\theta_1 = 0^\circ$$

Snapshot Analysis (one input angle)

Given this mechanism and $\theta_2 = 70^\circ$, calculate θ_4 and r_4 .

θ_4 (deg)	r_4 (m)
150.5	0.191

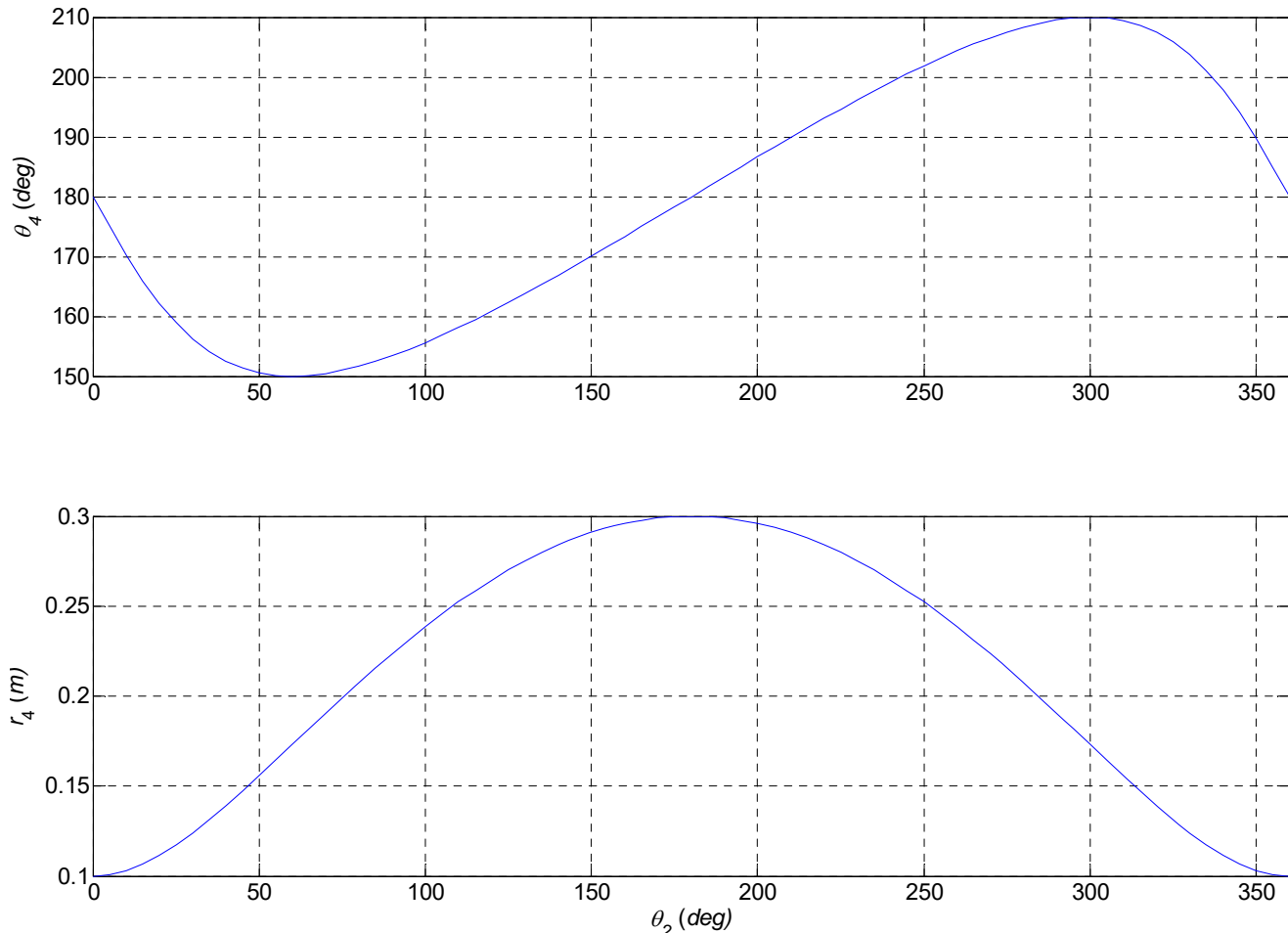
This Term Example 3 position solution is demonstrated in the figure below.



Term Example 3 Position Snapshot

Full-Range-Of-Motion (F.R.O.M.) Analysis: Term Example 3

A more meaningful result from position analysis is to report the position analysis unknowns for the entire range of mechanism motion. The subplots below gives r_4 (m) and θ_4 (deg), for all $0^\circ \leq \theta_2 \leq 360^\circ$, for Term Example 3.



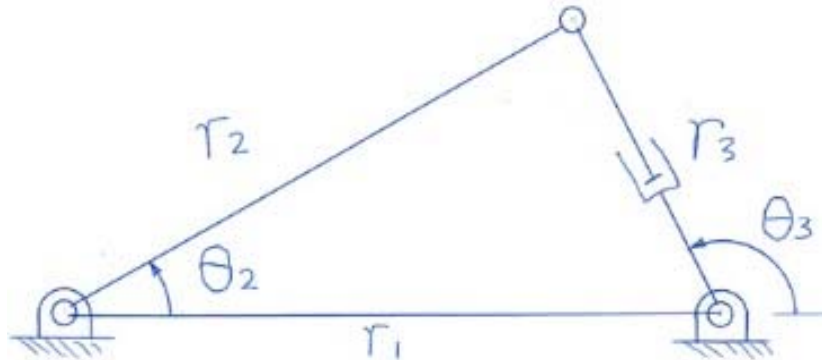
Term Example 3 θ_4 and r_4

θ_4 varies symmetrically about 180° , being 180° at $\theta_2 = 0, 180, 360^\circ$. r_4 varies like a negative cosine function with minimum displacement $r_1 - r_2 = 0.1$ at $\theta_2 = 0, 360^\circ$ and maximum displacement $r_1 + r_2 = 0.3$. Since r_1 is twice r_2 in this example, whenever $\theta_2 = 60, 300^\circ$, a perfect $30^\circ - 60^\circ - 90^\circ$ triangle is formed; the relative angle between links 2 and 4 is 90° which corresponds to the max and min of $\theta_4 = 150, 210^\circ$, respectively. At these special points, $r_4 = (\sqrt{3}/2)0.2 = 0.173$ m.

There is another right triangle that shows up for $\theta_2 = \pm 90^\circ$; in these cases $r_4 = \sqrt{0.2^2 + 0.1^2} = 0.224$ m and $\theta_4 = 153.4, 206.6^\circ$, respectively. Check all of these special values in the F.R.O.M. plot results.

Alternate Inversion-2 Slider Crank Mechanism with r_3 Input

In this subsection we solve the position kinematics for an alternate second-inversion slider-crank mechanism. In this case link 2 is no longer the input, so θ_2 is no longer given. Instead, the input is a length, called r_3 , the total variable length between the R joints at the end of link 2 and also at the end of the ground link. This mechanism is used in dump trucks and foot-operated bicycle pumps. As seen in the figure below, this mechanism position analysis requires the intersection of two circles, which the 4-bar mechanism also required. Given r_1 and r_2 (plus $\theta_1 = 0$), and input length r_3 , find θ_2 and θ_3 .



The Vector Loop-Closure Equation is:

$$\mathbf{r}_2 = \mathbf{r}_1 + \mathbf{r}_3$$

Length r_3 is given, but angles θ_2 and θ_3 are unknown. The X and Y scalar component equations are:

$$\begin{aligned} r_2 c_2 &= r_1 + r_3 c_3 \\ r_2 s_2 &= r_3 s_3 \end{aligned}$$

These are two coupled nonlinear equations in the two unknowns θ_2 and θ_3 . Unlike the standard slider-crank mechanism, there is no decoupling of X and Y. However, unlike the four-bar mechanism, there are less terms so the solution is easier than the four-bar mechanism. The above XY equations already have unknown θ_2 isolated. Now square and add the XY equations to eliminate θ_2 and solve for θ_3 .

$$\begin{aligned} r_2^2 c_2^2 &= r_1^2 + r_3^2 c_3^2 + 2r_1 r_3 c_3 \\ r_2^2 s_2^2 &= r_3^2 s_3^2 \end{aligned}$$

$$r_2^2 (c_2^2 + s_2^2) = r_1^2 + r_3^2 (c_3^2 + s_3^2) + 2r_1 r_3 c_3$$

$$r_2^2 = r_1^2 + r_3^2 + 2r_1 r_3 c_3$$

$$\theta_3 = \cos^{-1} \left[\frac{r_2^2 - r_1^2 - r_3^2}{2r_1 r_3} \right]$$

What about trigonometric uncertainty? These mechanisms are generally designed to work only in one branch, often the + one; so just take the primary inverse cosine solution and the secondary one (negative) will not be admissible. To finish the solution,

$$\theta_2 = \sin^{-1} \left[\frac{r_3 s_3}{r_2} \right]$$

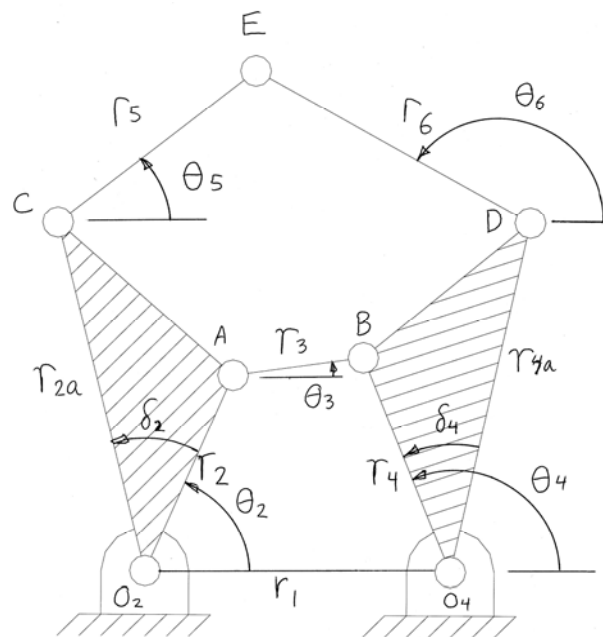
where we must substitute the value of θ_3 solved above. Again, trigonometric uncertainty is not a problem; just take the primary inverse sine solution. Certainly, you should validate the correct branch is obtained by a graphical solution.

2.4 Multi-Loop Mechanism Position Analysis

Thus far we have presented position analysis for the single-loop four-bar, slider-crank, and inverted slider-crank mechanisms. The position analysis for mechanisms of more than one loop is handled using the same general procedures developed for the single loop mechanisms. A good rule of thumb is to look for four-bar (or slider-crank) parts of the multi-loop mechanism as we already know how to solve the complete position analyses for these.

This section presents position analysis for the two-loop Stephenson I six-bar mechanism shown below as an example multi-loop mechanism. This is one of the five possible six-bar mechanisms shown in Dr. Bob's on-line Atlas of Structures, Mechanisms, and Robots:

ohio.edu/mechanical-faculty/williams/html/PDF/MechanismAtlas.pdf



Stephenson I 6-Bar Mechanism

We immediately see that the bottom loop of the Stephenson I six-bar mechanism is identical to our standard four-bar mechanism model. Since we number the links the same as in the four-bar, and if we define the angles identically, the position analysis solution is identical to the four-bar presented earlier. With the complete position analysis of the bottom loop thus solved, we see that points C and D can be easily calculated. Then the solution for the top loop is essentially another four-bar solution: graphically, the circle of radius r_5 about point C must intersect the circle of radius r_6 about point D to form point E (yielding two possible intersections in general). The analytical solution is very similar to the standard four-bar position solution, as we will show.

For multi-loop mechanisms, the number of solution branches for position analysis increases compared to the single-loop mechanisms. Most single-loop mechanisms mathematically have two solution branches. For multi-loop mechanisms composed of multiple single-loop mechanisms, the number of solution branches is 2^n , where n is the number of mechanism loops. For the two-loop Stephenson I six-bar mechanism, the number of solution branches for the position analysis problem is 4, two from the standard four-bar part, and two for each of these branches from the upper loop.

Now let us solve the position analysis problem for the two-loop Stephenson I six-bar mechanism using the formal position analysis steps presented earlier. Assume link 2 is the input link.

Step 1. Draw the Kinematic Diagram this is done in the figure above.

r_1	constant ground link length	θ_1	constant ground link angle
r_2	constant input link length to point A	θ_2	variable input link angle
r_{2a}	constant input link length to point C	δ_2	constant angle on link 2
r_3	constant coupler link length, loop I	θ_3	variable coupler link angle, loop I
r_4	constant output link length, loop I	θ_4	variable output link angle, loop I
r_{4a}	constant input link length to point D	δ_4	constant angle on link 4
r_5	constant coupler link length, loop II	θ_5	variable coupler link angle, loop II
r_6	constant output link length, loop II	θ_6	variable output link angle, loop II

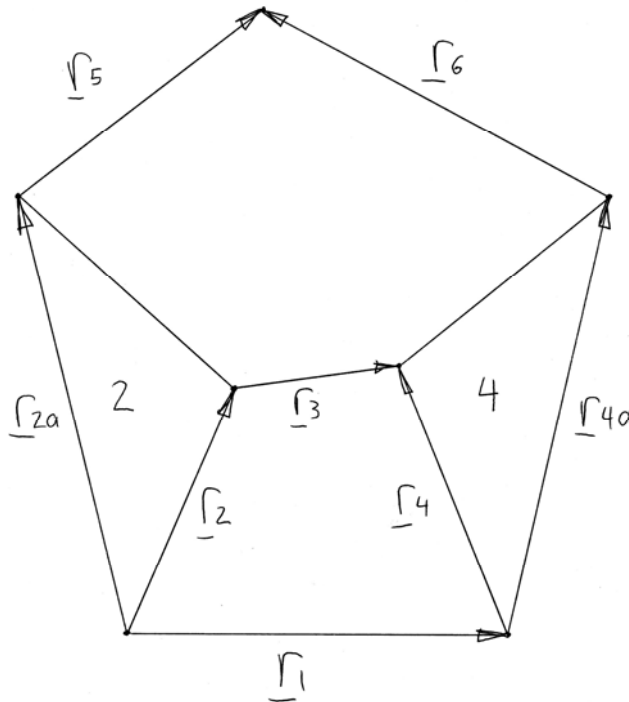
As usual, all angles are measured in a right-hand sense from the absolute horizontal to the link, as shown in the kinematic diagram.

Step 2. State the Problem

Given $r_1, \theta_1, r_2, r_3, r_4, r_{2a}, r_{4a}, r_5, r_6, \delta_2, \delta_4$; plus 1-dof position input θ_2

Find $\theta_3, \theta_4, \theta_5, \theta_6$

Step 3. Draw the Vector Diagram. Define all angles in a positive sense, measured with the right hand from the right horizontal to the link vector (tail-to-head with the right-hand thumb at the vector tail and right-hand fingers towards the arrow in the vector diagram below).



Step 4. Derive the Vector-Loop-Closure Equations. One VLCE is required for each mechanism loop. Start at one point, add vectors tail-to-head until you reach a second point. Write each vector equation by starting and ending at the same points, but choosing a different path.

$$\underline{r}_2 + \underline{r}_3 = \underline{r}_1 + \underline{r}_4$$

$$\underline{r}_{2a} + \underline{r}_5 = \underline{r}_1 + \underline{r}_{4a} + \underline{r}_6$$

Note an alternative to the second vector loop equation is $\underline{r}_{2b} + \underline{r}_5 = \underline{r}_3 + \underline{r}_{4b} + \underline{r}_6$. See if you can identify \underline{r}_{2b} and \underline{r}_{4b} , plus their angles θ_{2b} and θ_{4b} .

Step 5. Write the XY Components for each Vector-Loop-Closure Equation. Separate the two vector equations into four XY scalar component equations.

$$r_2 c_2 + r_3 c_3 = r_1 c_1 + r_4 c_4$$

$$r_2 s_2 + r_3 s_3 = r_1 s_1 + r_4 s_4$$

$$r_{2a} c_{2a} + r_5 c_5 = r_1 c_1 + r_{4a} c_{4a} + r_6 c_6$$

$$r_{2a} s_{2a} + r_5 s_5 = r_1 s_1 + r_{4a} s_{4a} + r_6 s_6$$

where

$$\theta_{2a} = \theta_2 + \delta_2$$

$$\theta_{4a} = \theta_4 - \delta_4$$

Step 6. Solve for the Unknowns from the four XY Equations. The four coupled nonlinear equations in the four unknowns $\theta_3, \theta_4, \theta_5, \theta_6$ can be solved in two stages, one for each mechanism loop.

Loop I. This solution is identical to the standard four-bar mechanism solution for θ_3, θ_4 , summarized here from earlier. From the first two XY scalar equations above, isolate θ_3 terms, square and add both equations to obtain one equation in one unknown θ_4 . This equation has the form $E \cos \theta_4 + F \sin \theta_4 + G = 0$, where terms E, F , and G are known functions of constants and the input angle θ_2 . Solve this equation for two possible values of θ_4 using the tangent half-angle substitution. The two θ_4 values correspond to the open and crossed branches. Then return to the original XY scalar equations with θ_3 terms isolated, divide the Y by the X equations, and solve for θ_3 using the **atan2** function, substituting the solved values for θ_4 . One unique θ_3 will result for each of the two possible θ_4 values.

Loop II. The method is analogous to the Loop I solution above. Since θ_4 is now known, we also know $\theta_{4a} = \theta_4 - \delta_4$. From the second two XY scalar equations above, isolate θ_5 terms, square and add both equations to obtain one equation in one unknown θ_6 . This equation is of the form $E_2 \cos \theta_6 + F_2 \sin \theta_6 + G_2 = 0$, where terms E_2, F_2 , and G_2 are known functions of constants and the known angles $\theta_{2a} = \theta_2 + \delta_2$ and $\theta_{4a} = \theta_4 - \delta_4$. Solve this equation for two possible values of θ_6 using the tangent

half-angle substitution. The two θ_6 values correspond to open and crossed branches, for each of the Loop I open and crossed branches. Then return to the original XY scalar equations with θ_5 terms isolated, divide the Y by the X equations, and solve for θ_5 using the **atan2** function, substituting the solved values for θ_6 . One unique θ_5 will result for each of the two possible θ_6 values from each θ_4 .

Branches. There are two θ_5 , θ_6 branches for each of the two θ_3 , θ_4 branches, so there are four overall mechanism branches for the two-loop Stephenson I six-bar mechanism.

Full-rotation condition

The range of motion of a multi-loop mechanism may be more limited than that of single-loop mechanisms. One can perform a compound Grashof analysis when four-bars are the component mechanisms. For the two-loop Stephenson I six-bar mechanism, the second loop may constrain the first loop (e.g. it may change an expected crank motion of the input link to a rocker). This is an important issue in design of multi-loop mechanisms if the input link must still rotate fully.

Graphical Solution

The two-loop Stephenson I six-bar mechanism position analysis may readily be solved *graphically*, by drawing the mechanism, determining the mechanism closure, and measuring the unknowns. This is an excellent method to validate your computer results at a given snapshot.

Loop I (this part is identical to the standard four-bar graphical solution)

- Draw the known ground link (points O_2 and O_4 separated by r_1 at the fixed angle θ_1).
- Draw the given input link length r_2 at the given angle θ_2 to yield point A .
- Draw a circle of radius r_3 , centered at point A .
- Draw a circle of radius r_4 , centered at point O_4 .
- These circles intersect in general in two places to yield two possible points B .
- Connect the two branches and measure the unknown angles θ_3 and θ_4 .

Loop II (this part is a modification of the standard four-bar graphical solution). Start with the end of the procedure above, on the same drawing. For each solution branch above, perform the following steps.

- Draw the link r_{2a} at angle $\theta_{2a} = \theta_2 + \delta_2$ from point O_2 .
- Draw the link r_{4a} at angle $\theta_{4a} = \theta_4 - \delta_4$ from point O_4 .
- Draw a circle of radius r_5 , centered at point C .
- Draw a circle of radius r_6 , centered at point D .
- These circles intersect in general in two places to yield two possible points E .
- Connect the two branches and measure the unknown values θ_5 and θ_6 .

In general, there are four overall position solution branches.

3. Velocity Kinematics Analysis

3.1 Velocity Analysis Introduction

Here are a couple of fun scalar velocity problems involving average speed, time, and distance to get started with.

1. A cyclist travels uphill at a constant speed of 20 kph for 30 min; then the cyclist travels downhill at a constant speed of 60 kph for the next 30 min. What is the cyclist's average speed for this motion?

Solution:

$$\begin{array}{l} \text{uphill:} \quad 20 \text{ kph} \times 0.5 \text{ hr} = 10 \text{ km} \\ \text{downhill:} \quad 60 \text{ kph} \times 0.5 \text{ hr} = 30 \text{ km} \\ \text{total:} \quad 40 \text{ km} \div 1 \text{ hr} = 40 \text{ kph} \end{array}$$

This answer is obvious, no? (i.e. the simple average of 20 and 60 kph) But how does the problem change if the distances are the same for both portions of the motion, rather than the times being the same as above?

2. A cyclist travels uphill at a constant speed of 20 kph for 10 km; then the cyclist travels downhill at a constant speed of 60 kph for the next 10 km. What is the cyclist's average speed for this motion?

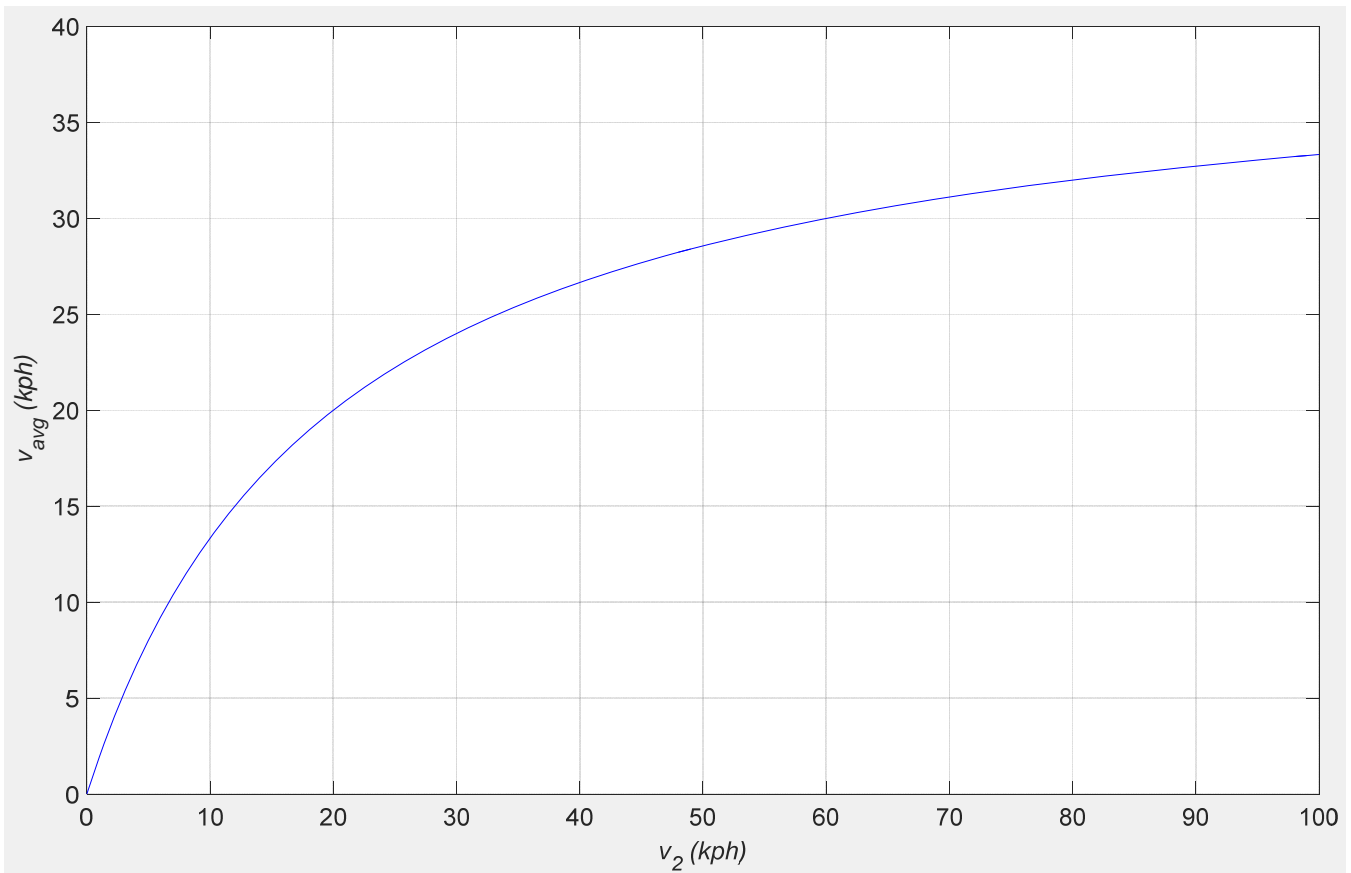
Solution:

$$\begin{array}{l} \text{uphill:} \quad 10 \text{ km} \times \frac{\text{hr}}{20 \text{ km}} = \frac{1}{2} \text{ hr} \\ \text{downhill:} \quad 10 \text{ km} \times \frac{\text{hr}}{60 \text{ km}} = \frac{1}{6} \text{ hr} \\ \text{total:} \quad 20 \text{ km} \div \frac{2}{3} \text{ hr} = 30 \text{ kph} \end{array}$$

So the cyclist travels slower than the simple average when the distances are the same for both portions of the motion, rather than the times being the same. This phenomenon is called the **Harmonic Mean of Velocity**. The Harmonic Mean of a set of numbers is the inverse of the simple average of the inverse numbers of that set. For our second example, if a distance is covered at speed v_1 and the same distance is then covered at speed v_2 , the Harmonic Mean applies to calculate average speed:

$$v_{avg} = \frac{n}{\frac{1}{v_1} + \frac{1}{v_2} + \dots + \frac{1}{v_n}} \qquad v_{avg} = \frac{2}{\frac{1}{v_1} + \frac{1}{v_2}} = \frac{2v_1v_2}{v_1 + v_2}$$

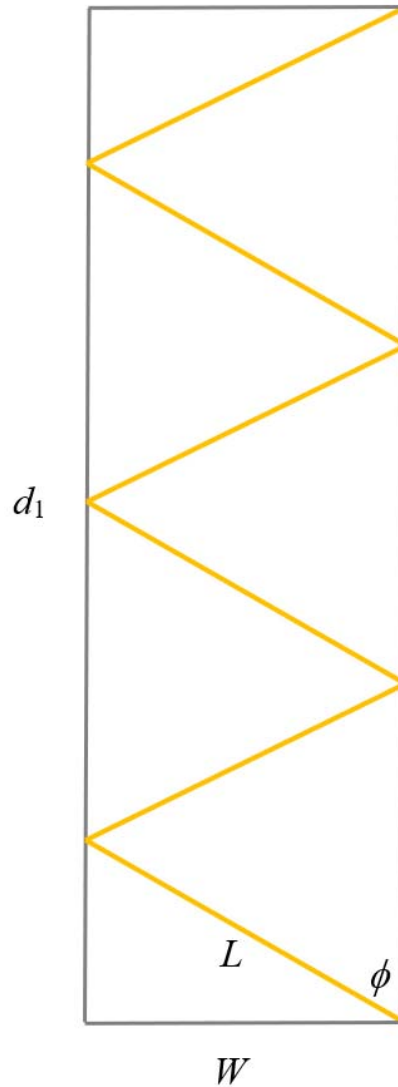
For the numerical example:
$$v_{avg} = \frac{2(20)(60)}{20 + 60} = 30 \text{ kph}$$



The plot above shows the average speed v_{avg} for various downhill speeds v_2 in this Example 2. The numerical result of this example is visible on this graph (i.e. $v_{avg} = 30$ kph for $v_2 = 60$ kph). We see that an average speed of 40 kph, as in Example 1, would be out of reach for any real human cyclist (off the graph). In fact, the downhill speed for average speed of 40 kph would have to be $v_2 = \infty$!! (Why?)

Cyclist Zig-Zagging Uphill

Often when there is not much traffic, a cyclist will zig-zag up a steep hill in order to reduce strain and increase speed. However, more distance is required, so while the uphill speed will be increased, will time actually be saved? Then we can add a downhill leg with the Harmonic Mean of Velocity, as introduced in the previous section. Will the overall average speed increased or decreased by zig-zagging? The current model is intended to investigate this problem and answer some of these questions. The zig-zagging parameters are shown in the figure below.



Parameters for a Cyclist Zig-Zagging Uphill

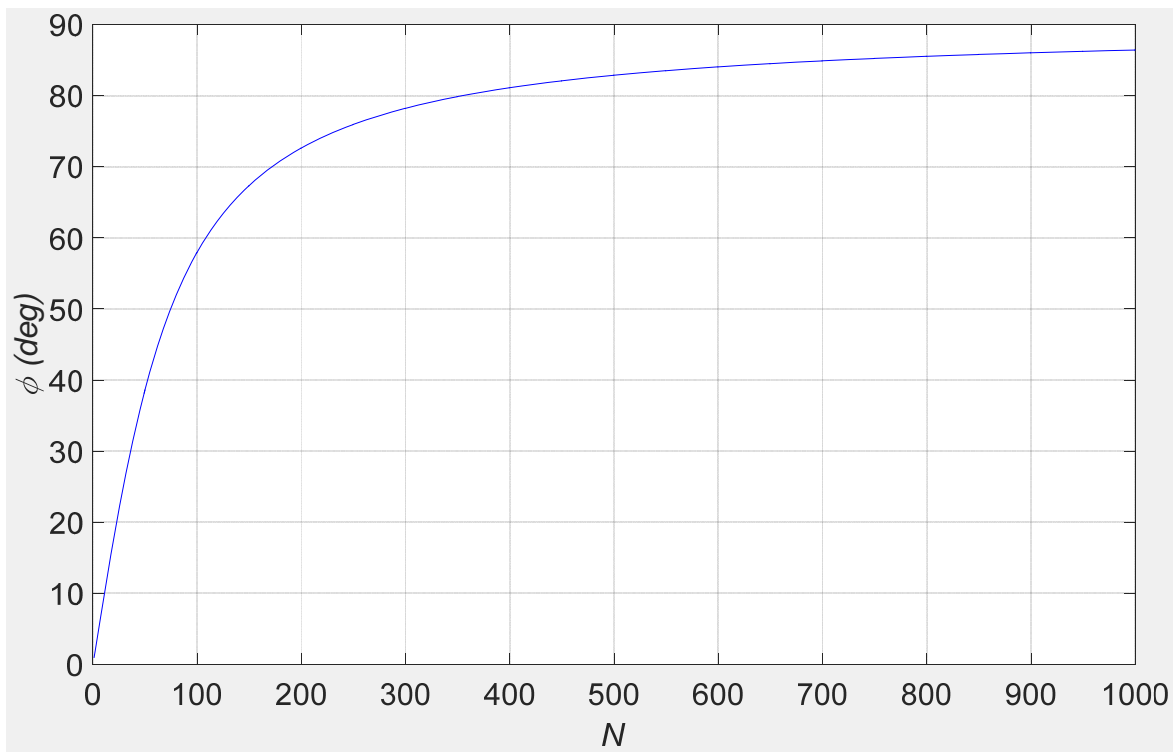
Assumptions and relationships:

- The hill has a constant uphill grade.
- The road is perfectly straight.
- The road is a standard 2-lane highway with a width of $W = 8$ m.
- The distance travelled on one zig or zag across the road is L .
- The uphill distance is $d_1 = 1$ km. The total distance travelled while zig-zagging is $d_1^* = 2NL > d_1$. The distance travelled straight along the road on one zig-zag is $D_1 = d_1/N$.
- The cyclist maintains a constant uphill speed v_1 (despite continually turning sharp corners!).
- There are no interruptions due to pesky traffic.
- The cyclist must divide the hill into a perfect N sections for zig-zagging.
- v_1 represents the straight-uphill speed and v_1^* represents the uphill speed with zig-zagging. $v_1 < v_1^*$

First, to eliminate one variable with infinite possibilities, let us determine the angle of zig-zagging ϕ to ensure the cyclist divides the hill into N perfect sections, as in the penultimate assumption. As shown in the figure, angle ϕ is measured from the road direction to the direction of the cyclist's heading when zig-zagging. From geometry we have:

$$\phi = \tan^{-1} \left[\frac{2NW}{d_1} \right] = \tan^{-1}(0.016N)$$

That is, the possible zig-zagging angles are a function of N ; the possibilities are plotted below. This graph really should be plotted as a bar graph, since we can only choose integer values of N . When N is 0, this is associated with no zig-zagging (straight up the hill), so the angle ϕ should be 0 as shown. At the opposite extreme, for large integers dividing the hill, the angle approaches $\phi = 90^\circ$. Of course, if the angle is exactly $\phi = 90^\circ$, the cyclist will go nowhere uphill, but the zig-zag becomes a perfect horizontal back-and-forth. Arguably an angle near $\phi = 45^\circ$ would be a good choice balancing these two extremes. Let us tabulate a few values in that region.

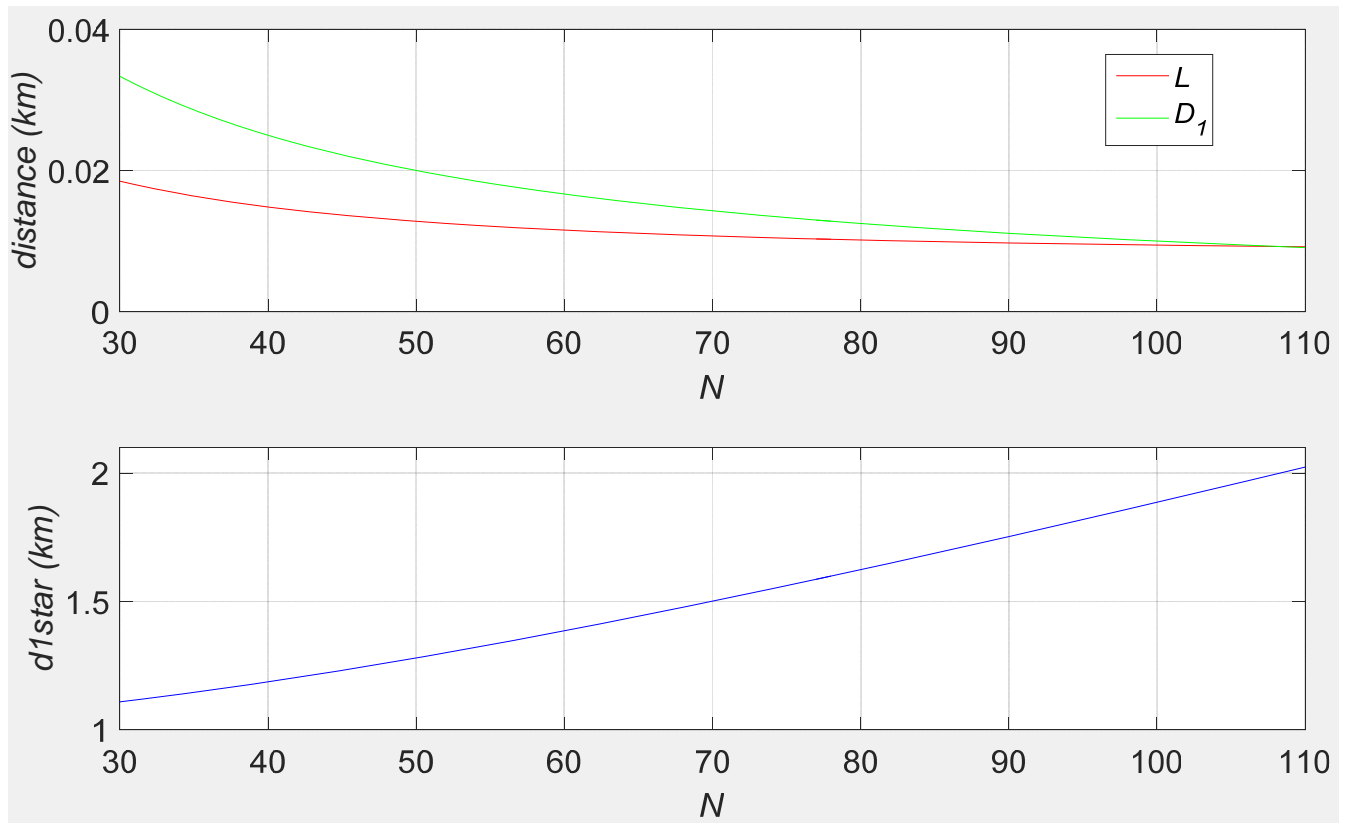


N	ϕ
61	44.3°
62	44.8°
63	45.2°
64	45.7°

For further study in this problem, let us use:

N	ϕ
36	29.9°
62	44.8°
108	59.9°

Why? No special reason, other than the human need to force nice angles (essentially 30°, 45°, 60°). The plots below show some of the other important kinematic parameters (L, D_1, d_1^*), in this zone of interest.



The L and D_1 curves cross near $N = 108$ (because this is closest to $\phi = 60^\circ$). The d_1^* curve reveals that the actual distance travelled doubles at $N = 108$ ($\phi = 60^\circ$).

Now let's a little more Harmonic Mean of Velocity fun, adding a downhill leg 2. Here are some additional assumptions, added to the previous assumptions:

- The hill has a constant downhill grade
- The road is perfectly straight.
- The downhill distance is $d_2 = 1$ km .
- The cyclist maintains a constant downhill speed $v_2 = 50$ kph .

The speed/distance relationships are:

$$d_1 = v_1 t_1 \qquad d_1^* = v_1^* t_1^* \qquad d_2 = v_2 t_2$$

where 1 indicates uphill and 2 indicates downhill. Again, the asterisk notation indicates the uphill zig-zagging. The average speed for the entire uphill and downhill 2 km trip is:

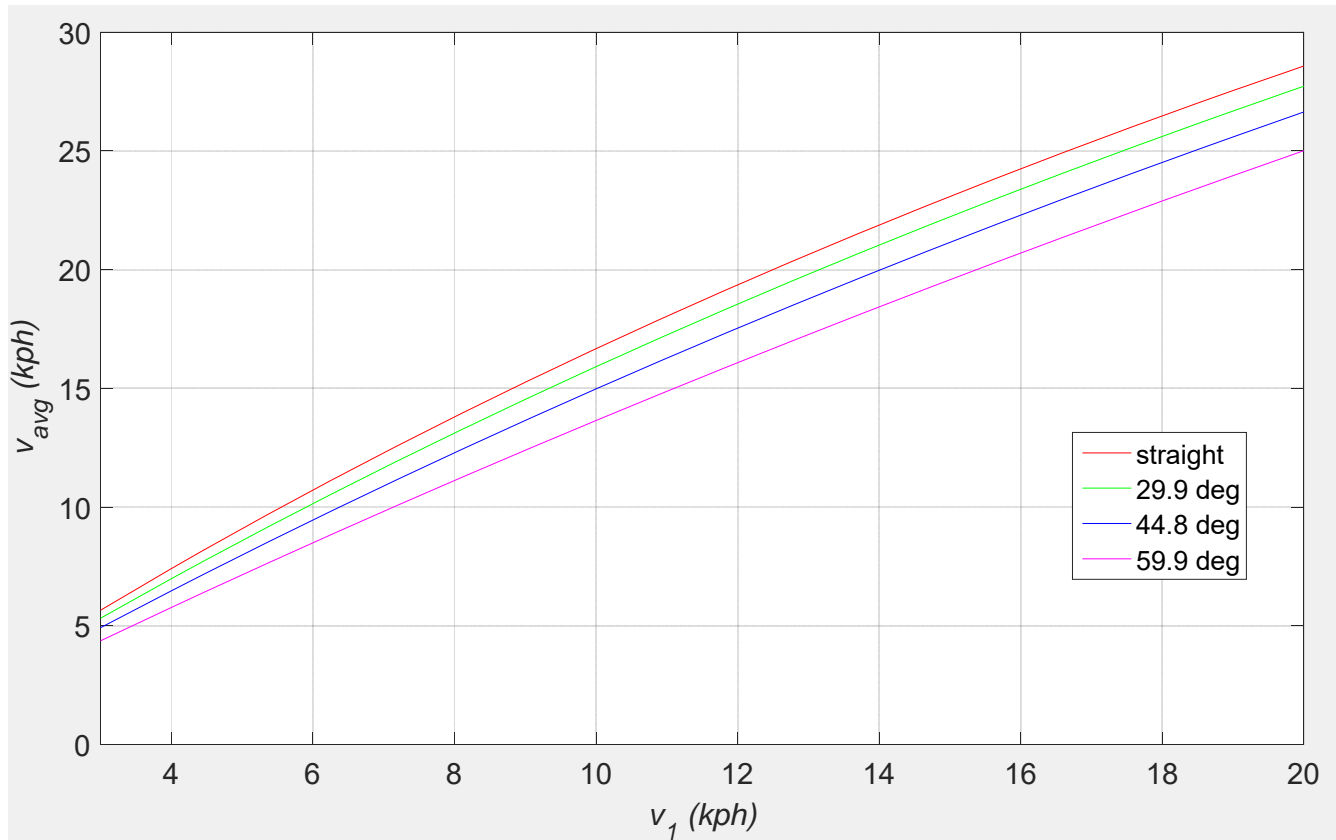
$$v_{avg} = \frac{d_1 + d_2}{t_1 + t_2} \qquad v_{avg}^* = \frac{d_1^* + d_2}{t_1^* + t_2}$$

Substituting the above relationships and simplifying yields:

$$v_{avg} = \frac{(d_1 + d_2)v_1}{d_1 + \frac{d_2 v_1}{v_2}}$$

$$v_{avg}^* = \frac{(d_1^* + d_2)v_1^*}{d_1^* + \frac{d_2 v_1^*}{v_2}}$$

We now plot the average speed results, with v_1 (and v_1^*) as the independent variable, for the three zig-zag angle values closest to $30^\circ, 45^\circ, 60^\circ$.



At first glance it appears that riding straight uphill is preferred, because that leads to the highest average speed for a given v_1 .

However, that ignores the fact that $v_1 < v_1^*$, since zig-zagging leads to a smaller effective slope and hence a faster speed. Looking at $v_1^* = 12$ kph for $\phi = 59.9^\circ$, the same v_{avg} can be reached by the other angle conditions by drawing an horizontal line to the left and projecting down to read the required v_1 for that case. This results (approximately) in average speeds of 12, 10.5, 9.75, and 8.5 kph, respectively.

In reality, that line would be rotated down from horizontal, for example passing through the magenta curve at 12 kph and the red curve at 6 kph.

To determine the optimal zig-zag angle ϕ would require knowledge of the function relating slope and uphill speed, which is not known, and hence not included in this analysis.

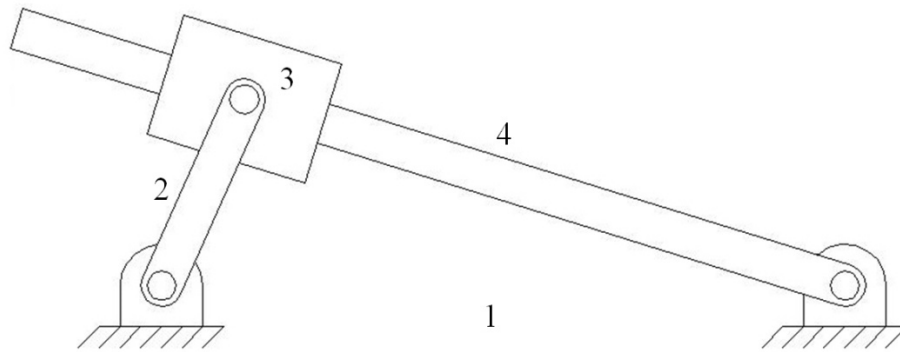
3.5 Inverted Slider-Crank Mechanism Velocity Analysis

Again, link 2 (the crank) is the input and link 4 is the output. Remember r_4 is a variable so $\dot{r}_4 \neq 0$ in this problem.

Step 1. The inverted slider-crank mechanism **Position Analysis** must first be complete.

Given r_1 , $\theta_1 = 0$, r_2 , and θ_2 , we solved for r_4 and θ_4

Step 2. Draw the inverted slider-crank mechanism **Velocity Diagram**.



where ω_i ($i = 2, 4$) is the absolute angular velocity of link i . \dot{r}_4 is the slider velocity along link 4. $\omega_3 = \omega_4$ since the slider cannot rotate relative to link 4.

Step 3. State the Problem

Given the mechanism r_1 , $\theta_1 = 0$, r_2

the position analysis θ_2 , r_4 , θ_4

1-dof of velocity input ω_2

Find the velocity unknowns \dot{r}_4 and ω_4

Step 4. Derive the velocity equations. Take the first time derivative of the vector loop closure equations from position analysis, in XY component form.

Here are the inverted slider-crank mechanism position equations from earlier.

$$\underline{r}_2 = \underline{r}_1 + \underline{r}_4$$

$$r_2 c_2 = r_1 + r_4 c_4$$

$$r_2 s_2 = r_4 s_4$$

The first time derivative of the position equations is given below.

$$-r_2 \omega_2 s_2 = \dot{r}_4 c_4 - r_4 \omega_4 s_4$$

$$r_2 \omega_2 c_2 = \dot{r}_4 s_4 + r_4 \omega_4 c_4$$

These two linear equations in two unknowns can be written in matrix form.

$$\begin{bmatrix} c_4 & -r_4 s_4 \\ s_4 & r_4 c_4 \end{bmatrix} \begin{Bmatrix} \dot{r}_4 \\ \omega_4 \end{Bmatrix} = \begin{Bmatrix} -r_2 \omega_2 s_2 \\ r_2 \omega_2 c_2 \end{Bmatrix}$$

Step 5. Solve the velocity equations for the unknowns \dot{r}_4, ω_4 .

$$\begin{Bmatrix} \dot{r}_4 \\ \omega_4 \end{Bmatrix} = \frac{1}{r_4} \begin{bmatrix} r_4 c_4 & r_4 s_4 \\ -s_4 & c_4 \end{bmatrix} \begin{Bmatrix} -r_2 \omega_2 s_2 \\ r_2 \omega_2 c_2 \end{Bmatrix} = \begin{Bmatrix} \frac{r_2 \omega_2 (-s_2 c_4 + c_2 s_4)}{r_4} \\ \frac{r_2 \omega_2 (s_2 s_4 + c_2 c_4)}{r_4} \end{Bmatrix}$$

$$\begin{Bmatrix} \dot{r}_4 \\ \omega_4 \end{Bmatrix} = \begin{Bmatrix} \frac{r_2 \omega_2 \sin(\theta_4 - \theta_2)}{r_4} \\ \frac{r_2 \omega_2 \cos(\theta_4 - \theta_2)}{r_4} \end{Bmatrix}$$

where we have used the trigonometric identities:

$$\cos(a \pm b) = \cos a \cos b \mp \sin a \sin b$$

$$\sin(a \pm b) = \sin a \cos b \pm \cos a \sin b$$

$$\sin(-a) = -\sin(a)$$

$$\cos(-a) = \cos(a)$$

The units are all correct in the solution above, m/s and rad/s , respectively.

Inverted slider-crank mechanism singularity condition

When does the solution fail? This is an inverted slider-crank mechanism singularity, when the determinant of the coefficient matrix goes to zero. The result is dividing by zero, resulting in infinite \dot{r}_4, ω_4 .

$$[A] = \begin{bmatrix} c_4 & -r_4 s_4 \\ s_4 & r_4 c_4 \end{bmatrix}$$

$$|A| = r_4 c_4^2 - (-r_4 s_4^2) = r_4 (c_4^2 + s_4^2) = r_4 = 0$$

Physically, assuming $r_1 > r_2$ as in the full rotation condition from the inverted slider-crank mechanism position analysis, this is impossible, i.e. r_4 never goes to zero.

This matrix determinant $|A| = r_4$ was used in the solution of the previous page.

Inverted slider-crank mechanism velocity example – Term Example 3 continued

Given

$$\begin{array}{ll} r_1 = 0.20 & \theta_2 = 70^\circ \\ r_2 = 0.10 & \theta_4 = 150.5^\circ \quad (\text{deg and } m) \\ L_4 = 0.32 \text{ (m)} & r_4 = 0.191 \\ \theta_1 = 0^\circ & \end{array}$$

Snapshot Analysis

Given this mechanism position analysis plus $\omega_2 = 25 \text{ rad/s}$, calculate \dot{r}_4, ω_4 for this snapshot.

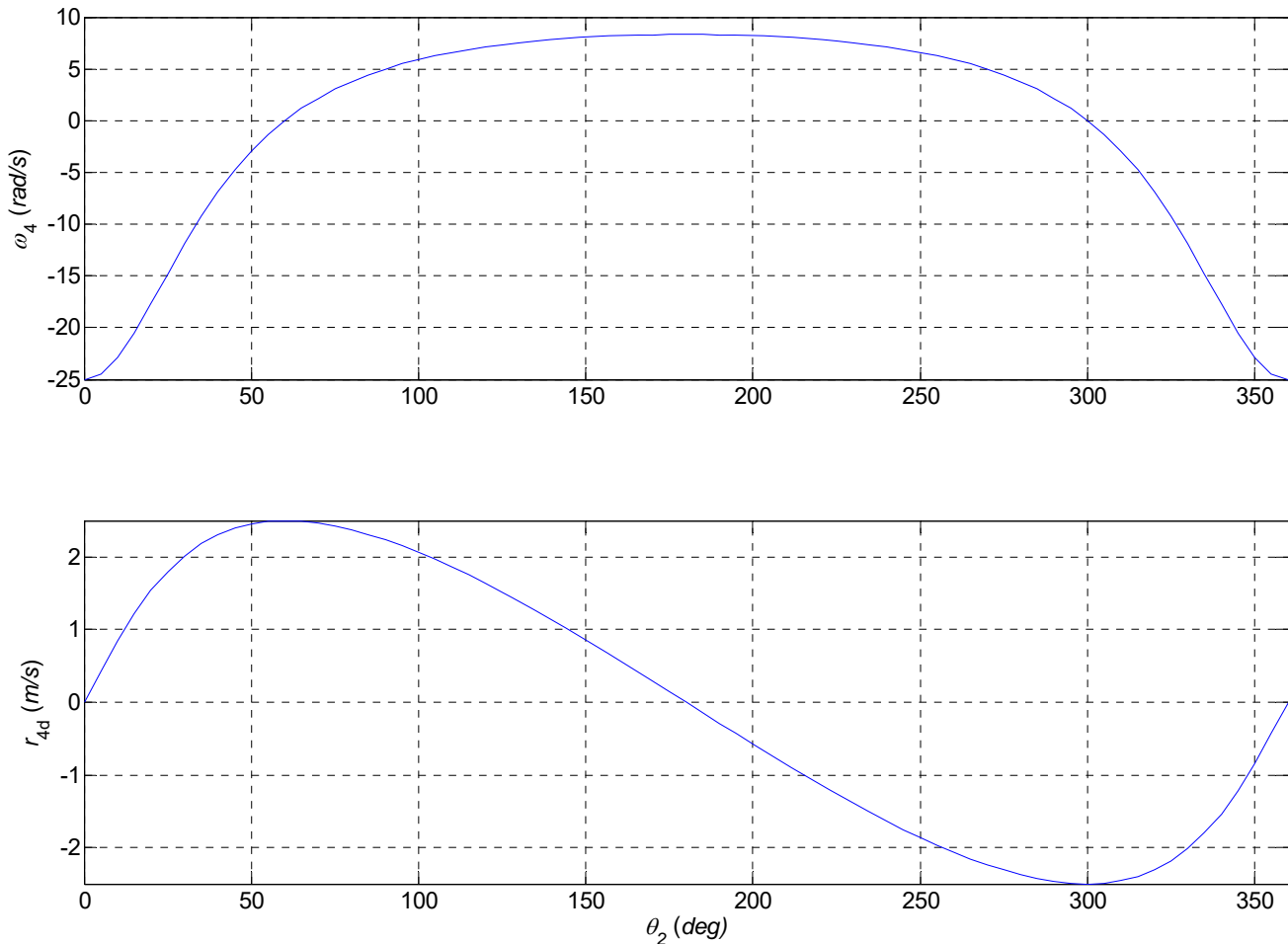
$$\begin{bmatrix} -0.870 & -0.094 \\ 0.493 & -0.166 \end{bmatrix} \begin{Bmatrix} \dot{r}_4 \\ \omega_4 \end{Bmatrix} = \begin{Bmatrix} -2.349 \\ 0.855 \end{Bmatrix}$$

$$\begin{Bmatrix} \dot{r}_4 \\ \omega_4 \end{Bmatrix} = \begin{Bmatrix} 2.47 \\ 2.18 \end{Bmatrix} \quad (\text{m/s and rad/s})$$

Both are positive, so the slider link 3 is currently traveling up link 4 and link 4 is currently rotating in the ccw direction, which makes sense from the physical problem.

Full-Range-Of-Motion (F.R.O.M.) Analysis – Term Example 3 continued

A more meaningful result from velocity analysis is to report the velocity analysis results for the entire range of mechanism motion. The subplot below gives ω_4 (top, *rad/s*) and \dot{r}_4 (bottom, *m/s*), for all $0^\circ \leq \theta_2 \leq 360^\circ$, for Term Example 3. Since ω_2 is constant, we can plot the velocity results vs. θ_2 (since it is related to time t via $\theta_2 = \omega_2 t$).



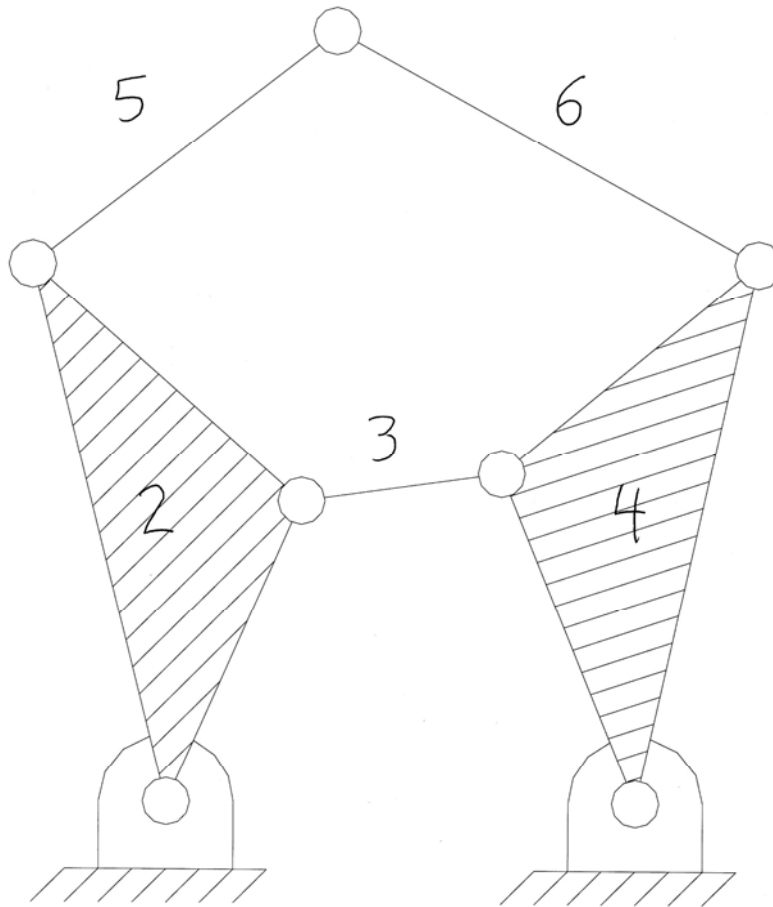
Term Example 3 F.R.O.M., ω_4 and \dot{r}_4

As expected, ω_4 is zero at the max and min for θ_4 (at $\theta_2 = \pm 60^\circ$); also, ω_4 has a large range of nearly constant positive velocity near the middle of motion – this can be seen in a MATLAB animation. \dot{r}_4 is zero at the beginning, middle, and end of motion and is max at $\theta_2 = \pm 60^\circ$.

3.6 Multi-Loop Mechanism Velocity Analysis

Thus far we have presented velocity analysis for the single-loop four-bar, slider-crank, and inverted slider-crank mechanisms. The velocity analysis for mechanisms of more than one loop is handled using the same general procedures developed for the single loop mechanisms.

This section presents velocity analysis for the two-loop Stephenson I six-bar mechanism shown below as an example multi-loop mechanism. It follows the position analysis for the same mechanism presented earlier.



Stephenson I 6-Bar Mechanism

The bottom loop of the Stephenson I six-bar mechanism is identical to the standard four-bar mechanism model and so the velocity analysis solution is identical to the four-bar presented earlier. With the complete velocity analysis of the bottom loop thus solved, the solution for the top loop is essentially another four-bar velocity solution.

As in all velocity analysis, the velocity solution for multi-loop mechanisms is a linear analysis yielding a unique solution (assuming the given mechanism position is not singular) for each position solution branch considered. The position analysis must be complete prior to the velocity solution.

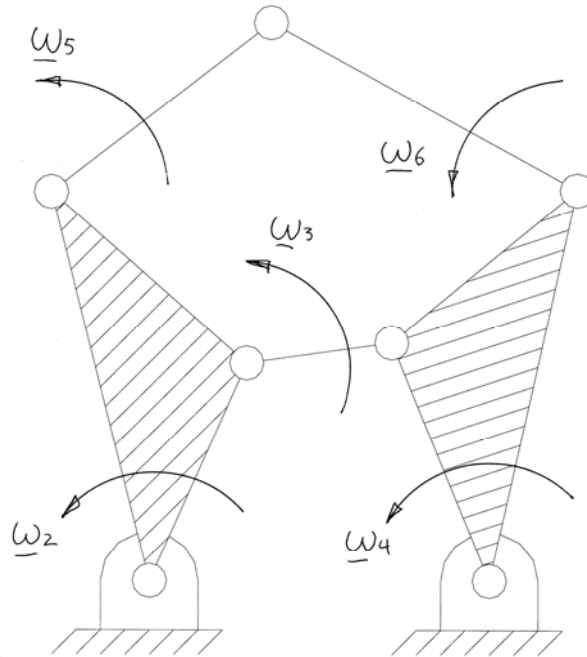
Now let us solve the velocity analysis problem for the two-loop Stephenson I six-bar mechanism using the formal velocity analysis steps presented earlier. Again, assume link 2 is the input link.

Step 1. The Stephenson I six-bar mechanism **Position Analysis** must first be complete.

Given $r_1, \theta_1, r_2, r_3, r_4, r_{2a}, r_{4a}, r_5, r_6, \delta_2, \delta_4,$ and θ_2 we solved for $\theta_3, \theta_4, \theta_5, \theta_6$.

Step 2. Draw the Stephenson I six-bar mechanism **Velocity Diagram**.

This should include all the information from the position diagram, plus the new velocity information. For clarity, we show only the new velocity information here. Refer to the previous Stephenson I position kinematics diagram for complete information.



where ω_i ($i = 2,3,4,5,6$) is the absolute angular velocity of link i . Triangular links 2 and 4 each have a single angular velocity for the whole link. $\dot{r}_i = 0$ for all links since all links are of fixed length (no sliders).

Step 3. State the Problem

Given the mechanism $r_1, \theta_1, r_2, r_3, r_4, r_{2a}, r_{4a}, r_5, r_6, \delta_2, \delta_4,$

the position analysis $\theta_2, \theta_3, \theta_4, \theta_5, \theta_6,$

1-dof velocity input ω_2

Find the velocity unknowns $\omega_3, \omega_4, \omega_5, \omega_6$

Step 4. Derive the velocity equations. Take the first time derivative of each of the two vector loop closure equations from position analysis, in XY component form.

Here are the Stephenson I six-bar mechanism position equations.

Vector equations

$$\underline{r}_2 + \underline{r}_3 = \underline{r}_1 + \underline{r}_4$$

$$\underline{r}_{2a} + \underline{r}_5 = \underline{r}_1 + \underline{r}_{4a} + \underline{r}_6$$

XY scalar equations

$$r_2 c_2 + r_3 c_3 = r_1 c_1 + r_4 c_4$$

$$r_2 s_2 + r_3 s_3 = r_1 s_1 + r_4 s_4$$

$$r_{2a} c_{2a} + r_5 c_5 = r_1 c_1 + r_{4a} c_{4a} + r_6 c_6$$

$$r_{2a} s_{2a} + r_5 s_5 = r_1 s_1 + r_{4a} s_{4a} + r_6 s_6$$

where

$$\theta_{2a} = \theta_2 + \delta_2$$

$$\theta_{4a} = \theta_4 - \delta_4$$

The first time derivatives of the Loop I position equations are identical to those for the standard four-bar mechanism.

$$-r_2 \omega_2 s_2 - r_3 \omega_3 s_3 = -r_4 \omega_4 s_4$$

$$r_2 \omega_2 c_2 + r_3 \omega_3 c_3 = r_4 \omega_4 c_4$$

These equations can be written in matrix form.

$$\begin{bmatrix} r_3 s_3 & -r_4 s_4 \\ -r_3 c_3 & r_4 c_4 \end{bmatrix} \begin{Bmatrix} \omega_3 \\ \omega_4 \end{Bmatrix} = \begin{Bmatrix} -r_2 \omega_2 s_2 \\ r_2 \omega_2 c_2 \end{Bmatrix}$$

The first time derivative of the Loop II position equations is

$$-r_{2a} \omega_{2a} s_{2a} - r_5 \omega_5 s_5 = -r_{4a} \omega_{4a} s_{4a} - r_6 \omega_6 s_6$$

$$r_{2a} \omega_{2a} c_{2a} + r_5 \omega_5 c_5 = r_{4a} \omega_{4a} c_{4a} + r_6 \omega_6 c_6$$

These equations can be written in matrix form.

$$\begin{bmatrix} r_5 s_5 & -r_6 s_6 \\ -r_5 c_5 & r_6 c_6 \end{bmatrix} \begin{Bmatrix} \omega_5 \\ \omega_6 \end{Bmatrix} = \begin{Bmatrix} -r_{2a} \omega_{2a} s_{2a} + r_{4a} \omega_{4a} s_{4a} \\ r_{2a} \omega_{2a} c_{2a} - r_{4a} \omega_{4a} c_{4a} \end{Bmatrix}$$

where we have used $\omega_{2a} = \omega_2$ since δ_2 and δ_4 are constant angles.
 $\omega_{4a} = \omega_4$

Step 5. Solve the velocity equations for the unknowns ω_3 , ω_4 , ω_5 , ω_6 .

The two mechanism loops decouple so we find ω_3 and ω_4 from Loop I first and then use ω_4 to find ω_5 and ω_6 from Loop II. The solutions are given below.

Loop I (identical to the standard four-bar mechanism)

$$\begin{Bmatrix} \omega_3 \\ \omega_4 \end{Bmatrix} = \begin{bmatrix} r_3 s_3 & -r_4 s_4 \\ -r_3 c_3 & r_4 c_4 \end{bmatrix}^{-1} \begin{Bmatrix} -r_2 \omega_2 s_2 \\ r_2 \omega_2 c_2 \end{Bmatrix}$$

Loop II (similar to the standard four-bar mechanism)

$$\begin{Bmatrix} \omega_5 \\ \omega_6 \end{Bmatrix} = \begin{bmatrix} r_5 s_5 & -r_6 s_6 \\ -r_5 c_5 & r_6 c_6 \end{bmatrix}^{-1} \begin{Bmatrix} -r_{2a} \omega_2 s_{2a} + r_{4a} \omega_4 s_{4a} \\ r_{2a} \omega_2 c_{2a} - r_{4a} \omega_4 c_{4a} \end{Bmatrix}$$

Remember, Gaussian elimination is more efficient and robust than the matrix inverse. Also, these equations may be solved algebraically instead of using matrix methods to yield the same answers.

Stephenson I six-bar mechanism singularity condition

The velocity solution fails when the determinant of either coefficient matrix above goes to zero. The result is dividing by zero, resulting in infinite angular velocities for the associated loop.

For the first loop, the singularity condition is identical to the singularity condition of the standard four-bar mechanism, i.e. when links 3 and 4 either line up or fold upon each other, causing a link 2 joint limit. For the second loop, the singularity condition is similar, occurring when links 5 and 6 either line up or fold upon each other. These conditions also cause angle limit problems for the position analysis, so the velocity singularities are known problems.

4. Acceleration Kinematics Analysis

4.2 Five-Part Acceleration Formula

We can derive the Five-Part Acceleration Formula using vectors and vector derivation. In order to do this we need the **Transport Theorem** (for kinematics, not the Reynolds Transport Theorem from fluid mechanics). The Transport Theorem states that to take the time derivative of a vector in a rotating coordinate frame, we must take the time derivative of the vector within the frame, and then add ω cross the original vector, where ω is the angular velocity vector of the rotating frame. The kinematic diagram for the 4-dof moving link with sliding collar is identical to that in the ME 3011 NotesBook, Section 4.2.

Below the use of the **Transport Theorem** is highlighted in **RED** font.

Two-Part Position Formula:

$$\underline{P}_p = \underline{P}_0 + \underline{L}$$

Three-Part Velocity Formula:

$$\underline{V}_p = \frac{d}{dt}(\underline{P}_0 + \underline{L})$$

$$\underline{V}_p = \underline{V}_0 + \underline{V} + \underline{\omega} \times \underline{L}$$

Five-Part Acceleration Formula:

$$\underline{A}_p = \frac{d}{dt}(\underline{V}_0 + \underline{V} + \underline{\omega} \times \underline{L})$$

$$\underline{A}_p = \underline{A}_0 + \underline{A} + \underline{\omega} \times \underline{V} + \underline{\alpha} \times \underline{L} + \underline{\omega} \times \dot{\underline{L}}$$

$$\underline{A}_p = \underline{A}_0 + \underline{A} + \underline{\omega} \times \underline{V} + \underline{\alpha} \times \underline{L} + \underline{\omega} \times (\underline{V} + \underline{\omega} \times \underline{L})$$

$$\underline{A}_p = \underline{A}_0 + \underline{A} + 2\underline{\omega} \times \underline{V} + \underline{\alpha} \times \underline{L} + \underline{\omega} \times (\underline{\omega} \times \underline{L})$$

We can carry on this example to one more time derivative to find the vector jerk expression.

Eight-Part Jerk Formula:

$$\underline{J}_p = \frac{d}{dt}(\underline{A}_0 + \underline{A} + 2\underline{\omega} \times \underline{V} + \underline{\alpha} \times \underline{L} + \underline{\omega} \times (\underline{\omega} \times \underline{L}))$$

$$\underline{J}_p = \underline{J}_0 + \underline{J} + \underline{\omega} \times \underline{A} + 2\underline{\alpha} \times \underline{V} + 2\underline{\omega} \times \dot{\underline{V}} + \underline{\beta} \times \underline{L} + \underline{\alpha} \times \dot{\underline{L}} + \underline{\alpha} \times (\underline{\omega} \times \underline{L}) + \underline{\omega} \times (\underline{\alpha} \times \underline{L}) + \underline{\omega} \times (\underline{\omega} \times \dot{\underline{L}})$$

$$\underline{J}_p = \underline{J}_0 + \underline{J} + \underline{\omega} \times \underline{A} + 2\underline{\alpha} \times \underline{V} + 2\underline{\omega} \times (\underline{A} + \underline{\omega} \times \underline{V}) + \underline{\beta} \times \underline{L} + \underline{\alpha} \times (\underline{V} + \underline{\omega} \times \underline{L}) + 2\underline{\omega} \times (\underline{\alpha} \times \underline{L}) + \underline{\omega} \times (\underline{\omega} \times (\underline{V} + \underline{\omega} \times \underline{L}))$$

$$\underline{J}_p = \underline{J}_0 + \underline{J} + 3\underline{\omega} \times \underline{A} + 3\underline{\alpha} \times \underline{V} + 3\underline{\omega} \times (\underline{\omega} \times \underline{V}) + \underline{\beta} \times \underline{L} + 3\underline{\omega} \times (\underline{\alpha} \times \underline{L}) + \underline{\omega} \times (\underline{\omega} \times (\underline{\omega} \times \underline{L}))$$

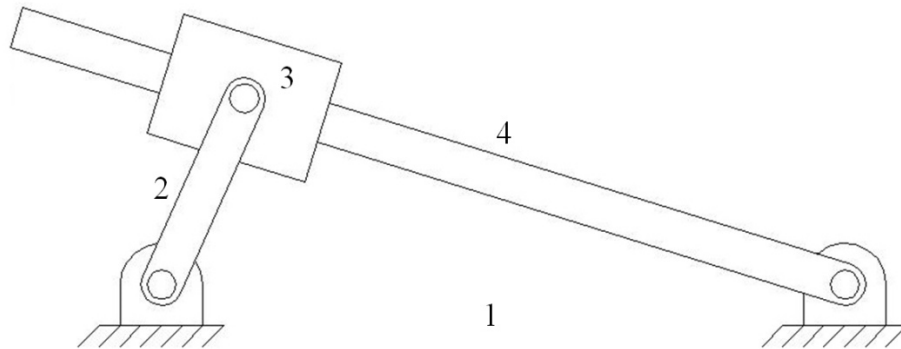
4.5 Inverted Slider-Crank Mechanism Acceleration Analysis

Again, link 2 (the crank) is the input and link 4 is the output.

Step 1. The inverted slider-crank mechanism **Position and Velocity Analyses** must first be complete.

Given r_1 , $\theta_1 = 0$, r_2 , and θ_2 we solved for r_4 and θ_4 ; then given ω_2 we solved for \dot{r}_4 and ω_4 .

Step 2. Draw the inverted slider-crank mechanism **Acceleration Diagram**.



where $\underline{\alpha}_i$ ($i = 2,4$) is the absolute angular acceleration of link i . \ddot{r}_4 is the slider acceleration along link 4. $\underline{\alpha}_3 = \underline{\alpha}_4$ since the slider cannot rotate relative to link 4.

Step 3. State the Problem

Given the mechanism r_1 , $\theta_1 = 0$, r_2
 the position analysis θ_2 , r_4 , θ_4
 the velocity analysis ω_2 , \dot{r}_4 , ω_4
 1-dof acceleration input α_2

Find the acceleration unknowns \ddot{r}_4 and α_4

Step 4. Derive the acceleration equations. Take the first time derivative of the inverted slider-crank mechanism velocity equations from velocity analysis, in XY component form.

Here are the inverted slider-crank mechanism velocity equations.

$$\begin{aligned}\dot{r}_4 c_4 - r_4 \omega_4 s_4 &= -r_2 \omega_2 s_2 \\ \dot{r}_4 s_4 + r_4 \omega_4 c_4 &= r_2 \omega_2 c_2\end{aligned}$$

The first time derivative of the velocity equations is given below.

$$\begin{aligned}\ddot{r}_4 c_4 - 2\dot{r}_4 \omega_4 s_4 - r_4 \alpha_4 s_4 - r_4 \omega_4^2 c_4 &= -r_2 \alpha_2 s_2 - r_2 \omega_2^2 c_2 \\ \ddot{r}_4 s_4 + 2\dot{r}_4 \omega_4 c_4 + r_4 \alpha_4 c_4 - r_4 \omega_4^2 s_4 &= r_2 \alpha_2 c_2 - r_2 \omega_2^2 s_2\end{aligned}$$

These equations can be written in matrix form.

$$\begin{bmatrix} c_4 & -r_4 s_4 \\ s_4 & r_4 c_4 \end{bmatrix} \begin{Bmatrix} \ddot{r}_4 \\ \alpha_4 \end{Bmatrix} = \begin{Bmatrix} -r_2 \alpha_2 s_2 - r_2 \omega_2^2 c_2 + 2\dot{r}_4 \omega_4 s_4 + r_4 \omega_4^2 c_4 \\ r_2 \alpha_2 c_2 - r_2 \omega_2^2 s_2 - 2\dot{r}_4 \omega_4 c_4 + r_4 \omega_4^2 s_4 \end{Bmatrix}$$

Step 5. Solve the acceleration equations for the unknowns \ddot{r}_4, α_4 .

$$\begin{Bmatrix} \ddot{r}_4 \\ \alpha_4 \end{Bmatrix} = \frac{1}{r_4} \begin{bmatrix} r_4 c_4 & r_4 s_4 \\ -s_4 & c_4 \end{bmatrix} \begin{Bmatrix} -r_2 \alpha_2 s_2 - r_2 \omega_2^2 c_2 + 2\dot{r}_4 \omega_4 s_4 + r_4 \omega_4^2 c_4 \\ r_2 \alpha_2 c_2 - r_2 \omega_2^2 s_2 - 2\dot{r}_4 \omega_4 c_4 + r_4 \omega_4^2 s_4 \end{Bmatrix}$$

$$\begin{Bmatrix} \ddot{r}_4 \\ \alpha_4 \end{Bmatrix} = \begin{Bmatrix} \frac{r_2 \alpha_2 \sin(\theta_4 - \theta_2) - r_2 \omega_2^2 \cos(\theta_4 - \theta_2) + r_4 \omega_4^2}{r_4} \\ \frac{r_2 \alpha_2 \cos(\theta_4 - \theta_2) + r_2 \omega_2^2 \sin(\theta_4 - \theta_2) - 2\dot{r}_4 \omega_4}{r_4} \end{Bmatrix}$$

where we have again used the trigonometric identities:

$$\begin{aligned}\cos(a \pm b) &= \cos a \cos b \mp \sin a \sin b & \sin(-a) &= -\sin(a) \\ \sin(a \pm b) &= \sin a \cos b \pm \cos a \sin b & \cos(-a) &= \cos(a)\end{aligned}$$

A major amount of algebra and trigonometry is required to get the final analytical solution for \ddot{r}_4, α_4 above. Interestingly, the link 4 Coriolis term $2\dot{r}_4 \omega_4$ cancelled in \ddot{r}_4 while the link 4 centripetal term $r_4 \omega_4^2$ cancelled in α_4 . The units are all correct, m/s^2 and rad/s^2 , respectively.

Inverted slider-crank mechanism singularity condition

The acceleration problem has the same coefficient matrix $[A]$ as the velocity problem, so the singularity condition is identical (see the singularity discussion in the inverted slider-crank mechanism velocity section – the only singularity is when r_4 goes to zero; this will never occur if $r_1 > r_2$).

Inverted slider-crank mechanism acceleration example – Term Example 3 continued

Given

$$\begin{array}{lll}
 r_1 = 0.20 & & \omega_2 = 25 \\
 r_2 = 0.10 & \theta_2 = 70^\circ & \\
 L_4 = 0.32 \text{ (m)} & \theta_4 = 150.5^\circ \text{ (deg and m)} & \dot{r}_4 = 2.47 \text{ (rad/s and m/s)} \\
 \theta_1 = 0^\circ & r_4 = 0.191 & \omega_4 = 2.18
 \end{array}$$

Snapshot Analysis

Given this mechanism position and velocity analyses, plus $\alpha_2 = 0 \text{ rad/s}^2$, calculate \ddot{r}_4, α_4 for this snapshot.

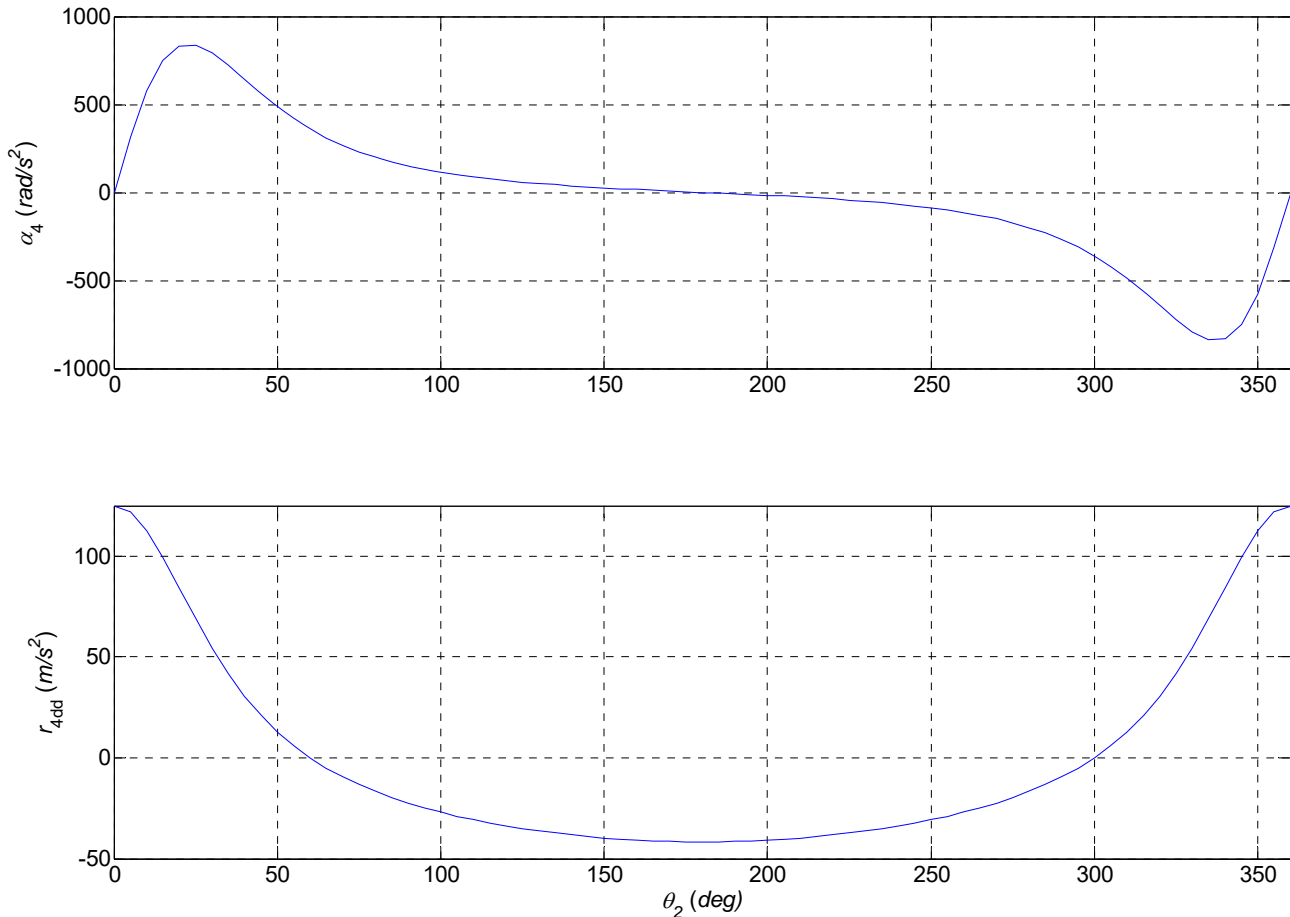
$$\begin{bmatrix} -0.870 & -0.094 \\ 0.493 & -0.166 \end{bmatrix} \begin{Bmatrix} \ddot{r}_4 \\ \alpha_4 \end{Bmatrix} = \begin{Bmatrix} -16.873 \\ -48.957 \end{Bmatrix}$$

$$\begin{Bmatrix} \ddot{r}_4 \\ \alpha_4 \end{Bmatrix} = \begin{Bmatrix} -9.46 \\ 267.14 \end{Bmatrix} \quad (\text{m/s}^2 \text{ and rad/s}^2)$$

\ddot{r}_4 is negative, so the slider link 3 is currently slowing down its positive velocity up link 4 and α_4 is positive, so the link 4 angular velocity is currently increasing in the *ccw* direction.

Full-Range-Of-Motion (F.R.O.M.) Analysis – Term Example 3 continued

A more meaningful result from acceleration analysis is to report the acceleration analysis results for the entire range of mechanism motion. The subplot below gives α_4 (top, rad/s^2) and \ddot{r}_4 (bottom, m/s^2), for all $0^\circ \leq \theta_2 \leq 360^\circ$, for Term Example 3. Again, since ω_2 is constant, we can plot the acceleration results vs. θ_2 (since it is related to time t via $\theta_2 = \omega_2 t$).



Term Example 3 F.R.O.M., α_4 and \ddot{r}_4

As expected, α_4 is zero at the beginning, middle, and end since the ω_4 curve flattens out at those points. The maximum (and minimum) α_4 values correspond to the greatest slopes for ω_4 . \ddot{r}_4 is maximum (and minimum) at the beginning, middle, and end since the \dot{r}_4 curve is steepest at those points; \ddot{r}_4 is zero when the \dot{r}_4 curve is flat, i.e. $\theta_2 = \pm 60^\circ$.

Derivative/Integral Relationships

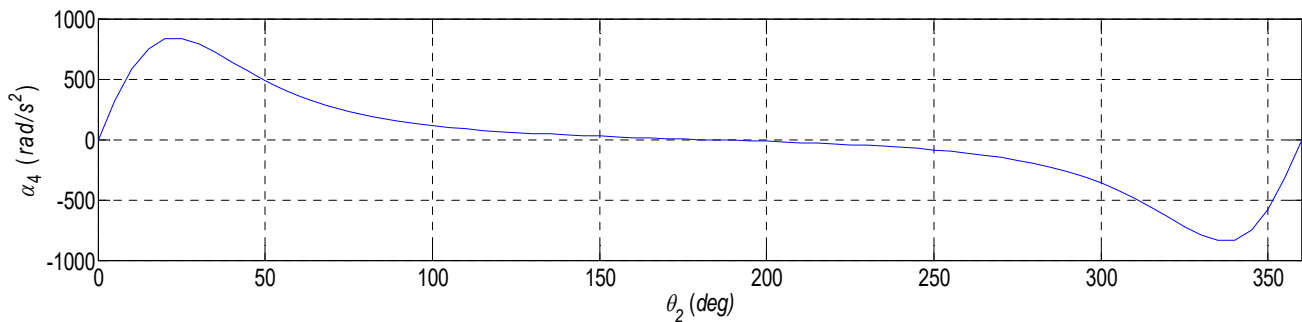
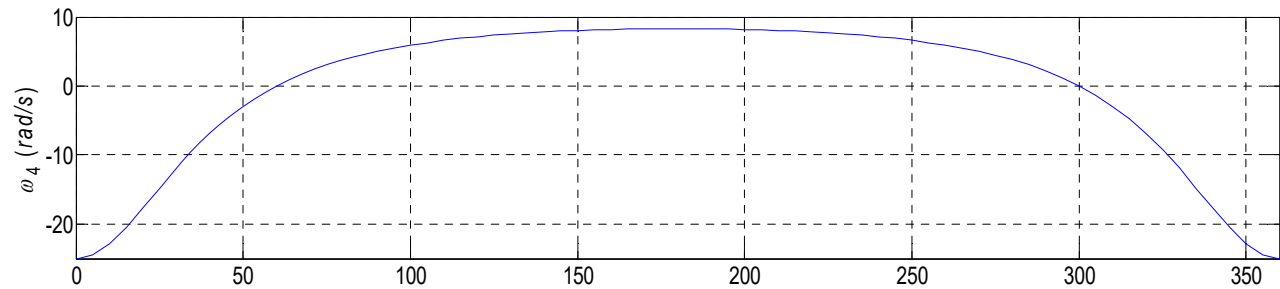
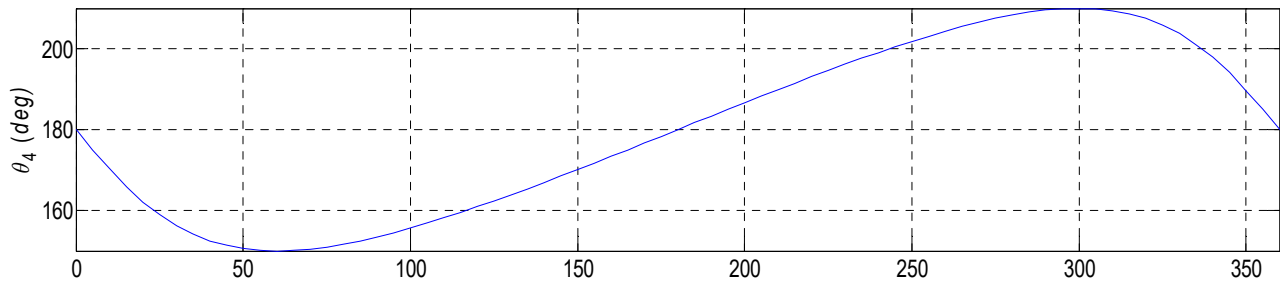
When one variable is the derivative of another, recall the relationships from calculus (the derivative is the slope of the above curve at each point; the integral is the area under the curve up to that point, taking into account the initial value). For example:

$$\omega_4(t) = \frac{d\theta_4(t)}{dt}$$

$$\theta_4(t) = \theta_{40} + \int \omega_4(t) dt$$

$$\alpha_4(t) = \frac{d\omega_4(t)}{dt}$$

$$\omega_4(t) = \omega_{40} + \int \alpha_4(t) dt$$

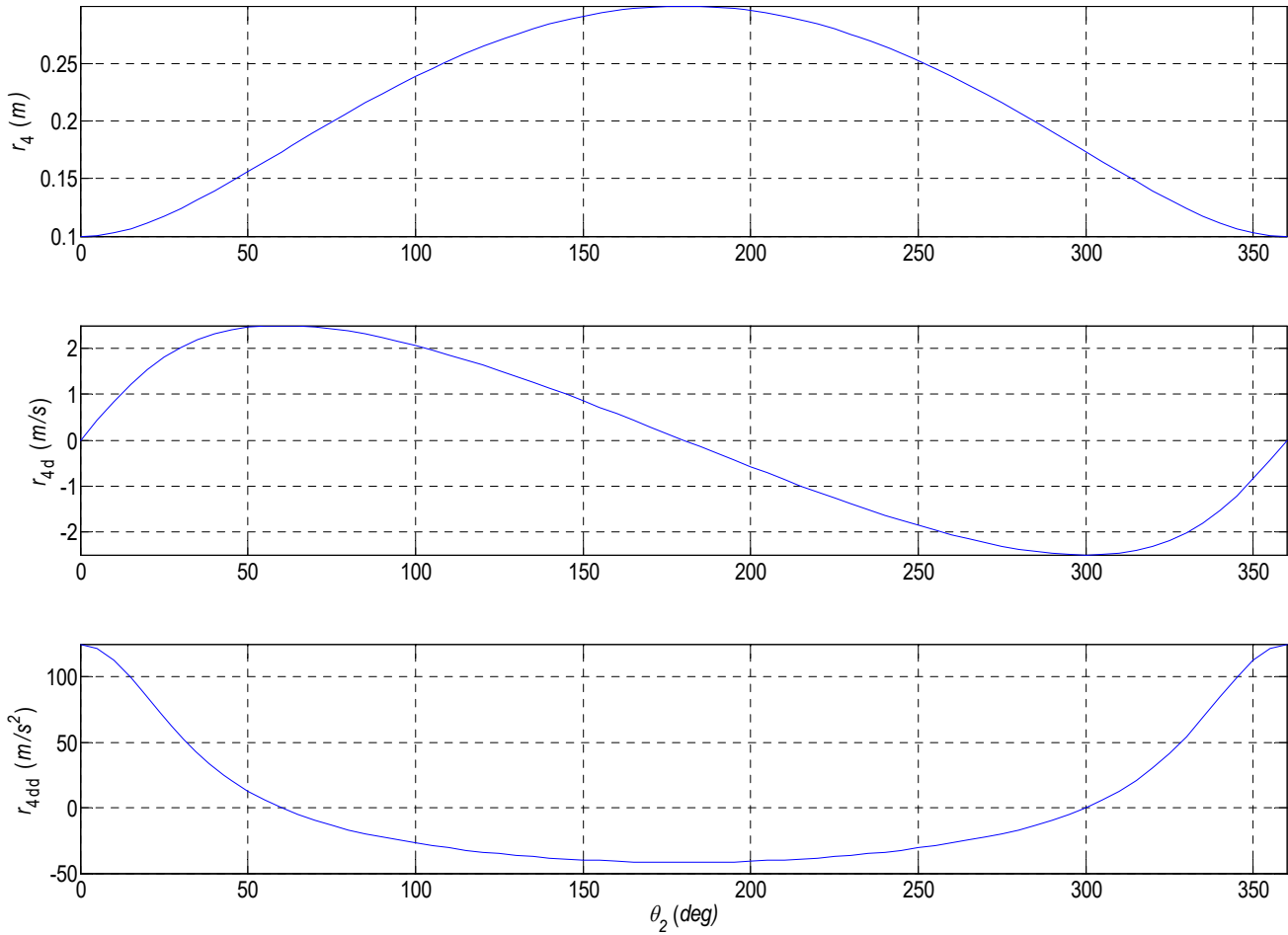


$$\dot{r}_4(t) = \frac{dr_4(t)}{dt}$$

$$r_4(t) = r_{40} + \int \dot{r}_4(t) dt$$

$$\ddot{r}_4(t) = \frac{d\dot{r}_4(t)}{dt}$$

$$\dot{r}_4(t) = \dot{r}_{40} + \int \ddot{r}_4(t) dt$$

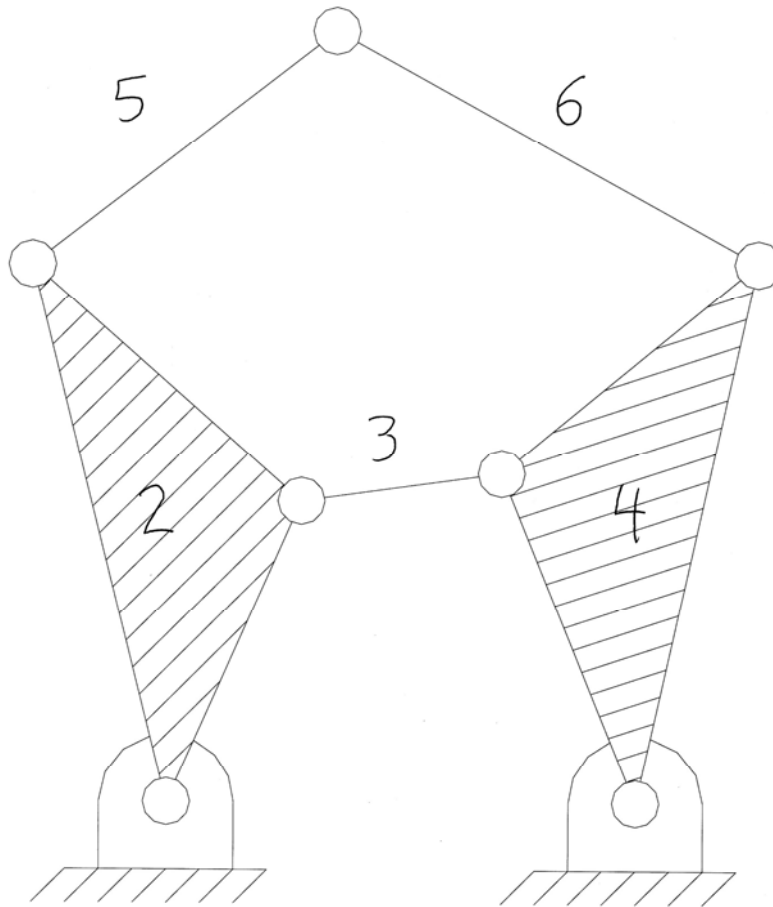


These plots are all from Term Example 3.

4.6 Multi-Loop Mechanism Acceleration Analysis

Thus far we have presented acceleration analysis for the single-loop four-bar, slider-crank, and inverted slider-crank mechanisms. The acceleration analysis for mechanisms of more than one loop is handled using the same general procedures developed for the single loop mechanisms.

This section presents acceleration analysis for the two-loop Stephenson I six-bar mechanism shown below as an example multi-loop mechanism. It follows the position and velocity analyses for the same mechanism presented earlier.



Stephenson I 6-Bar Mechanism

The bottom loop of the Stephenson I six-bar mechanism is identical to the standard four-bar mechanism model and so the acceleration analysis solution is identical to the four-bar presented earlier. With the complete acceleration analysis of the bottom loop thus solved, the solution for the top loop is essentially another four-bar acceleration solution.

As in all acceleration analysis, the acceleration solution for multi-loop mechanisms is a linear analysis yielding a unique solution (assuming the given mechanism position is not singular) for each solution branch considered. The position and velocity analyses must be complete prior to the acceleration solution.

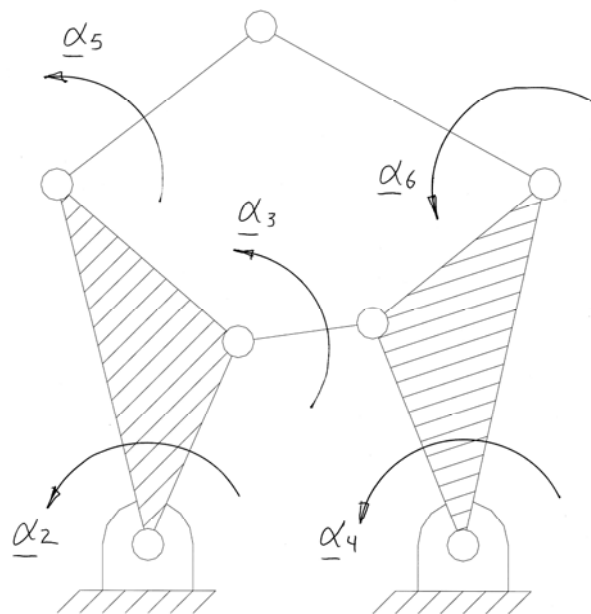
Now let us solve the acceleration analysis problem for the two-loop Stephenson I six-bar mechanism using the formal acceleration analysis steps presented earlier. Again, assume link 2 is the input link.

Step 1. The Stephenson I six-bar mechanism **Position and Velocity Analyses** must first be complete.

Given $r_1, \theta_1, r_2, r_3, r_4, r_{2a}, r_{4a}, r_5, r_6, \delta_2, \delta_4, \theta_2$, and ω_2 , we solved for $\theta_3, \theta_4, \theta_5, \theta_6, \omega_3, \omega_4, \omega_5, \omega_6$.

Step 2. Draw the Stephenson I six-bar mechanism **Acceleration Diagram**.

This should include all the information from the position and velocity diagrams, plus the new acceleration information. For clarity, we show only the new acceleration information here. Refer to the previous Stephenson I position and velocity kinematics diagrams for complete information.



where α_i ($i = 2,3,4,5,6$) is the absolute angular acceleration of link i . Triangular links 2 and 4 each have a single angular acceleration for the whole link. $\ddot{r}_i = 0$ for all links since all links are of fixed length (no sliders).

Step 3. State the Problem

Given the mechanism $r_1, \theta_1, r_2, r_3, r_4, r_{2a}, r_{4a}, r_5, r_6, \delta_2, \delta_4$,
the position analysis $\theta_2, \theta_3, \theta_4, \theta_5, \theta_6$,
the velocity analysis $\omega_2, \omega_3, \omega_4, \omega_5, \omega_6$,
1-dof acceleration input α_2

Find the acceleration unknowns $\alpha_3, \alpha_4, \alpha_5, \alpha_6$

Step 4. Derive the acceleration equations. Take the first time derivative of both sides of each of the four scalar XY velocity equations.

The Stephenson I six-bar mechanism velocity equations are given below.

XY scalar velocity equations

$$\begin{aligned} -r_2\omega_2s_2 - r_3\omega_3s_3 &= -r_4\omega_4s_4 \\ r_2\omega_2c_2 + r_3\omega_3c_3 &= r_4\omega_4c_4 \end{aligned}$$

$$\begin{aligned} -r_{2a}\omega_{2a}s_{2a} - r_5\omega_5s_5 &= -r_{4a}\omega_{4a}s_{4a} - r_6\omega_6s_6 \\ r_{2a}\omega_{2a}c_{2a} + r_5\omega_5c_5 &= r_{4a}\omega_{4a}c_{4a} + r_6\omega_6c_6 \end{aligned}$$

where

$$\begin{aligned} \theta_{2a} &= \theta_2 + \delta_2 \\ \theta_{4a} &= \theta_4 - \delta_4 \end{aligned}$$

The first time derivative of the Loop I velocity equations is identical to that for the standard four-bar mechanism.

$$\begin{aligned} -r_2\alpha_2s_2 - r_2\omega_2^2c_2 - r_3\alpha_3s_3 - r_3\omega_3^2c_3 &= -r_4\alpha_4s_4 - r_4\omega_4^2c_4 \\ r_2\alpha_2c_2 - r_2\omega_2^2s_2 + r_3\alpha_3c_3 - r_3\omega_3^2s_3 &= r_4\alpha_4c_4 - r_4\omega_4^2s_4 \end{aligned}$$

These equations can be written in matrix form.

$$\begin{bmatrix} r_3s_3 & -r_4s_4 \\ -r_3c_3 & r_4c_4 \end{bmatrix} \begin{Bmatrix} \alpha_3 \\ \alpha_4 \end{Bmatrix} = \begin{Bmatrix} -r_2\alpha_2s_2 - r_2\omega_2^2c_2 - r_3\omega_3^2c_3 + r_4\omega_4^2c_4 \\ r_2\alpha_2c_2 - r_2\omega_2^2s_2 - r_3\omega_3^2s_3 + r_4\omega_4^2s_4 \end{Bmatrix}$$

The first time derivatives of the Loop II velocity equations are:

$$\begin{aligned} -r_{2a}\alpha_{2a}s_{2a} - r_{2a}\omega_{2a}^2c_{2a} - r_5\alpha_5s_5 - r_5\omega_5^2c_5 &= -r_{4a}\alpha_{4a}s_{4a} - r_{4a}\omega_{4a}^2c_{4a} - r_6\alpha_6s_6 - r_6\omega_6^2c_6 \\ r_{2a}\alpha_{2a}c_{2a} - r_{2a}\omega_{2a}^2s_{2a} + r_5\alpha_5c_5 - r_5\omega_5^2s_5 &= r_{4a}\alpha_{4a}c_{4a} - r_{4a}\omega_{4a}^2s_{4a} + r_6\alpha_6c_6 - r_6\omega_6^2s_6 \end{aligned}$$

These equations can be written in matrix form.

$$\begin{bmatrix} r_5s_5 & -r_6s_6 \\ -r_5c_5 & r_6c_6 \end{bmatrix} \begin{Bmatrix} \alpha_5 \\ \alpha_6 \end{Bmatrix} = \begin{Bmatrix} -r_{2a}\alpha_{2a}s_{2a} - r_{2a}\omega_{2a}^2c_{2a} - r_5\omega_5^2c_5 + r_{4a}\alpha_{4a}s_{4a} + r_{4a}\omega_{4a}^2c_{4a} + r_6\omega_6^2c_6 \\ r_{2a}\alpha_{2a}c_{2a} - r_{2a}\omega_{2a}^2s_{2a} - r_5\omega_5^2s_5 - r_{4a}\alpha_{4a}c_{4a} + r_{4a}\omega_{4a}^2s_{4a} + r_6\omega_6^2s_6 \end{Bmatrix}$$

where we have used $\omega_{2a} = \omega_2$ and $\alpha_{2a} = \alpha_2$ since δ_2 and δ_4 are constant angles.
 $\omega_{4a} = \omega_4$ and $\alpha_{4a} = \alpha_4$

Step 5. Solve the acceleration equations for the unknowns α_3 , α_4 , α_5 , α_6 .

The two loops decouple so we find α_3 and α_4 from Loop I first and then use α_4 to find α_5 and α_6 from Loop II. The solutions are given below.

Loop I (identical to the standard four-bar mechanism)

$$\begin{Bmatrix} \alpha_3 \\ \alpha_4 \end{Bmatrix} = \begin{bmatrix} r_3 s_3 & -r_4 s_4 \\ -r_3 c_3 & r_4 c_4 \end{bmatrix}^{-1} \begin{Bmatrix} -r_2 \alpha_2 s_2 - r_2 \omega_2^2 c_2 - r_3 \omega_3^2 c_3 + r_4 \omega_4^2 c_4 \\ r_2 \alpha_2 c_2 - r_2 \omega_2^2 s_2 - r_3 \omega_3^2 s_3 + r_4 \omega_4^2 s_4 \end{Bmatrix}$$

Loop II (similar to the standard four-bar mechanism)

$$\begin{Bmatrix} \alpha_5 \\ \alpha_6 \end{Bmatrix} = \begin{bmatrix} r_5 s_5 & -r_6 s_6 \\ -r_5 c_5 & r_6 c_6 \end{bmatrix}^{-1} \begin{Bmatrix} -r_{2a} \alpha_2 s_{2a} - r_{2a} \omega_2^2 c_{2a} - r_5 \omega_5^2 c_5 + r_{4a} \alpha_4 s_{4a} + r_{4a} \omega_4^2 c_{4a} + r_6 \omega_6^2 c_6 \\ r_{2a} \alpha_2 c_{2a} - r_{2a} \omega_2^2 s_{2a} - r_5 \omega_5^2 s_5 - r_{4a} \alpha_4 c_{4a} + r_{4a} \omega_4^2 s_{4a} + r_6 \omega_6^2 s_6 \end{Bmatrix}$$

Remember, Gaussian elimination is more efficient and robust than the matrix inverse. Also, these equations may easily be solved algebraically instead of using matrix methods.

Stephenson I six-bar mechanism singularity condition

The acceleration solution fails when the determinant of either coefficient matrix above goes to zero. The result is dividing by zero, resulting in infinite angular accelerations for the associated loop. Note the two coefficient matrices in the acceleration solutions are identical to those for the velocity solutions. Therefore, the acceleration singularity conditions are identical to the velocity singularity conditions.

For the first loop, the singularity condition is identical to the singularity condition of the standard four-bar mechanism, i.e. when links 3 and 4 either line up or fold upon each other, causing a link 2 joint limit. For the second loop, the singularity condition is similar, occurring when 5 and 6 either line up or fold upon each other. These conditions also cause problems for the velocity and position analyses, so the acceleration singularities are known problems.

5. Other Kinematics Topics

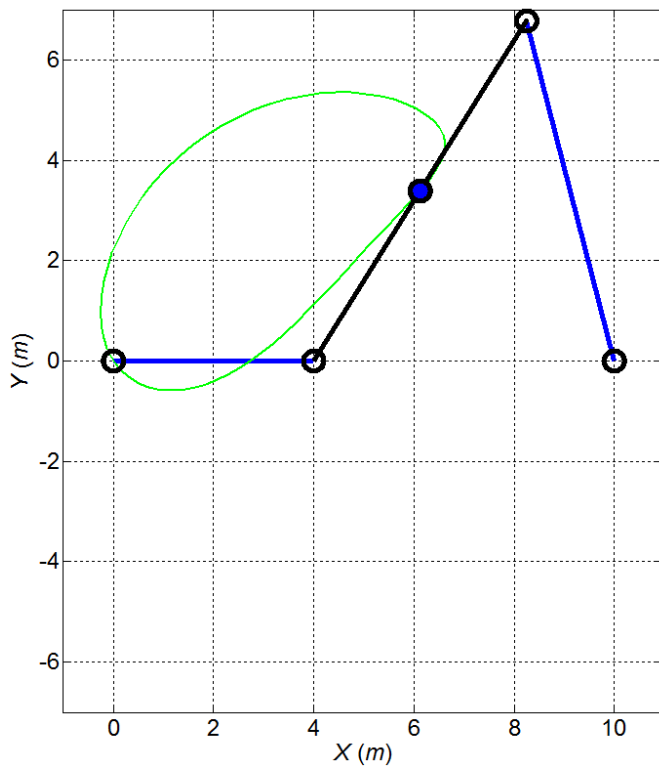
5.4 Branch Symmetry in Kinematics Analysis

We have been doing F.R.O.M. analysis for the open-branch only (four-bar mechanism) and the right-branch only (slider-crank mechanism). What do the kinematics results look like for the crossed and left branches? Are there any relationships amongst the various analyses for the two branches? The reader is left to draw their own conclusions.

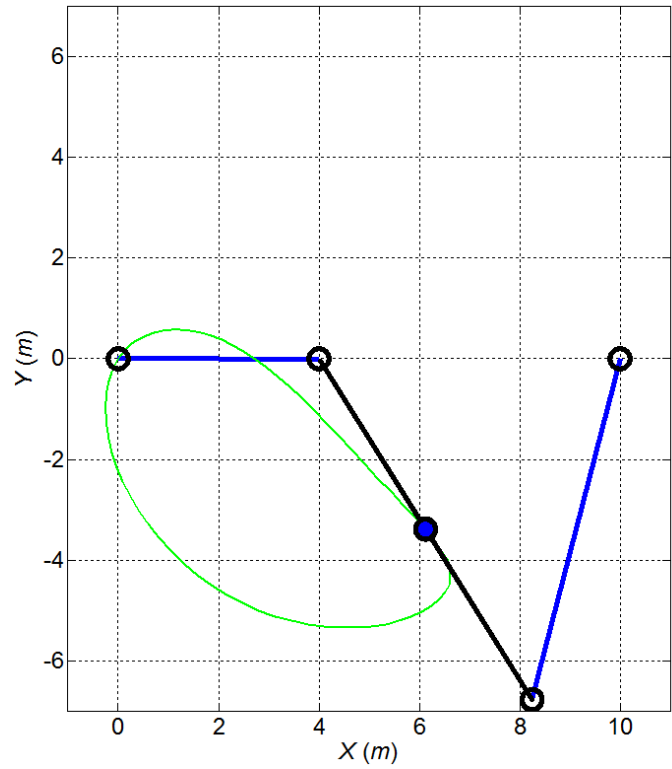
5.4.1 Four-Bar Mechanism

Given:	$r_1 = 10$	$\theta_1 = 0$
	$r_2 = 4$	$r_{CA} = 4$
	$r_3 = 8$	$\delta_3 = 0$
	$r_4 = 7$	$\omega_2 = 10$ (constant)

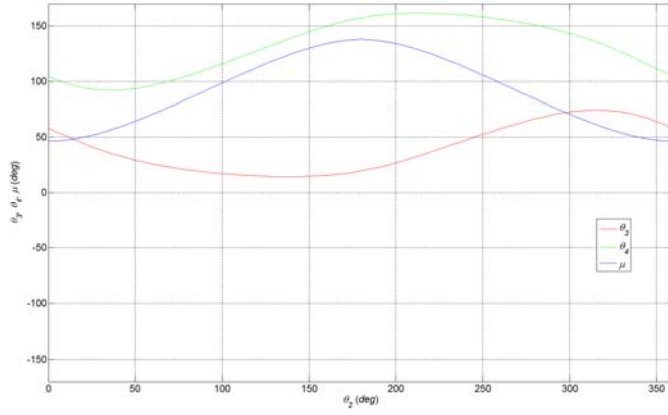
Open Branch



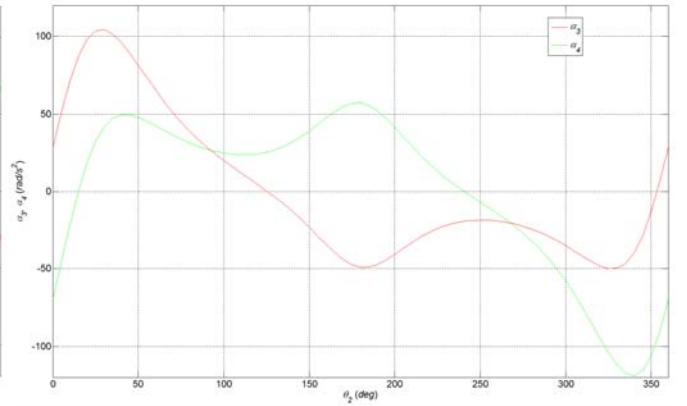
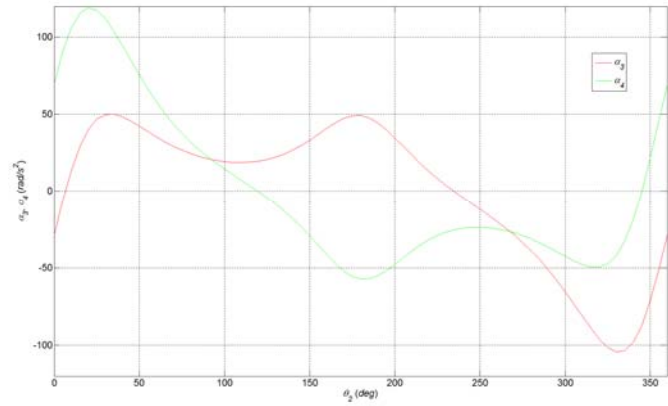
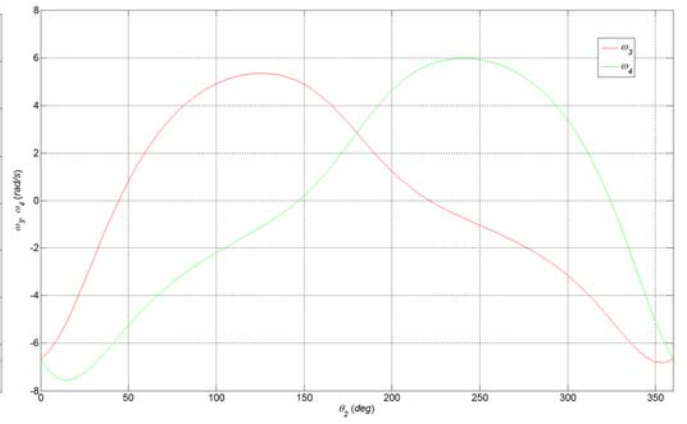
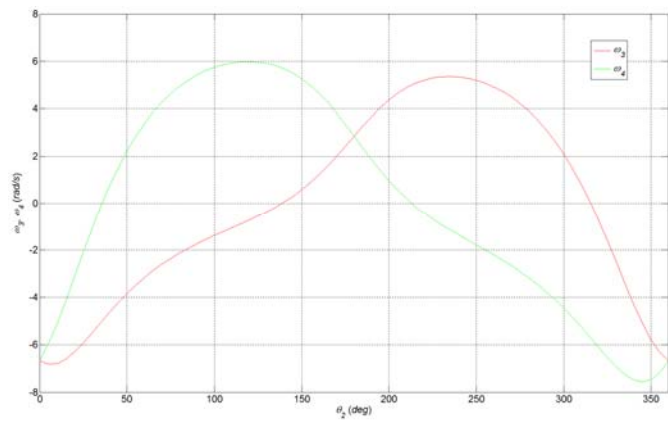
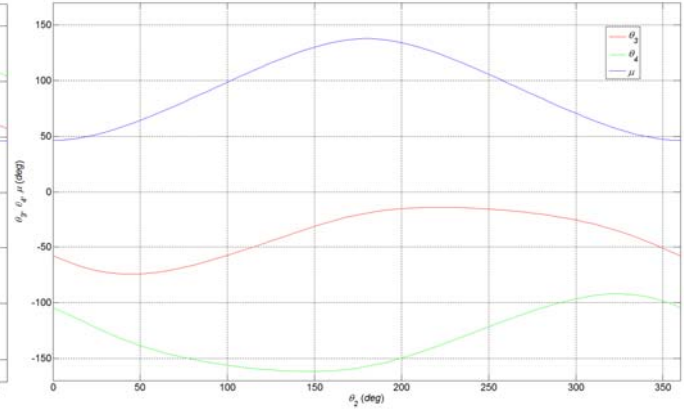
Crossed Branch



Open Branch



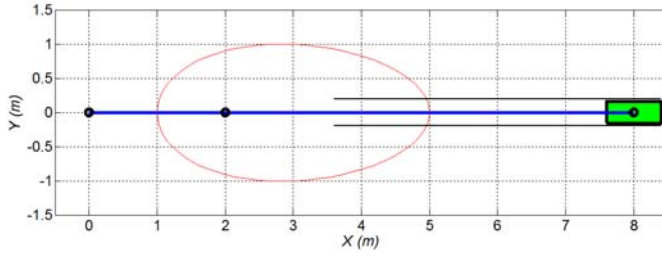
Crossed Branch



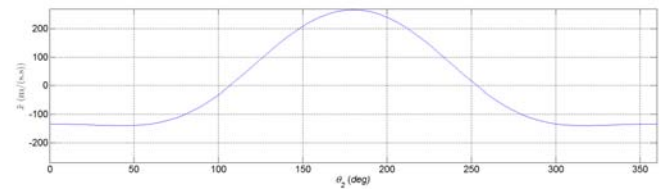
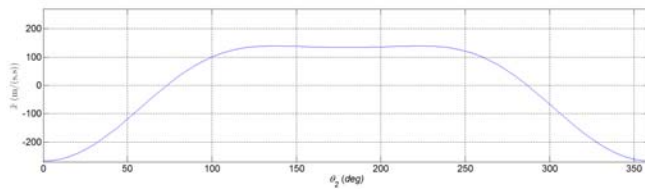
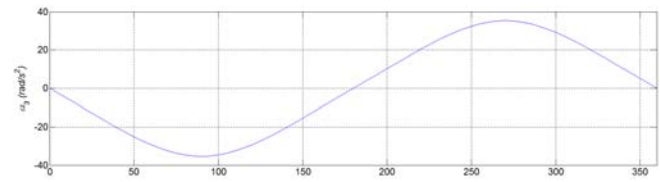
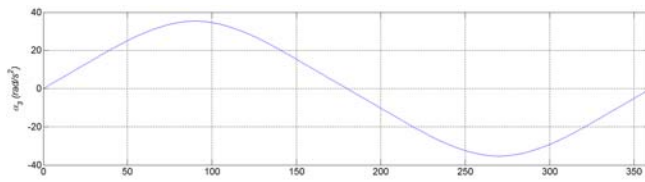
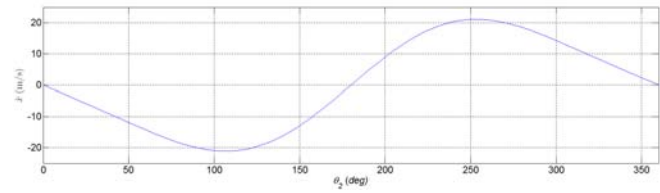
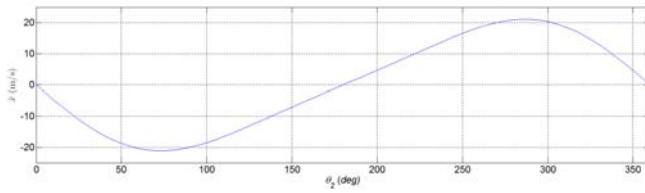
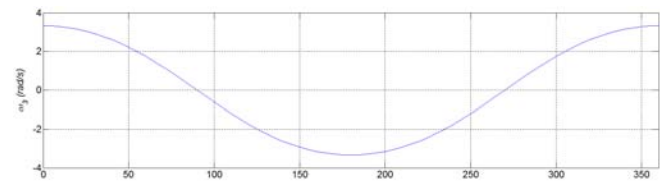
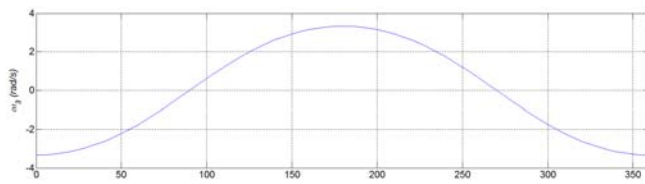
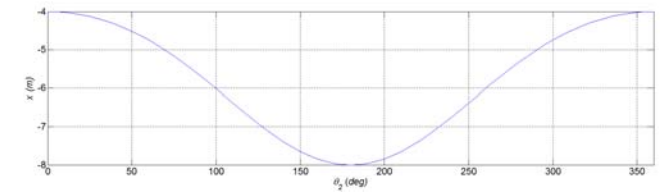
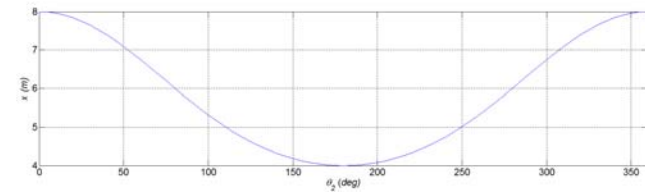
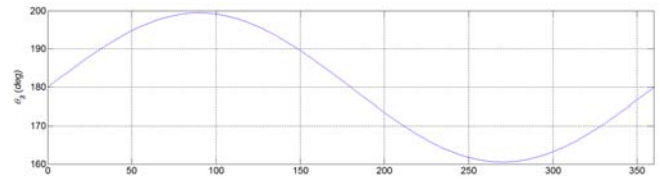
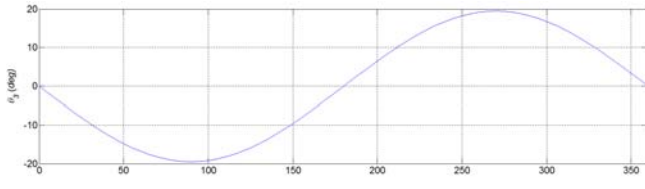
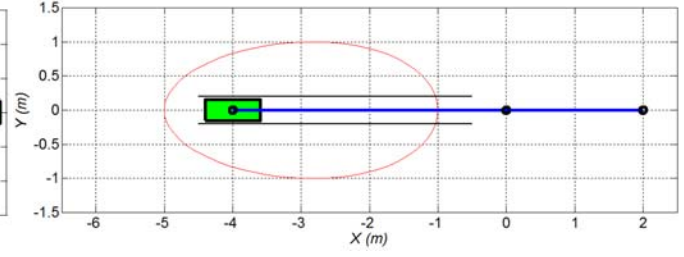
5.4.2 Slider-Crank Mechanism

Given: $r_2=2, r_3=6, h=0, r_{CA}=3, \delta_3=0, \omega_2=10$ (constant)

Right Branch



Left Branch



We see a great deal of symmetry for both four-bar and slider crank mechanism kinematic analyses. The coupler point curves and all plots have either horizontal midpoint $\theta_2 = 180^\circ$ or vertical zero point flip-symmetry (some have both).

However, for the \dot{x} and \ddot{x} slider-crank mechanism results, this symmetry is not immediately evident. This special symmetry is revealed when first cutting the plots at $\theta_2 = 180^\circ$, and then performing the horizontal and/or vertical flipping.

6. Inverse Dynamics Analysis

6.1 Dynamics Introduction

D'Alembert's Principle

We can convert dynamics problems into statics problems by the inclusion of a vector inertial force $\underline{F}_0 = -m\underline{A}_G$ and a vector inertial moment $\underline{M}_0 = -I_G\underline{\alpha}$. Centrifugal force $-mr\omega^2$, directed away from the center of rotation, is an example of an inertial force vector. It's not really a force but a felt effect of an inertia in acceleration. Using D'Alembert's principle, the right-hand side of the translational and rotational dynamics equations is subtracted to the other side of the equation. Then the forces and moments balance to zero as in statics, when the inertial forces are included in the FBD.

We won't use this method, but it is mentioned for completeness. We would instead prefer to consider statics problems as a subset of dynamics problems, with zero accelerations.

$$\underline{R} - m\underline{A}_G = 0$$

$$\underline{R} + \underline{F}_0 = 0$$

$$\underline{T} + \underline{r} \times \underline{R} - I_G \underline{\alpha} = 0$$

$$\underline{T} + \underline{r} \times \underline{R} + \underline{M}_0 = 0$$

6.4 Four-Bar Mechanism Inverse Dynamics Analysis

Four-bar mechanism inverse dynamics matrix equation

$$\begin{bmatrix} -1 & 0 & 1 & 0 & 0 & 0 & 0 & 0 & 0 \\ 0 & -1 & 0 & 1 & 0 & 0 & 0 & 0 & 0 \\ r_{12Y} & -r_{12X} & -r_{32Y} & r_{32X} & 0 & 0 & 0 & 0 & 1 \\ 0 & 0 & -1 & 0 & 1 & 0 & 0 & 0 & 0 \\ 0 & 0 & 0 & -1 & 0 & 1 & 0 & 0 & 0 \\ 0 & 0 & r_{23Y} & -r_{23X} & -r_{43Y} & r_{43X} & 0 & 0 & 0 \\ 0 & 0 & 0 & 0 & -1 & 0 & 1 & 0 & 0 \\ 0 & 0 & 0 & 0 & 0 & -1 & 0 & 1 & 0 \\ 0 & 0 & 0 & 0 & r_{34Y} & -r_{34X} & -r_{14Y} & r_{14X} & 0 \end{bmatrix} \begin{Bmatrix} F_{21X} \\ F_{21Y} \\ F_{32X} \\ F_{32Y} \\ F_{43X} \\ F_{43Y} \\ F_{14X} \\ F_{14Y} \\ \tau_2 \end{Bmatrix} = \begin{Bmatrix} m_2 A_{G2X} \\ m_2 (A_{G2Y} + g) \\ I_{G2Z} \alpha_2 \\ m_3 A_{G3X} - F_{E3X} \\ m_3 (A_{G3Y} + g) - F_{E3Y} \\ I_{G3Z} \alpha_3 - r_{E3X} F_{E3Y} + r_{E3Y} F_{E3X} - M_{E3} \\ m_4 A_{G4X} - F_{E4X} \\ m_4 (A_{G4Y} + g) - F_{E4Y} \\ I_{G4Z} \alpha_4 - r_{E4X} F_{E4Y} + r_{E4Y} F_{E4X} - M_{E4} \end{Bmatrix}$$

$$[A]\{v\} = \{b\}$$

Step 6. Solve for the unknowns (alternate solution)

It is possible to partially decouple the solution to this problem¹. If we consider the FBDs of only links 3 and 4 first, this is 6 equations in 6 unknowns – this is verified by looking at the original 9x9 matrix and noting three 6x1 columns of zeros (1, 2, 9) in rows 4 through 9. Here is a more efficient solution. The reduced 6x6 set of equations for links 3 and 4 are given below.

$$\begin{bmatrix} -1 & 0 & 1 & 0 & 0 & 0 \\ 0 & -1 & 0 & 1 & 0 & 0 \\ r_{23Y} & -r_{23X} & -r_{43Y} & r_{43X} & 0 & 0 \\ 0 & 0 & -1 & 0 & 1 & 0 \\ 0 & 0 & 0 & -1 & 0 & 1 \\ 0 & 0 & r_{34Y} & -r_{34X} & -r_{14Y} & r_{14X} \end{bmatrix} \begin{Bmatrix} F_{32X} \\ F_{32Y} \\ F_{43X} \\ F_{43Y} \\ F_{14X} \\ F_{14Y} \end{Bmatrix} = \begin{Bmatrix} m_3 A_{G3X} - F_{E3X} \\ m_3 (A_{G3Y} + g) - F_{E3Y} \\ I_{G3Z} \alpha_3 - r_{E3X} F_{E3Y} + r_{E3Y} F_{E3X} - M_{E3} \\ m_4 A_{G4X} - F_{E4X} \\ m_4 (A_{G4Y} + g) - F_{E4Y} \\ I_{G4Z} \alpha_4 - r_{E4X} F_{E4Y} + r_{E4Y} F_{E4X} - M_{E4} \end{Bmatrix}$$

$$[A_{34}]\{v_{34}\} = \{b_{34}\}$$

Solve for six unknowns $\{v_{34}\} = [A_{34}]^{-1} \{b_{34}\}$ and then use F_{32X} and F_{32Y} in the following 3x3 set of linear equations, from the link 2 FBD, very similar to the single rotating link.

$$\begin{bmatrix} -1 & 0 & 0 \\ 0 & -1 & 0 \\ r_{12Y} & -r_{12X} & 1 \end{bmatrix} \begin{Bmatrix} F_{21X} \\ F_{21Y} \\ \tau_2 \end{Bmatrix} = \begin{Bmatrix} m_2 A_{G2X} - F_{32X} \\ m_2 (A_{G2Y} + g) - F_{32Y} \\ I_{G2Z} \alpha_2 + r_{32Y} F_{32X} - r_{32X} F_{32Y} \end{Bmatrix}$$

¹ R.L. Williams II, 2009, "Partial Decoupling of the Matrix Method for Planar Mechanisms Inverse Dynamics", CD Proceedings of the ASME International Design Technical Conferences, 33rd Mechanisms and Robotics Conference, Paper # DETC2009-87054, San Diego CA, August 30-September 2.

We do not need a matrix solution here since the X and Y force equations are decoupled. The solution is:

$$F_{21X} = -m_2 A_{G2X} + F_{32X}$$

$$F_{21Y} = -m_2 (A_{G2Y} + g) + F_{32Y}$$

$$\tau_2 = I_{G2Z} \alpha_2 + r_{32Y} F_{32X} - r_{32X} F_{32Y} - r_{12Y} F_{21X} + r_{12X} F_{21Y}$$

Matrix inversion requires approximately $\frac{3n^3}{\log n}$ and Gaussian elimination requires approximately $\frac{(n^2 - 1)n}{3} + n^2$ multiplications/divisions².

Number of Multiplications/Divisions for Four-bar Inverse Dynamics Solution

Method	Inversion	Gaussian	Reduction
9x9	2292	321	86%
6x6 plus decoupled link 2	840	113	87%
Reduction in cost	63%	65%	

There is a substantial **65% reduction in computational cost** for Gaussian elimination with the 6x6 plus decoupled link 2 method. Also, the numerical accuracy may also improve with this method since we needn't do unnecessary calculations with the three 6x1 columns of zeros.

² E.D. Nering, 1974, Elementary Linear Algebra, W.B. Saunders Company, Philadelphia: 38-39.

6.5 Slider-Crank Mechanism Inverse Dynamics Analysis

Slider-crank mechanism inverse dynamics matrix equation

$$\begin{bmatrix} -1 & 0 & 1 & 0 & 0 & 0 & 0 & 0 \\ 0 & -1 & 0 & 1 & 0 & 0 & 0 & 0 \\ r_{12Y} & -r_{12X} & -r_{32Y} & r_{32X} & 0 & 0 & 0 & 1 \\ 0 & 0 & -1 & 0 & 1 & 0 & 0 & 0 \\ 0 & 0 & 0 & -1 & 0 & 1 & 0 & 0 \\ 0 & 0 & r_{23Y} & -r_{23X} & -r_{43Y} & r_{43X} & 0 & 0 \\ 0 & 0 & 0 & 0 & -1 & 0 & \pm\mu & 0 \\ 0 & 0 & 0 & 0 & 0 & -1 & 1 & 0 \end{bmatrix} \begin{Bmatrix} F_{21X} \\ F_{21Y} \\ F_{32X} \\ F_{32Y} \\ F_{43X} \\ F_{43Y} \\ F_{14Y} \\ \tau_2 \end{Bmatrix} = \begin{Bmatrix} m_2 A_{G2X} \\ m_2 (A_{G2Y} + g) \\ I_{G2Z} \alpha_2 \\ m_3 A_{G3X} - F_{E3X} \\ m_3 (A_{G3Y} + g) - F_{E3Y} \\ I_{G3Z} \alpha_3 - r_{E3X} F_{E3Y} + r_{E3Y} F_{E3X} - M_{E3} \\ m_4 A_{G4X} - F_{E4X} \\ m_4 g - F_{E4Y} \end{Bmatrix}$$

$$[A]\{v\} = \{b\}$$

Step 6. Solve for the unknowns (alternate solution)

Like the four-bar mechanism, it is possible to partially decouple the solution to this problem¹. If we consider the FBDs of only links 3 and 4 first, this is 5 equations in 5 unknowns – this is verified by looking at the original 8x8 matrix and noting three 5x1 columns of zeros (1, 2, 8) in rows 4 through 8. Here is a more efficient solution. The reduced 5x5 set of equations for links 3 and 4 are given below.

$$\begin{bmatrix} -1 & 0 & 1 & 0 & 0 \\ 0 & -1 & 0 & 1 & 0 \\ r_{23Y} & -r_{23X} & -r_{43Y} & r_{43X} & 0 \\ 0 & 0 & -1 & 0 & \pm\mu \\ 0 & 0 & 0 & -1 & 1 \end{bmatrix} \begin{Bmatrix} F_{32X} \\ F_{32Y} \\ F_{43X} \\ F_{43Y} \\ F_{14Y} \end{Bmatrix} = \begin{Bmatrix} m_3 A_{G3X} - F_{E3x} \\ m_3 (A_{G3Y} + g) - F_{E3y} \\ I_{G3Z} \alpha_3 - r_{E3x} F_{E3y} + r_{E3y} F_{E3x} - M_{E3} \\ m_4 A_{G4X} - F_{E4x} \\ m_4 g - F_{E4y} \end{Bmatrix}$$

$$[A_{34}]\{v_{34}\} = \{b_{34}\}$$

Solve for five unknowns $\{v_{34}\} = [A_{34}]^{-1} \{b_{34}\}$ and then use F_{32X} and F_{32Y} in the following 3x3 set of linear equations, from the link 2 FBD.

$$\begin{bmatrix} -1 & 0 & 0 \\ 0 & -1 & 0 \\ r_{12Y} & -r_{12X} & 1 \end{bmatrix} \begin{Bmatrix} F_{21X} \\ F_{21Y} \\ \tau_2 \end{Bmatrix} = \begin{Bmatrix} m_2 A_{G2X} - F_{32X} \\ m_2 (A_{G2Y} + g) - F_{32Y} \\ I_{G2Z} \alpha_2 + r_{32Y} F_{32X} - r_{32X} F_{32Y} \end{Bmatrix}$$

We do not need a matrix solution here since the X and Y force equations are decoupled. The solution is identical to that of the four-bar mechanism.

$$F_{21X} = -m_2 A_{G2X} + F_{32X}$$

$$F_{21Y} = -m_2 (A_{G2Y} + g) + F_{32Y}$$

$$\tau_2 = I_{G2Z} \alpha_2 + r_{32Y} F_{32X} - r_{32X} F_{32Y} - r_{12Y} F_{21X} + r_{12X} F_{21Y}$$

Matrix inversion requires approximately $\frac{3n^3}{\log n}$ and Gaussian elimination requires approximately

$\frac{(n^2-1)n}{3} + n^2$ multiplications/divisions (Nering, 1974).

Number of Multiplications/Divisions for Slider-Crank Inverse Dynamics Solution

Method	Inversion	Gaussian	Reduction
8x8	1701	232	86%
5x5 plus decoupled link 2	544	72	87%
Reduction in cost	68%	69%	

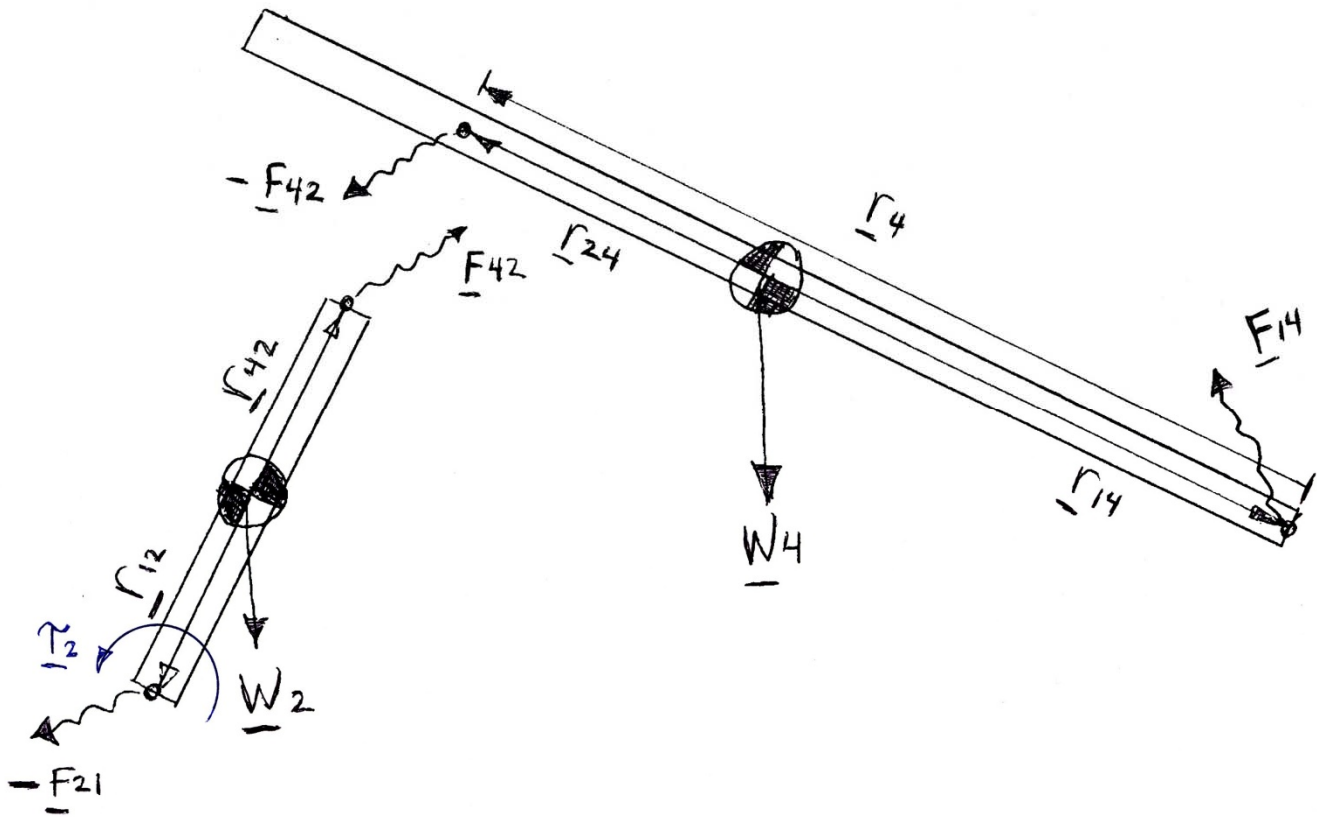
There is a substantial **69% reduction in computational cost** for Gaussian elimination with the 5x5 plus decoupled link 2 method. Also, the numerical accuracy may also improve with this method since we needn't do unnecessary calculations with the three 5x1 columns of zeros.

6.6 Inverted Slider-Crank Mechanism Inverse Dynamics Analysis

This problem can be solved with a 9x9 matrix, after eliminating a redundant equation. Let's try a simpler approach – assume the link 3 mass is small and use only FBDs for links 2 and 4. We further assume zero external forces and moments.

Step 1. The inverted slider-crank **Position, Velocity, and Acceleration Analyses** must be complete.

Step 2. Draw the Inverted Slider-Crank Mechanism Free-Body Diagrams



\underline{F}_{ij} unknown vector internal joint force of link i acting on link j .

\underline{r}_{ij} known vector moment arm pointing to the joint connection with link i from the CG of link j .

Step 3. State the Problem

Given $r_1, \theta_1 = 0, r_2$
 θ_2, r_4, θ_4
 $\omega_2, \dot{r}_4, \omega_4$
 $\alpha_2, \ddot{r}_4, \alpha_4$
 assume zero external forces and moments

Find $\underline{F}_{21}, \underline{F}_{42}, \underline{F}_{14}$ and τ

Step 4. Derive the Newton-Euler Dynamics Equations.

Newton's Second Law

Link 2

$$\sum \underline{F}_2 = \underline{F}_{42} - \underline{F}_{21} + \underline{W}_2 = m_2 \underline{A}_{G2}$$

Link 4

$$\sum \underline{F}_4 = \underline{F}_{14} - \underline{F}_{42} + \underline{W}_4 = m_4 \underline{A}_{G4}$$

Euler's Rotational Dynamics Equation

Link 2

$$\sum \underline{M}_{G2z} = \tau_2 + r_{42} \times \underline{F}_{42} - r_{12} \times \underline{F}_{21} = I_{G2Z} \alpha_2$$

Link 4

$$\sum \underline{M}_{G4z} = r_{14} \times \underline{F}_{14} - r_{24} \times \underline{F}_{42} = I_{G4Z} \alpha_4$$

Count the number of unknowns and the number of equations: 6 scalar equations and 7 scalar unknowns. We need an additional equation; let us assume zero friction between links 2 and 4. Therefore, \underline{F}_{42} is always perpendicular to link 4 and there is only one unknown from this vector, the magnitude F_{42} .

$$\underline{F}_{42} = \begin{Bmatrix} F_{42X} \\ F_{42Y} \end{Bmatrix} = \begin{Bmatrix} F_{42} \cos(\theta_4 + \pi/2) \\ F_{42} \sin(\theta_4 + \pi/2) \end{Bmatrix}$$

Step 5. Derive the XYZ scalar dynamics equations from the vector dynamics equations.

Link 2

$$F_{42X} - F_{21X} = m_2 A_{G2X}$$

$$F_{42Y} - F_{21Y} = m_2 (A_{G2Y} + g)$$

$$\tau_2 + (r_{42X} F_{42Y} - r_{42Y} F_{42X}) - (r_{12X} F_{21Y} - r_{12Y} F_{21X}) = I_{G2Z} \alpha_2$$

Link 4

$$F_{14X} - F_{42X} = m_4 A_{G4X}$$

$$F_{14Y} - F_{42Y} = m_4 (A_{G4Y} + g)$$

$$(r_{14X} F_{14Y} - r_{14Y} F_{14X}) - (r_{24X} F_{42Y} - r_{24Y} F_{42X}) = I_{G4Z} \alpha_4$$

Express these scalar equations in matrix/vector form. The simplified inverted slider-crank mechanism inverse dynamics matrix equation is given below.

$$\begin{bmatrix} -1 & 0 & c & 0 & 0 & 0 \\ 0 & -1 & s & 0 & 0 & 0 \\ r_{12Y} & -r_{12X} & r_{42X}s - r_{42Y}c & 0 & 0 & 1 \\ 0 & 0 & -c & 1 & 0 & 0 \\ 0 & 0 & -s & 0 & 1 & 0 \\ 0 & 0 & -r_{24X}s + r_{24Y}c & -r_{14Y} & r_{14X} & 0 \end{bmatrix} \begin{Bmatrix} F_{21X} \\ F_{21Y} \\ F_{42} \\ F_{14X} \\ F_{14Y} \\ \tau_2 \end{Bmatrix} = \begin{Bmatrix} m_2 A_{G2X} \\ m_2 (A_{G2Y} + g) \\ I_{G2Z} \alpha_2 \\ m_4 A_{G4X} \\ m_4 (A_{G4Y} + g) \\ I_{G4Z} \alpha_4 \end{Bmatrix}$$

where: $\begin{Bmatrix} c \\ s \end{Bmatrix} = \begin{Bmatrix} \cos(\theta_4 + \pi/2) \\ \sin(\theta_4 + \pi/2) \end{Bmatrix}$

$$[A]\{v\} = \{b\}$$

Step 6. Solve for the unknowns

The coefficient matrix $[A]$ is dependent on the mechanism geometry (i.e. the angles from the position kinematics solution). The right-hand-side vector $\{b\}$ is dependent on inertial terms and gravity.

Matrix/vector solution $\{v\} = [A]^{-1} \{b\}$

MATLAB `v = inv(A)*b; % Solution via matrix inverse`

Using Gaussian elimination is more efficient and robust.

MATLAB `v = A\b; % Solution via Gaussian elimination`

The solution to the internal forces and input torque are contained in the components of \mathbf{v} . To save these values for later plotting, use the following MATLAB code, inside the \mathbf{i} loop.

```
f21x(i) = v(1);
f21y(i) = v(2);
:
:
tau2(i) = v(6);
```

Like the four-bar and slider-crank mechanisms, it is possible to partially decouple the solution to this problem. If we consider the FBDs of only 4 first, this is 3 equations in 3 unknowns – this is verified by looking at the original 6x6 matrix and noting three 3x1 columns of zeros (1, 2, 6) in rows 4 through 6. Here is a more efficient solution. The reduced 3x3 set of equations for link 4 is given below.

$$\begin{bmatrix} -c & 1 & 0 \\ -s & 0 & 1 \\ -r_{24X}s + r_{24Y}c & -r_{14Y} & r_{14X} \end{bmatrix} \begin{Bmatrix} F_{42} \\ F_{14X} \\ F_{14Y} \end{Bmatrix} = \begin{Bmatrix} m_4 A_{G4X} \\ m_4 (A_{G4Y} + g) \\ I_{G4Z} \alpha_4 \end{Bmatrix}$$

$$[A_4] \{v_4\} = \{b_4\}$$

Solve for three unknowns $\{v_4\} = [A_4]^{-1} \{b_4\}$ and then use F_{42} in the following 3x3 set of linear equations, from the link 2 FBD.

$$\begin{bmatrix} -1 & 0 & 0 \\ 0 & -1 & 0 \\ r_{12Y} & -r_{12X} & 1 \end{bmatrix} \begin{Bmatrix} F_{21X} \\ F_{21Y} \\ \tau_2 \end{Bmatrix} = \begin{Bmatrix} m_2 A_{G2X} - cF_{42} \\ m_2 (A_{G2Y} + g) - sF_{42} \\ I_{G2Z} \alpha_2 - (r_{42X}s - r_{42Y}c)F_{42} \end{Bmatrix}$$

We do not need a matrix solution here since the X and Y force equations are decoupled. The solution is identical to that of the four-bar mechanism.

$$\begin{aligned} F_{21X} &= -m_2 A_{G2X} + cF_{42} \\ F_{21Y} &= -m_2 (A_{G2Y} + g) + sF_{42} \\ \tau_2 &= I_{G2Z} \alpha_2 - r_{12Y} F_{21X} + r_{12X} F_{21Y} - (r_{42X}s - r_{42Y}c)F_{42} \end{aligned}$$

Matrix inversion requires approximately $\frac{3n^3}{\log n}$ and Gaussian elimination requires approximately $\frac{(n^2-1)n}{3} + n^2$ multiplications/divisions (Nering, 1974).

Number of Multiplications/Divisions			
Method	Inversion	Gaussian	Reduction
6x6	833	106	87%
3x3 plus decoupled link 2	177	24	86%
Reduction in cost	79%	77%	

There is a substantial **77% reduction in computational cost** for Gaussian elimination with the 3x3 plus decoupled link 2 method. Also, the numerical accuracy may also improve with this method since we needn't do unnecessary calculations with the three 3x1 columns of zeros.

Step 7. Calculate Shaking Force and Moment

After the basic inverse dynamics problem is solved, we can calculate the vector shaking force and vector shaking moment, which is the force/moment reaction on the ground link due to the motion, inertia, weight, and external loads (which we assumed to be zero in this problem). The shaking force and moment for the inverted slider-crank mechanism is identical to the four-bar in notation and terms.

Ground link force/moment diagram

Shaking force

$$\underline{F}_S = \underline{F}_{21} + \underline{F}_{41} = \underline{F}_{21} - \underline{F}_{14} = \begin{Bmatrix} F_{21X} - F_{14X} \\ F_{21Y} - F_{14Y} \end{Bmatrix}$$

Shaking moment

$$\begin{aligned} \underline{M}_S &= -\tau_2 + \underline{r}_{21} \times \underline{F}_{21} - \underline{r}_{41} \times \underline{F}_{14} \\ &= -\tau_2 + r_{21X}F_{21Y} - r_{21Y}F_{21X} - r_{41X}F_{14Y} + r_{41Y}F_{14X} \end{aligned}$$

Inverted slider-crank mechanism inverse dynamics example – Term Example 3 continued

Given

$$\begin{array}{ll}
 r_1 = 0.20 & \theta_2 = 70^\circ \\
 r_2 = 0.10 & \theta_4 = 150.5^\circ \text{ (deg and m)} \\
 L_4 = 0.32 \text{ (m)} & r_4 = 0.19 \\
 \theta_1 = 0^\circ & \\
 \\
 \omega_2 = 25 & \alpha_2 = 0 \\
 \dot{r}_4 = 2.47 \text{ (rad/s and m/s)} & \ddot{r}_4 = -9.46 \text{ (rad/s}^2 \text{ and m/s}^2\text{)} \\
 \omega_4 = 2.18 & \alpha_4 = 267.14
 \end{array}$$

In this problem the external forces and moments are zero for both links 2 and 4. In inverse dynamics we ignore the slider link mass and inertia. The mechanism links 2 and 4 are uniform, homogeneous rectangular solids made of steel ($\rho = 7850 \text{ kg/m}^3$) with a constant thickness of 2 cm and link widths of 3 cm. The CGs are in the geometric center of each link. This yields the following fixed dynamics parameters.

$$m_2 = 0.47 \text{ and } m_4 = 1.51 \text{ (kg)} \quad I_{GZ2} = 0.0004 \text{ and } I_{GZ4} = 0.013 \text{ (kg-m}^2\text{)}$$

Snapshot Analysis

Given the previous mechanism position, velocity, and acceleration analyses, solve the inverse dynamics problem for this snapshot ($\theta_2 = 70^\circ$). The matrix-vector equation to solve is given below.

$$\begin{bmatrix} -1 & 0 & -0.49 & 0 & 0 & 0 \\ 0 & -1 & -0.87 & 0 & 0 & 0 \\ -0.05 & 0.02 & 0.01 & 0 & 0 & 1 \\ 0 & 0 & 0.49 & 1 & 0 & 0 \\ 0 & 0 & 0.87 & 0 & 1 & 0 \\ 0 & 0 & -0.03 & 0.08 & 0.14 & 0 \end{bmatrix} \begin{Bmatrix} F_{21X} \\ F_{21Y} \\ F_{42} \\ F_{14X} \\ F_{14Y} \\ \tau_2 \end{Bmatrix} = \begin{Bmatrix} -5.03 \\ -9.21 \\ 0 \\ -30.77 \\ -41.82 \\ 3.47 \end{Bmatrix}$$

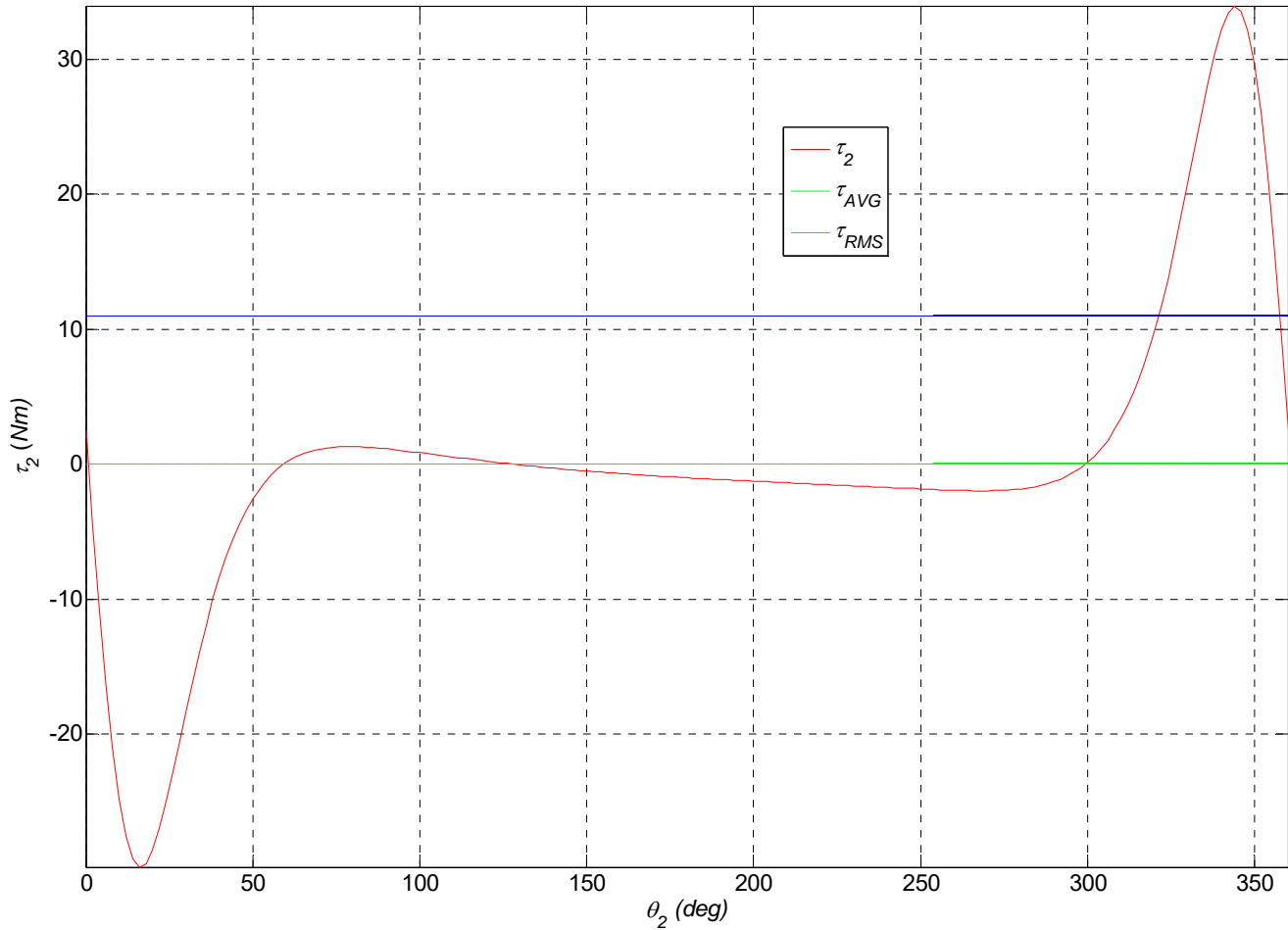
The answer is:

$$\begin{Bmatrix} F_{21X} \\ F_{21Y} \\ F_{42} \\ F_{14X} \\ F_{14Y} \\ \tau_2 \end{Bmatrix} = \begin{Bmatrix} 35.35 \\ 62.69 \\ -61.47 \\ -0.46 \\ 11.65 \\ 1.10 \end{Bmatrix}$$

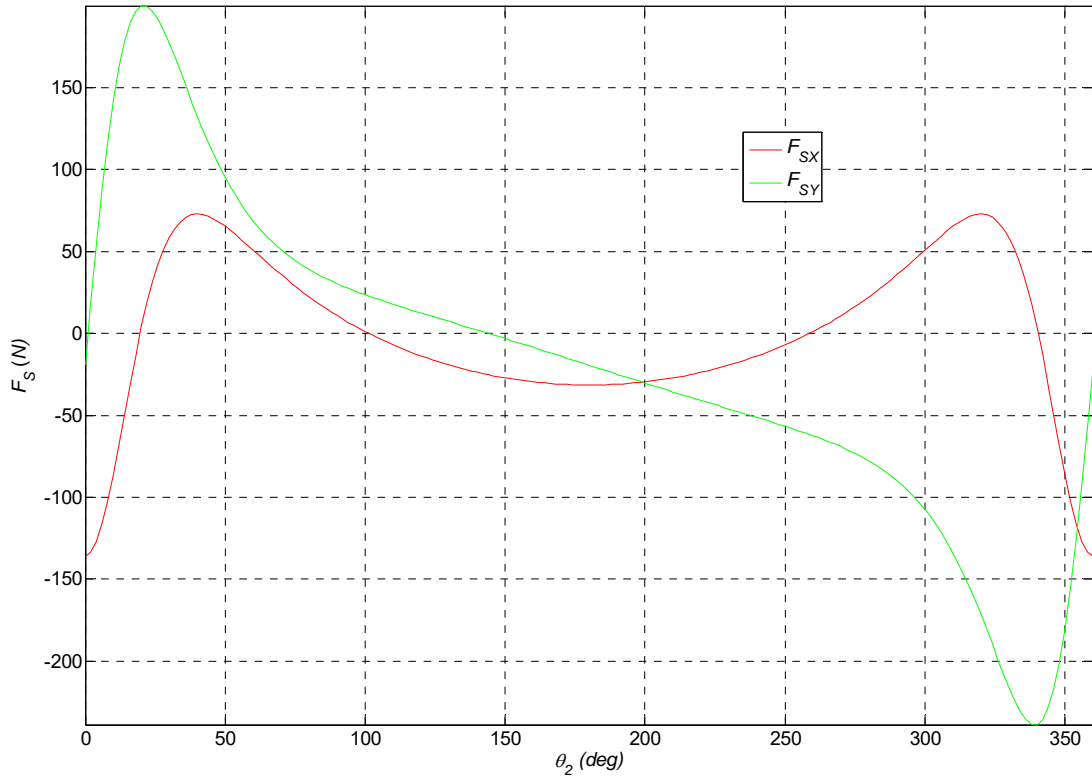
The associated vector shaking force and moment are $\underline{F}_s = \begin{Bmatrix} F_{sX} \\ F_{sY} \end{Bmatrix} = \begin{Bmatrix} 35.81 \\ 51.03 \end{Bmatrix} \text{ (N)}$ $\underline{M}_s = -8.53\hat{k} \text{ (Nm)}$

Full-Range-Of-Motion (F.R.O.M.) Analysis – Term Example 3 continued

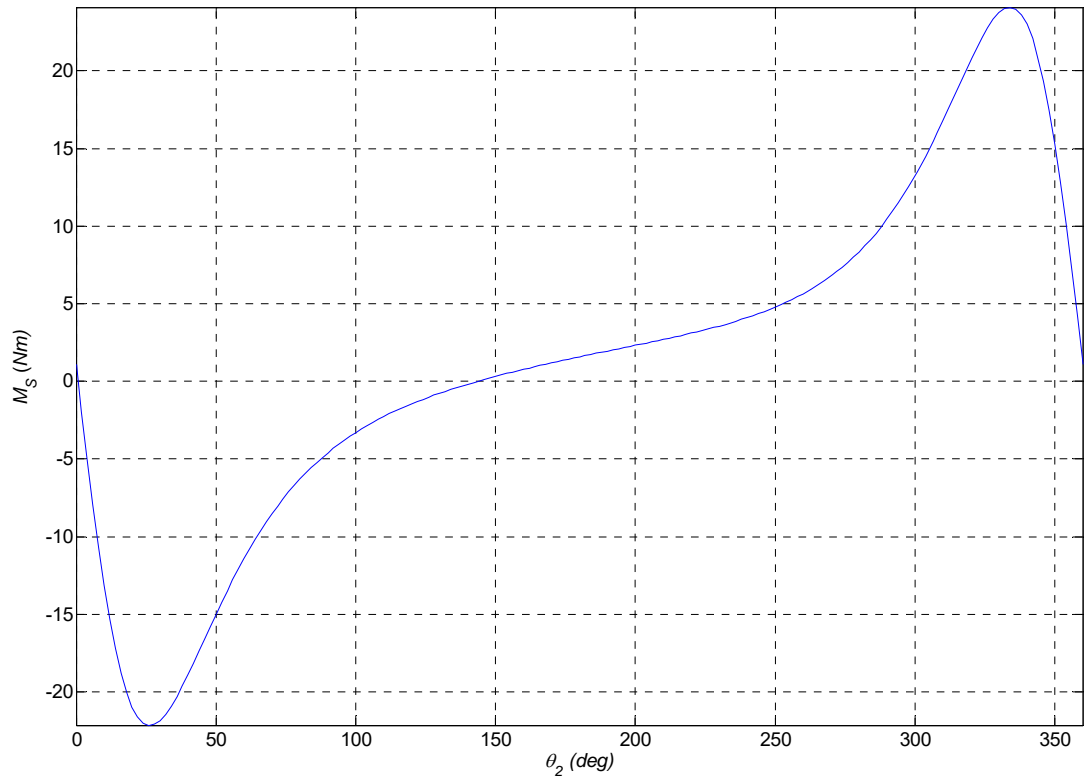
A more meaningful result is to solve and plot the inverse dynamics analysis results for the entire range of mechanism motion. The plots below give the inverse dynamics results for all $0^\circ \leq \theta_2 \leq 360^\circ$, for Term Example 3. Since ω_2 is constant, we can plot the velocity results vs. θ_2 (since it is related to time t via $\theta_2 = \omega_2 t$).



Input Torque τ_2



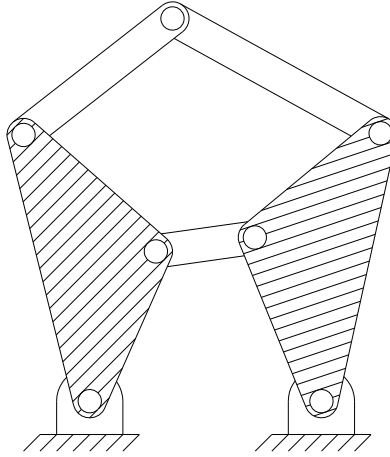
Shaking Force



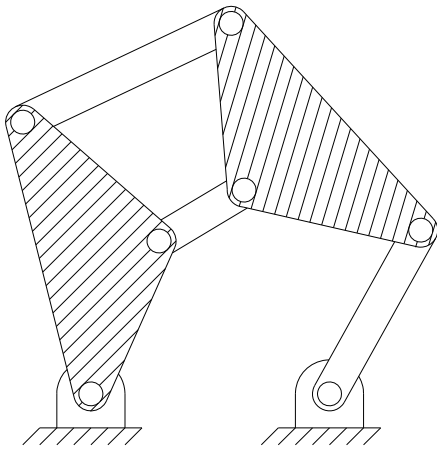
Shaking Moment

6.7 Multi-loop Mechanism Inverse Dynamics Analysis

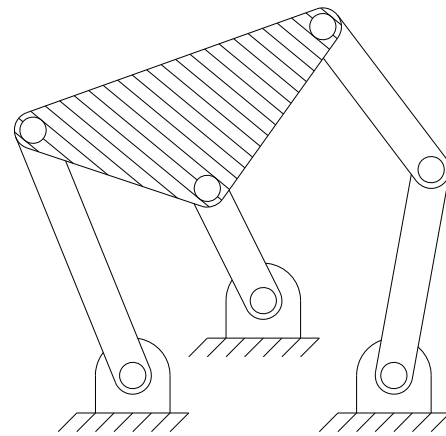
The **Matrix Method** can be applied to any planar mechanism inverse dynamics problem. Here are the five two-loop six-bar mechanisms from Dr. Bob's on-line Atlas of Structures, Mechanisms, and Robots (ohio.edu/mechanical-faculty/williams/html/PDF/MechanismAtlas.pdf).



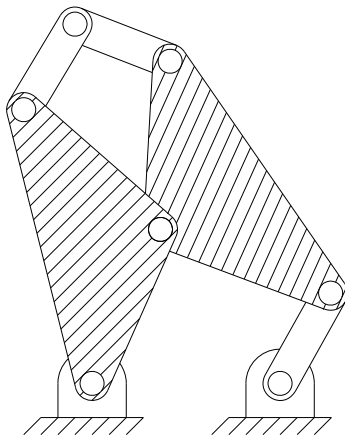
Stephenson I 6-Bar Mechanism



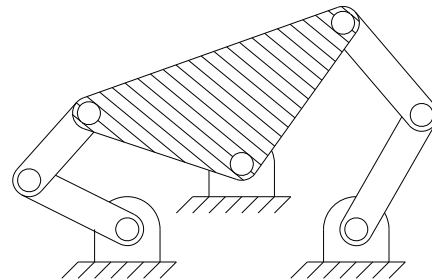
Stephenson II 6-Bar Mechanism



Stephenson III 6-Bar Mechanism

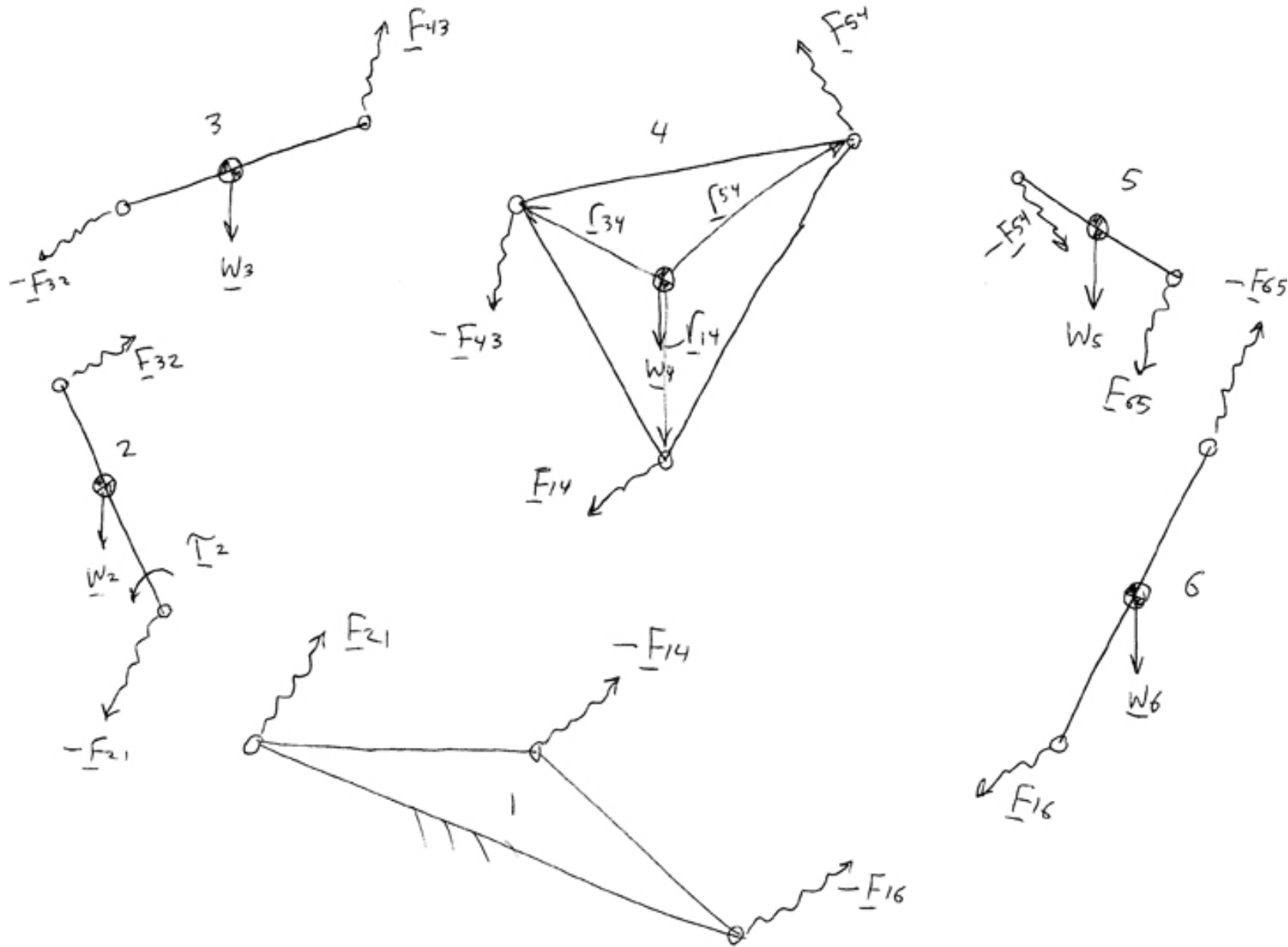


Watt I 6-Bar Mechanism



Watt II 6-Bar Mechanism

For example, here are the **Watt II six-bar mechanism** FBDs, ignoring external forces and moments.



The Watt II six-bar mechanism inverse dynamics 15x15 matrix-vector equation is given below.

$$\begin{bmatrix}
 -1 & 0 & 1 & 0 & 0 & 0 & 0 & 0 & 0 & 0 & 0 & 0 & 0 & 0 & 0 \\
 0 & -1 & 0 & 1 & 0 & 0 & 0 & 0 & 0 & 0 & 0 & 0 & 0 & 0 & 0 \\
 r_{12Y} & -r_{12X} & -r_{32Y} & r_{32X} & 0 & 0 & 0 & 0 & 0 & 0 & 0 & 0 & 0 & 0 & 1 \\
 0 & 0 & -1 & 0 & 1 & 0 & 0 & 0 & 0 & 0 & 0 & 0 & 0 & 0 & 0 \\
 0 & 0 & 0 & -1 & 0 & 1 & 0 & 0 & 0 & 0 & 0 & 0 & 0 & 0 & 0 \\
 0 & 0 & r_{23Y} & -r_{23X} & -r_{43Y} & r_{43X} & 0 & 0 & 0 & 0 & 0 & 0 & 0 & 0 & 0 \\
 0 & 0 & 0 & 0 & -1 & 0 & 1 & 0 & 1 & 0 & 0 & 0 & 0 & 0 & 0 \\
 0 & 0 & 0 & 0 & 0 & -1 & 0 & 1 & 0 & 1 & 0 & 0 & 0 & 0 & 0 \\
 0 & 0 & 0 & 0 & r_{34Y} & -r_{34X} & -r_{14Y} & r_{14X} & -r_{54Y} & r_{54X} & 0 & 0 & 0 & 0 & 0 \\
 0 & 0 & 0 & 0 & 0 & 0 & 0 & 0 & -1 & 0 & 1 & 0 & 0 & 0 & 0 \\
 0 & 0 & 0 & 0 & 0 & 0 & 0 & 0 & 0 & -1 & 0 & 1 & 0 & 0 & 0 \\
 0 & 0 & 0 & 0 & 0 & 0 & 0 & 0 & r_{45Y} & -r_{45X} & -r_{65Y} & r_{65X} & 0 & 0 & 0 \\
 0 & 0 & 0 & 0 & 0 & 0 & 0 & 0 & 0 & 0 & -1 & 0 & 1 & 0 & 0 \\
 0 & 0 & 0 & 0 & 0 & 0 & 0 & 0 & 0 & 0 & 0 & -1 & 0 & 1 & 0 \\
 0 & 0 & 0 & 0 & 0 & 0 & 0 & 0 & 0 & 0 & r_{56Y} & -r_{56X} & -r_{16Y} & r_{16X} & 0
 \end{bmatrix}
 \begin{Bmatrix}
 F_{21X} \\
 F_{21Y} \\
 F_{32X} \\
 F_{32Y} \\
 F_{43X} \\
 F_{43Y} \\
 F_{14X} \\
 F_{14Y} \\
 F_{54X} \\
 F_{54Y} \\
 F_{65X} \\
 F_{65Y} \\
 F_{16X} \\
 F_{16Y} \\
 \tau_2
 \end{Bmatrix}
 =
 \begin{Bmatrix}
 m_2 A_{G2X} \\
 m_2 (A_{G2Y} + g) \\
 I_{G2Z} \alpha_2 \\
 m_3 A_{G3X} \\
 m_3 (A_{G3Y} + g) \\
 I_{G3Z} \alpha_3 \\
 m_4 A_{G4X} \\
 m_4 (A_{G4Y} + g) \\
 I_{G4Z} \alpha_4 \\
 m_5 A_{G5X} \\
 m_5 (A_{G5Y} + g) \\
 I_{G5Z} \alpha_5 \\
 m_6 A_{G6X} \\
 m_6 (A_{G6Y} + g) \\
 I_{G6Z} \alpha_6
 \end{Bmatrix}$$

$$[A]\{v\} = \{b\}$$

Step 6. Solve for the unknowns (continued)

Like the four-bar mechanism, it is possible to partially decouple the solution to this problem. If we consider the FBDs of only links 5 and 6 first, this is 6 equations in 6 unknowns – this is verified by looking at the original 15x15 matrix and noting nine 6x1 columns of zeros (1, 2, 3, 4, 5, 6, 7, 8, 15) in the six rows 10 through 15. Here is a more efficient solution. The reduced 6x6 set of equations for links 5 and 6 is given below.

$$\begin{bmatrix} -1 & 0 & 1 & 0 & 0 & 0 \\ 0 & -1 & 0 & 1 & 0 & 0 \\ r_{45Y} & -r_{45X} & -r_{65Y} & r_{65X} & 0 & 0 \\ 0 & 0 & -1 & 0 & 1 & 0 \\ 0 & 0 & 0 & -1 & 0 & 1 \\ 0 & 0 & r_{56Y} & -r_{56X} & -r_{16Y} & r_{16X} \end{bmatrix} \begin{Bmatrix} F_{54X} \\ F_{54Y} \\ F_{65X} \\ F_{65Y} \\ F_{16X} \\ F_{16Y} \end{Bmatrix} = \begin{Bmatrix} m_5 A_{G5X} \\ m_5 (A_{G5Y} + g) \\ I_{G5Z} \alpha_5 \\ m_6 A_{G6X} \\ m_6 (A_{G6Y} + g) \\ I_{G6Z} \alpha_6 \end{Bmatrix}$$

$$[A_{56}] \{v_{56}\} = \{b_{56}\}$$

Solve for the six unknowns $\{v_{56}\} = [A_{56}]^{-1} \{b_{56}\}$. Second, consider the FBDs of only links 3 and 4: this is 6 equations in 6 unknowns – this is verified by looking at the original 15x15 matrix and noting seven 6x1 columns of zeros (1, 2, 11, 12, 13, 14, 15) in the six rows 4 through 9. Recognizing that now F_{54X} and F_{54Y} are now known from the above 6x6 partial solution, here is a more efficient solution. The reduced 6x6 set of equations for links 3 and 4 is given below.

$$\begin{bmatrix} -1 & 0 & 1 & 0 & 0 & 0 \\ 0 & -1 & 0 & 1 & 0 & 0 \\ r_{23Y} & -r_{23X} & -r_{43Y} & r_{43X} & 0 & 0 \\ 0 & 0 & -1 & 0 & 1 & 0 \\ 0 & 0 & 0 & -1 & 0 & 1 \\ 0 & 0 & r_{34Y} & -r_{34X} & -r_{14Y} & r_{14X} \end{bmatrix} \begin{Bmatrix} F_{32X} \\ F_{32Y} \\ F_{43X} \\ F_{43Y} \\ F_{14X} \\ F_{14Y} \end{Bmatrix} = \begin{Bmatrix} m_3 A_{G3X} \\ m_3 (A_{G3Y} + g) \\ I_{G3Z} \alpha_3 \\ m_4 A_{G4X} - F_{54X} \\ m_4 (A_{G4Y} + g) - F_{54Y} \\ I_{G4Z} \alpha_4 + r_{54Y} F_{54X} - r_{54X} F_{54Y} \end{Bmatrix}$$

$$[A_{34}] \{v_{34}\} = \{b_{34}\}$$

Solve for six unknowns $\{v_{34}\} = [A_{34}]^{-1} \{b_{34}\}$ and then use F_{32X} and F_{32Y} in the following 3x3 set of linear equations, from the link 2 FBD.

$$\begin{bmatrix} -1 & 0 & 0 \\ 0 & -1 & 0 \\ r_{12Y} & -r_{12X} & 1 \end{bmatrix} \begin{Bmatrix} F_{21X} \\ F_{21Y} \\ \tau_2 \end{Bmatrix} = \begin{Bmatrix} m_2 A_{G2X} - F_{32X} \\ m_2 (A_{G2Y} + g) - F_{32Y} \\ I_{G2Z} \alpha_2 + r_{32Y} F_{32X} - r_{32X} F_{32Y} \end{Bmatrix}$$

We do not need a matrix solution here since the X and Y force equations are decoupled. The solution is identical to that of the four-bar mechanism.

$$F_{21X} = -m_2 A_{G2X} + F_{32X}$$

$$F_{21Y} = -m_2 (A_{G2Y} + g) + F_{32Y}$$

$$\tau_2 = I_{G2Z} \alpha_2 + r_{32Y} F_{32X} - r_{32X} F_{32Y} - r_{12Y} F_{21X} + r_{12X} F_{21Y}$$

Matrix inversion requires approximately $\frac{3n^3}{\log n}$ and Gaussian elimination requires approximately $\frac{(n^2-1)n}{3} + n^2$ multiplications/divisions (Nering, 1974).

Number of Multiplications/Divisions

Method	Inversion	Gaussian	Reduction
15x15	8609	1345	84%
6x6 twice, plus decoupled link 2	1672	183	89%
Reduction in cost	81%	86%	

There is an astonishing **86% reduction in computational cost** for Gaussian elimination with the methods using 6x6 inversion twice, plus the decoupled link 2 solution. Also, the numerical accuracy may also improve with this method since we needn't do unnecessary calculations with the sixteen 6x1 columns of zeros.

Any mechanism with a dyad of binary links may be decoupled in this manner. Thus, the method is similar and the computational complexity identical for the **Stephenson I**, **Stephenson III**, **Watt I**, and **Watt II** six-bar mechanisms.

The **Stephenson II** six-bar mechanism does not include a dyad of binary links and so it cannot be solved like the other 4 six-bar mechanisms (first links 5 and 6, then links 3 and 4 with one unknown vector force from 5 and 6, then link 2 independently). But links 3, 4, 5, and 6 can be solved first independently of link 2: a 12x12 solution followed by the standard link 2 solution. The computational savings is not as impressive as in the former six-bar cases.

Number of Multiplications/Divisions, Stephenson II Six-Bar

Method	Inversion	Gaussian	Reduction
15x15	8609	1345	84%
12x12 plus decoupled link 2	4811	723	85%
Reduction in cost	44%	46%	

There is a **46% reduction in computational cost** for Gaussian elimination with the 12x12 plus decoupled link 2 method. Also, the numerical accuracy may also improve with this method since we needn't do unnecessary calculations with the three 12x1 columns of zeros.

6.8 Dynamic Balancing of Rotating Shafts

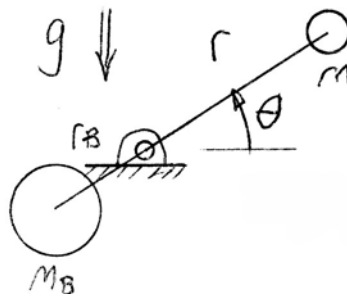
If high-speed shafts are unbalanced, this can lead to the following problems.

<ul style="list-style-type: none"> • unwanted vibrations • shaking forces • wear • noise 	<ul style="list-style-type: none"> • safety concerns • comfort of users/riders • less efficient • shorter service life
--	--

Let us start with the balancing of a single idealized point mass.

1) Static Balance

Moments about the rotating shaft must be balanced statically.



$$\sum \underline{M}_Z = 0 \quad -mgr \cos \theta + m_B g r_B \cos \theta = 0 \quad nr = m_B r_B$$

2) Dynamic Balance

Inertial forces due to motion must also be balanced.

Inertial forces are not actual forces but are effects of acceleration, e.g. centripetal force. Assuming constant input angular velocity ω , the inertial force is directed outward, opposite to the centripetal acceleration directed inward.

$$\underline{F}_I = -m \underline{A}_C = -m(\omega \times (\omega \times r)) \quad \text{the vector magnitude is } F_I = m r \omega^2$$

For dynamic balance, we again add a balance mass. The dynamic balance condition is:

$$\underline{F}_I + \underline{F}_{IB} = 0$$

The original and balance inertial forces must be equal in magnitude and opposite in direction. This vector balance condition is equivalent to the two scalar equations below.

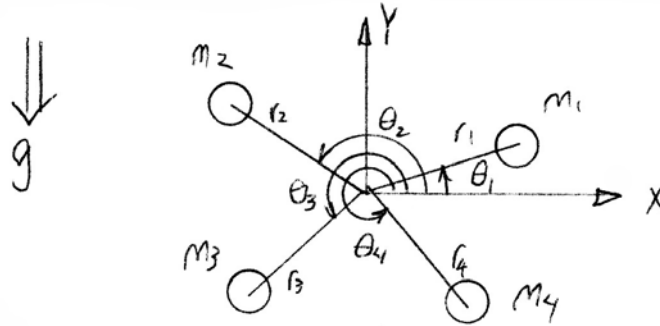
$$\begin{aligned} \sum F_x &= 0 & mr\omega^2 \cos \theta - m_B r_B \omega^2 \cos \theta &= 0 \\ \sum F_y &= 0 & mr\omega^2 \sin \theta - m_B r_B \omega^2 \sin \theta &= 0 \end{aligned}$$

Both equations yield the same condition as the static balance case, namely:

$$m\mathbf{r} = m_B \mathbf{r}_B$$

So, if a single mass is balanced statically, it is also balanced dynamically.

Now let us include a system of idealized point masses attached to the same rotating shaft.



1) Static Balance

The rotating shaft will be balanced statically if the system CG lies on the axis of rotation.

$$\underline{P}_{CG} = \begin{Bmatrix} \bar{X} \\ \bar{Y} \end{Bmatrix} = \begin{Bmatrix} 0 \\ 0 \end{Bmatrix}$$

Recall the scalar CG equations for a system of point masses:

$$X_{CG} = \bar{X} = \frac{\sum m_i x_i}{\sum m_i} \quad Y_{CG} = \bar{Y} = \frac{\sum m_i y_i}{\sum m_i}$$

Let us consider a system of four point masses. There are two equations to satisfy:

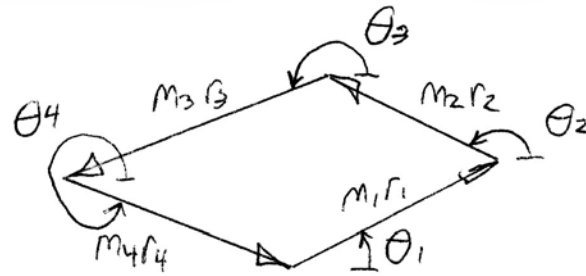
$$\sum_{i=1}^4 m_i r_i \cos \theta_i = 0 \quad \sum_{i=1}^4 m_i r_i \sin \theta_i = 0$$

where $x_i = r_i \cos \theta_i$, $y_i = r_i \sin \theta_i$, and the $\sum_{i=1}^4 m_i$ term in the denominator cancels out.

If we fix each $m_i r_i$, these are 2 equations in the four unknowns θ_i . Therefore, arbitrarily fix θ_1, θ_2 and solve for θ_3, θ_4 . This is equivalent to solving the four-bar linkage position problem.

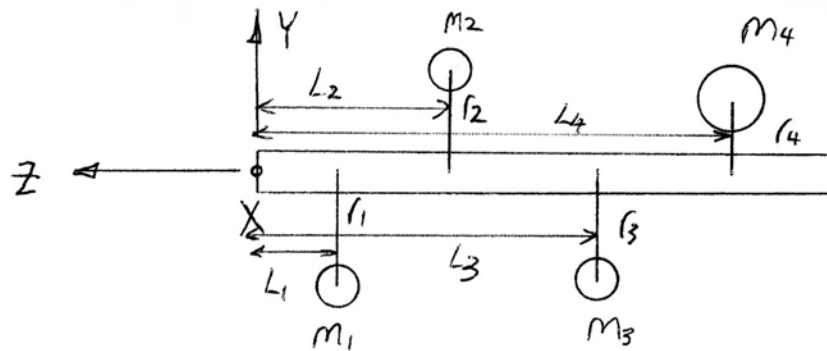
$$\begin{aligned} m_1 r_1 c_1 + m_2 r_2 c_2 + m_3 r_3 c_3 + m_4 r_4 c_4 &= 0 & r_2 c_2 + r_3 c_3 &= r_1 c_1 + r_4 c_4 \\ m_1 r_1 s_1 + m_2 r_2 s_2 + m_3 r_3 s_3 + m_4 r_4 s_4 &= 0 & r_2 s_2 + r_3 s_3 &= r_1 s_1 + r_4 s_4 \end{aligned}$$

Let $R_i = m_i r_i$; the vectors 1 and 4 are reversed compared to the four-bar mechanism. So we know how to solve these equations. The shaft will be statically balanced for any shaft angle θ . Here is the associated figure.



2) Dynamic Balance

For dynamic balance, we must consider the front view in addition to the previously-shown side view.



If the following conditions are satisfied assuming constant ω , we will have dynamic balance.

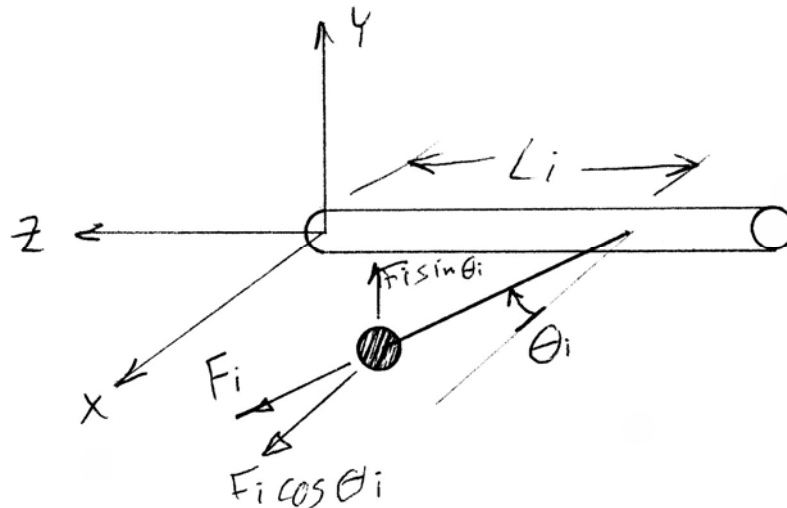
$$\begin{aligned} \sum F_x &= 0 & \sum M_x &= 0 \\ \sum F_y &= 0 & \sum M_y &= 0 \\ \sum F_z &= 0 & \sum M_z &= 0 \end{aligned}$$

Let us consider each in turn.

$$\begin{aligned} \sum F_x &= \sum_{i=1}^4 m_i r_i \omega^2 \cos \theta_i = \sum_{i=1}^4 m_i r_i \cos \theta_i = 0 \\ \sum F_y &= \sum_{i=1}^4 m_i r_i \omega^2 \sin \theta_i = \sum_{i=1}^4 m_i r_i \sin \theta_i = 0 \\ \sum F_z &\rightarrow 0 = 0 \end{aligned}$$

The $\sum F_x$ and $\sum F_y$ equations are already satisfied by the static balancing, because ω^2 divides out.

The $\sum F_z$ equation yields nothing because all inertial forces are in the XY plane.



$$\sum M_x = \sum_{i=1}^4 m_i r_i \omega^2 \sin \theta_i L_i = 0$$

$$\sum M_y = -\sum_{i=1}^4 m_i r_i \omega^2 \cos \theta_i L_i = 0$$

$$\sum M_z \rightarrow 0 = 0$$

The $\sum M_x$ and $\sum M_y$ equations must be solved to satisfy dynamic balancing. The $\sum M_z$ equation yields nothing because all inertial forces pass through the axis of rotation.

We fixed each $m_i r_i$, we previously determined θ_i , and the ω^2 term divides out. Therefore, we have two equations in the four unknowns L_i ; arbitrarily fix L_1, L_2 and solve for L_3, L_4 . The result is two linear equations in the two unknowns.

$$\begin{aligned} m_1 r_1 \sin \theta_1 L_1 + m_2 r_2 \sin \theta_2 L_2 + m_3 r_3 \sin \theta_3 L_3 + m_4 r_4 \sin \theta_4 L_4 &= 0 \\ m_1 r_1 \cos \theta_1 L_1 + m_2 r_2 \cos \theta_2 L_2 + m_3 r_3 \cos \theta_3 L_3 + m_4 r_4 \cos \theta_4 L_4 &= 0 \end{aligned}$$

$$\begin{bmatrix} m_3 r_3 \sin \theta_3 & m_4 r_4 \sin \theta_4 \\ m_3 r_3 \cos \theta_3 & m_4 r_4 \cos \theta_4 \end{bmatrix} \begin{Bmatrix} L_3 \\ L_4 \end{Bmatrix} = \begin{Bmatrix} -m_1 r_1 \sin \theta_1 L_1 - m_2 r_2 \sin \theta_2 L_2 \\ -m_1 r_1 \cos \theta_1 L_1 - m_2 r_2 \cos \theta_2 L_2 \end{Bmatrix}$$

Solve for L_3, L_4 and the system will be balanced statically and dynamically.

7. Gears and Cams

7.1 Gears

7.1.3 Gear Trains

To obtain a higher gear ratio than practical with a single pair of standard involute spur gears, one can mate any number of spur gears in a gearbox, or gear train. The leftmost gear is the driving gear and the rightmost is the output gear. All intermediate gears are first the driven gear and then the driving gear as we proceed from left to right. Let us calculate the overall gear ratio n_{GT} .

$$n_{GT} = \frac{\omega_{IN}}{\omega_{OUT}}$$

Example

We can find the overall gear ratio by canceling neighboring intermediate angular velocities.

Each term in the above product may be replaced by its known number of teeth ratio.

All intermediate ratios cancel, so

We could have done the same with pitch radii instead of number of teeth because they are in direct proportion.

So, the intermediate gears are **idlers**. Their number of teeth effect cancels out, but they do change direction. We should have included the +/- signs, by inspection. For gear trains composed of externally-meshing spur gear pairs:

odd number of gears

even number of gears

the output is in the same direction as the input

the output is in the opposite direction as the input

Improved gear train

That gear train concept did not work. Now let us mate any number of spur gears, where the driving and driven gears are distinct, because each pair is rigidly attached to the same shaft. Again, let us calculate the overall gear ratio.

$$n_{GT} = \frac{\omega_{IN}}{\omega_{OUT}}$$

Example

Again, we use the equation

But now the gears rigidly attached to the same shaft have the same angular velocity ratio, so

The general formula for this case is

Again, we must consider direction

For gear trains composed of externally-meshing spur gear pairs:

odd number of pairs	the output is in the opposite direction as the input
even number of pairs	the output is in the same direction as the input

7.1.4 Involute Spur Gear Standardization

Rolling Cylinders

Mating spur gears are based on two pitch circles rolling without slip. These are fictitious circles, i.e. you cannot look on a gear to see them. The actual gear teeth both roll and slide with respect to each other (via the two-dof gear joint).

Fundamental Law of Gearing

The angular velocity between the gears of a gearset must remain constant throughout the mesh.

From our study of linkage velocity, we know this is no easy feat. Velocity ratios in a linkage vary wildly over the range of motion.

$$\text{Velocity Ratio} \quad \text{VR} = \frac{\omega_{OUT}}{\omega_{IN}} = \pm \frac{r_{IN}}{r_{OUT}} = \frac{1}{n}$$

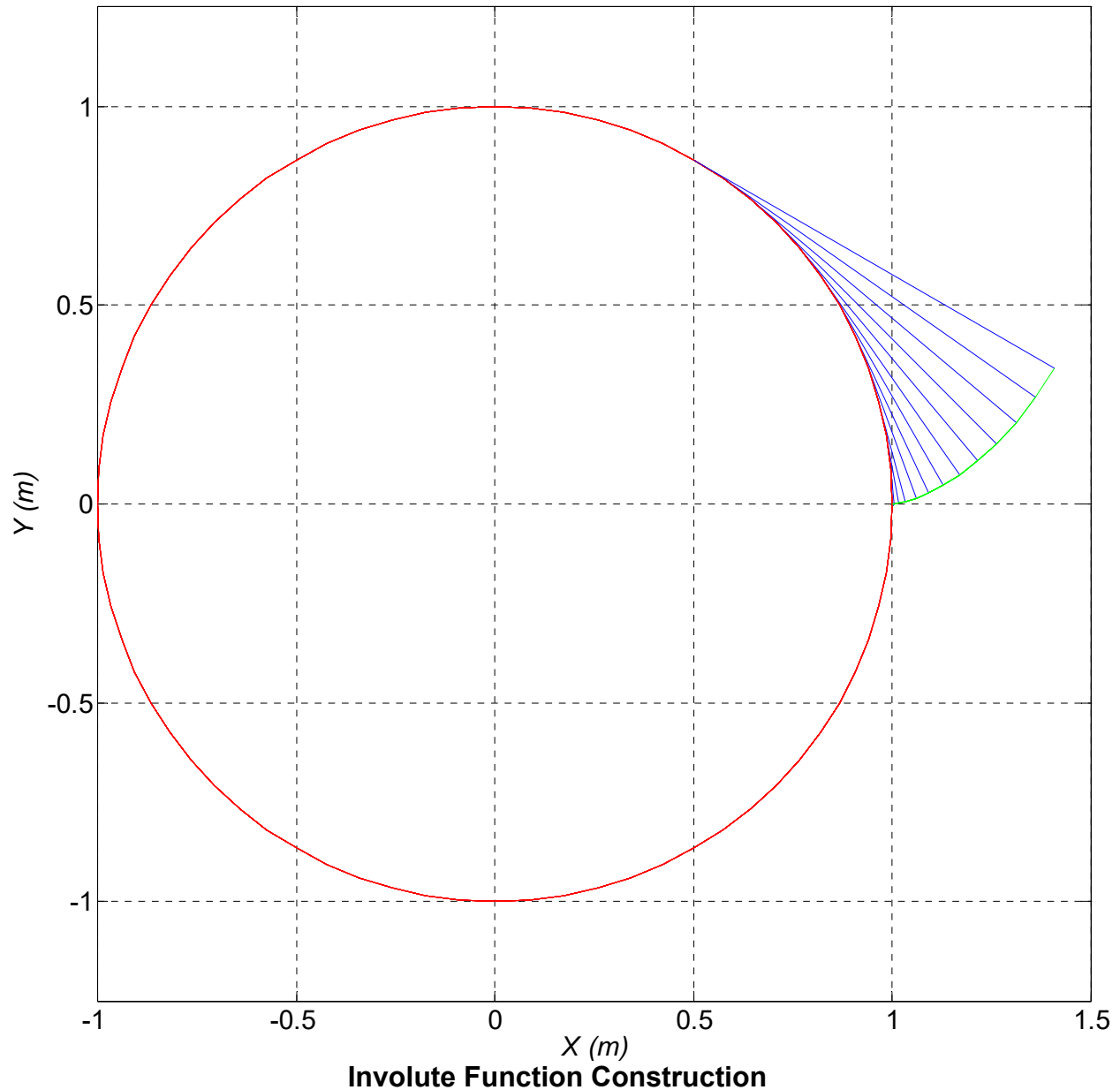
$$\text{Torque Ratio} \quad \text{TR} = \frac{\omega_{IN}}{\omega_{OUT}} = \pm \frac{r_{OUT}}{r_{IN}} = n$$

The velocity ratio is the inverse of the gear ratio n and the torque ratio is the same as the gear ratio n defined previously. The torque ratio is also called Mechanical Advantage (MA).

Involute Function

Standard spur gears have an involute tooth shape. If the gears' center distance is not perfect (tolerances, thermal expansion, wear – in design the center distance is increased slightly by the engineer to allow for these effects; this is called clearance), the angular velocity ratio will still be constant to satisfy the **Fundamental Law of Gearing**.

The **involute of a circle** is a curve generated by unwrapping a taut string from the circumference of a so-called base circle, always keeping it tangent to the circle. The figure below has $t_h = [0:5:60]^*DR$ and $r_b = 1\text{ m}$. The **red** circle is the gear base circle, the **blue** lines are the taut tangent construction lines, and the **green** curve is the involute function.



In polar coordinates (θ, r) , the parametric equations for the involute of a circle are given below.

$$\theta = \tan t - t$$

$$r = r_b \sec t$$

where t is the independent parameter and r_b is the base circle radius. In Cartesian coordinates (x_I, y_I) :

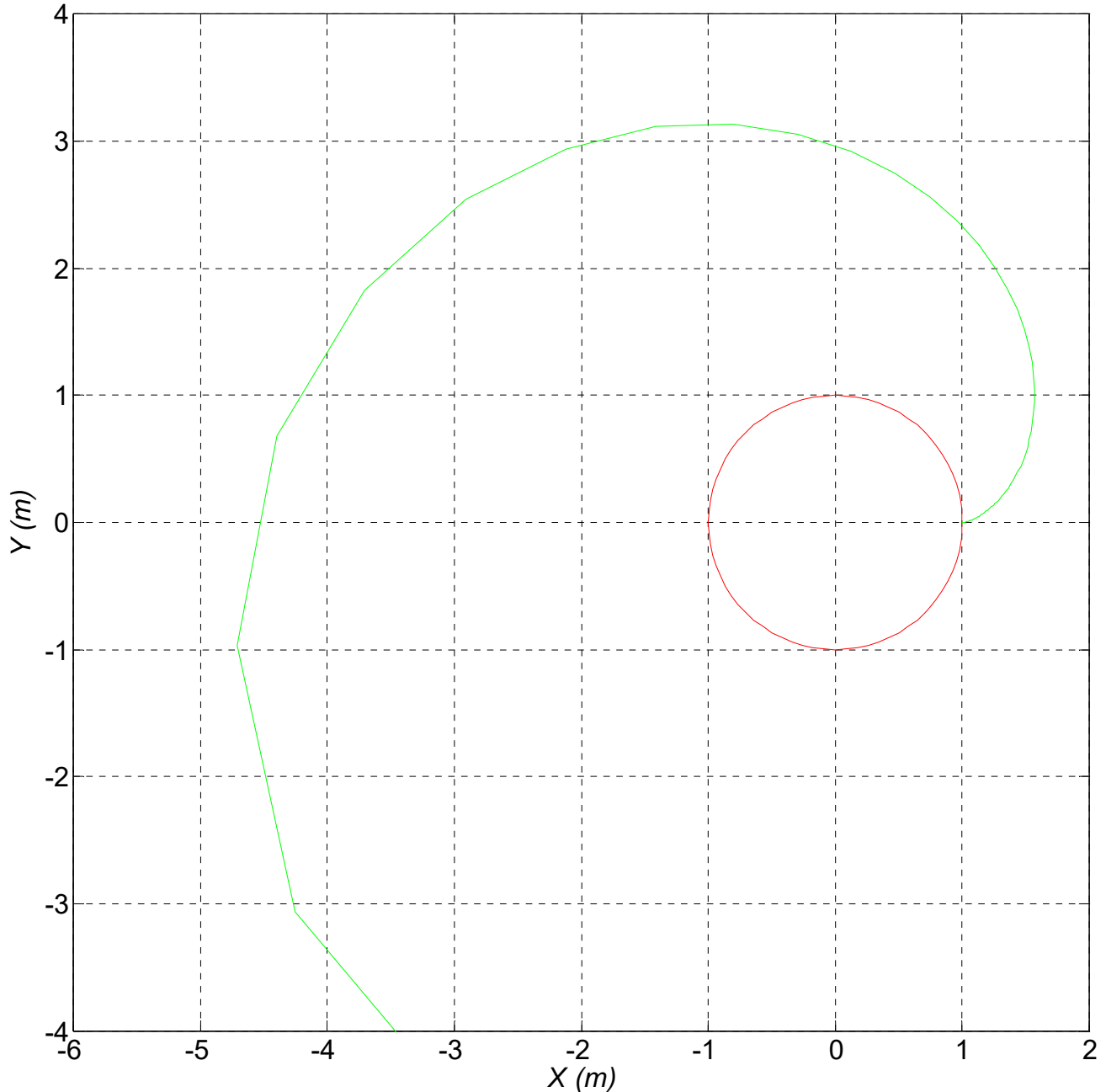
$$x_I = r \cos \theta = r_b \sec t \cos(\tan t - t)$$

$$y_I = r \sin \theta = r_b \sec t \sin(\tan t - t)$$

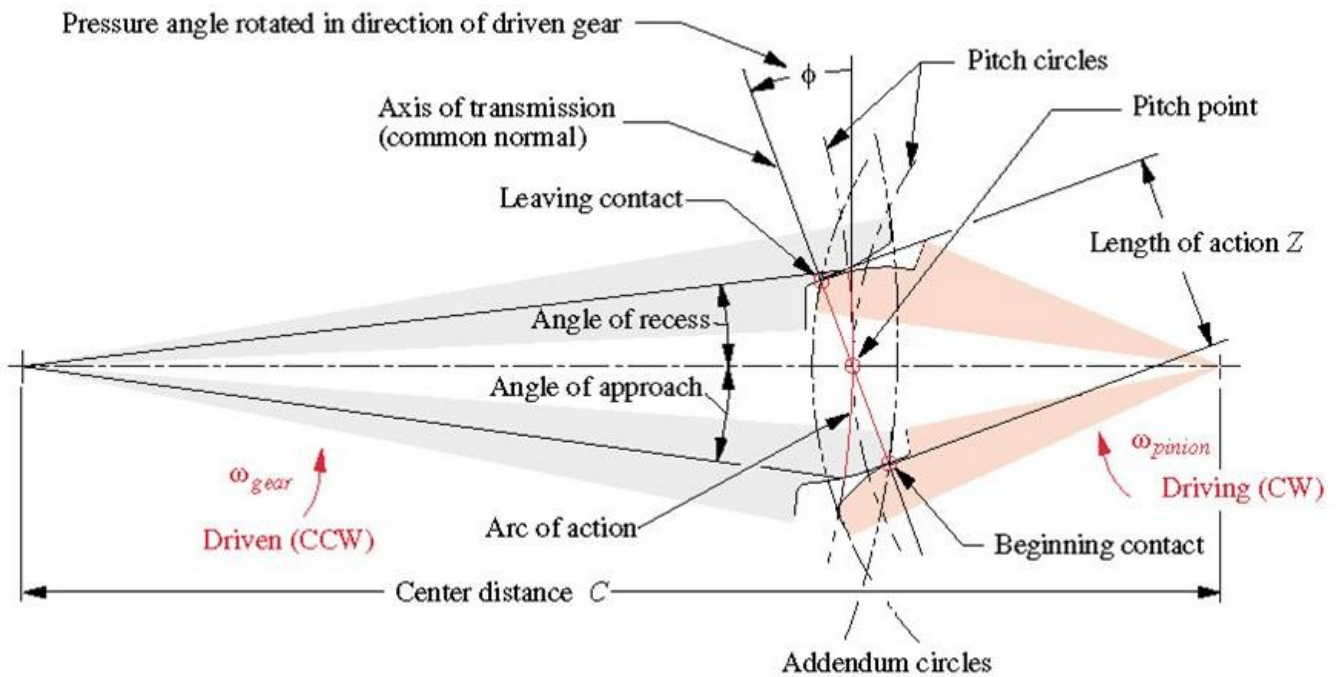
Involute Function Example

The plot below shows the involute function for a circle of $r_b = 1\text{ m}$. The parameter range is $\mathbf{t} = [0:1:80]*\mathbf{DR}$; near the circle the involute points are very close to each other and farther away the step size increases dramatically.

The involute function is symmetric (try $\mathbf{t} = [0:5:360]*\mathbf{DR}$) but watch out for those intermediate steps). Gear teeth only require the involute near the base circle, with two symmetric sides.



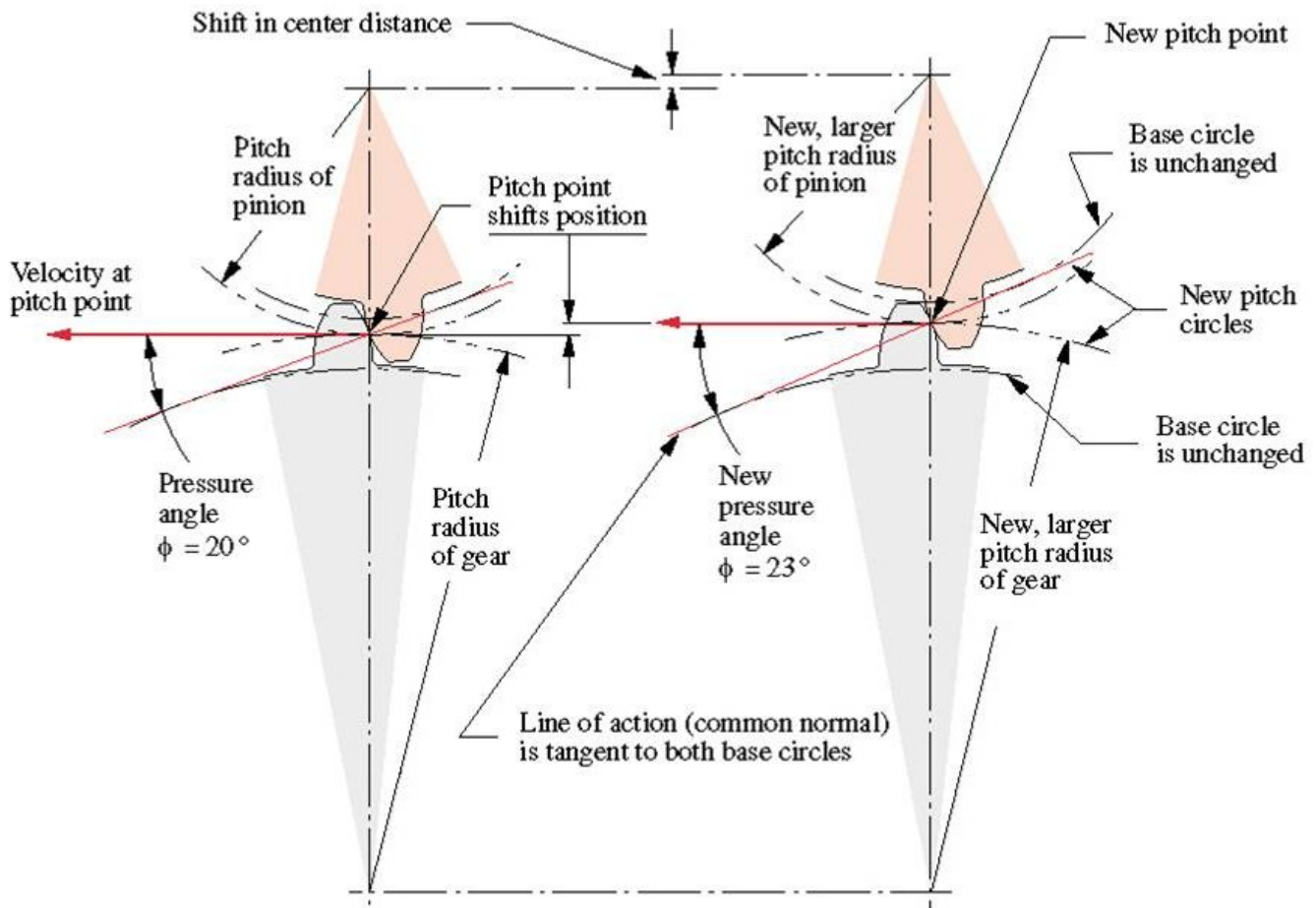
Involute Function of a Circle



Norton (2008)

The **length of contact** is measured along the axis of transmission. The beginning of contact is when the tip of the driven gear tooth intersects the axis of transmission. The end of contact is when the tip of driving gear tooth intersects the **axis of transmission**, as shown in the figure above. Only one or two teeth are in contact at any one time for standard spur gears.

For harmonic gearing, many teeth are in contact at any one time, which provides a higher gear ratio in a smaller package.



Norton (2008)

Increasing the center distance increases the **pressure angle** and increases the **pitch circle radii**, but doesn't change the **base circles** (obviously – the gears are made based on their own constant r_b). Thanks to the **involute tooth shape**, increasing the center distance does not affect the **angular velocity ratio**. This is why the involute function is so widely used in spur gears.

The relationship from before still applies with an increase in center distance.

$$r_b = r_p \cos \phi$$

Again, r_b is fixed, and r_p and ϕ both increase – the cosine function maintains the constant r_b .

Spur Gear Standardization

Gear standardization is used to allow interchangeability in manufacturing and to allow meshing of different size gears (different pitch radii and number of teeth) to achieve desired gear ratios. For two spur gears to mesh, they must have

- 1) the same **pressure angle** (see previous figures and definition)
- 2) the same **diametral pitch** (see the equation below)
- 3) **standard tooth proportions** (see the figure below)

diametral pitch
$$P_d = \frac{N}{d}$$

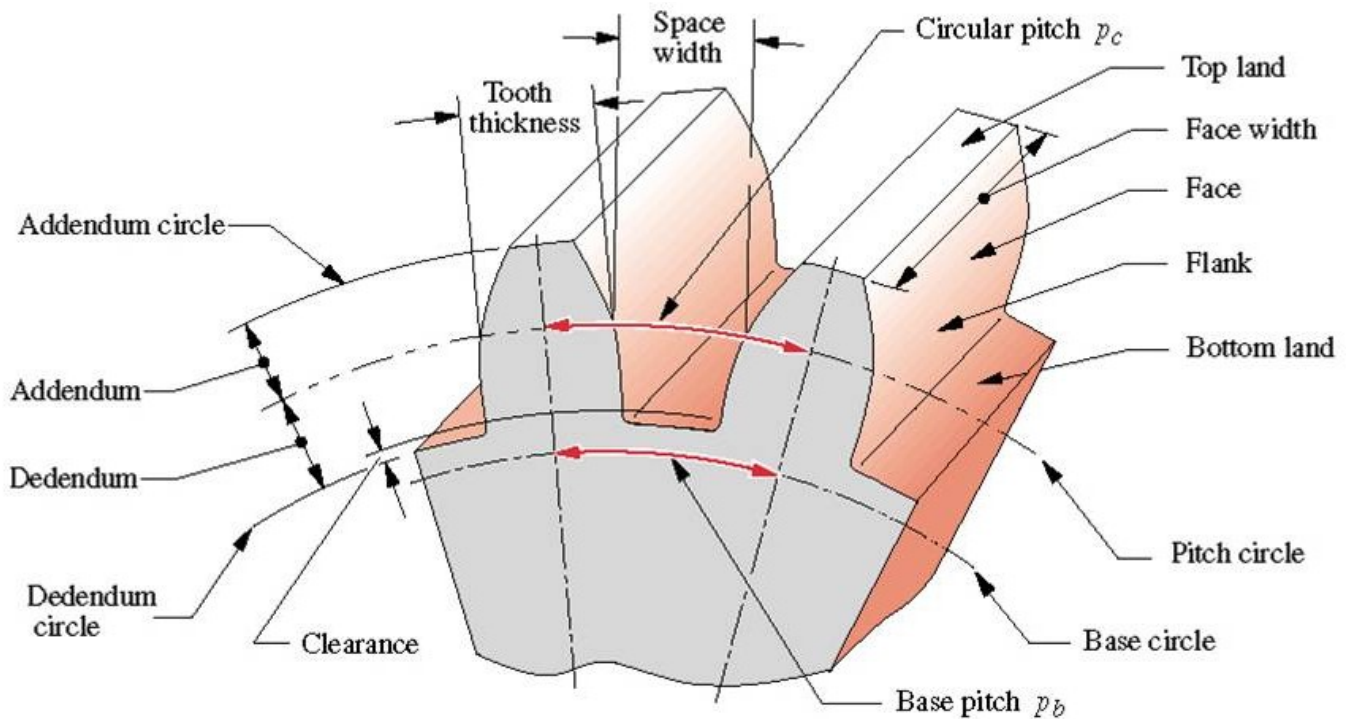
Where N is the number of teeth and d is the pitch diameter, both for each gear.

module
$$m = \frac{d}{N} = \frac{1}{P_d}$$

Module is the SI version of diametral pitch (it is the inverse). SI gears are not interchangeable with English system gears because of different tooth proportion standards.

circular pitch
$$P_c = \frac{\pi d}{N}$$

Circular pitch is the circumferential distance (arc length) between teeth along the pitch circle of a spur gear.



from Norton (2008)

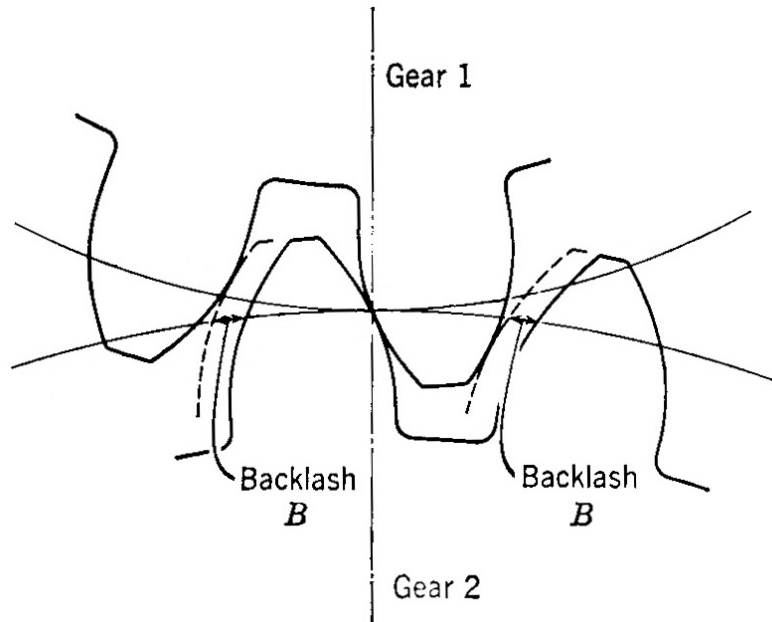
Standard involute tooth proportions

- **Addendum** is radial distance from pitch circle to *top land* of tooth.
- **Dedendum** is radial distance from pitch circle to *bottom land* of tooth (not to the base circle).
- **Clearance** is radial distance from *bottom land* to mating gear *top land* (radial backlash).
- **Face width** is thickness of tooth and gear (mating widths needn't be the same).
- **Tooth thickness** t is the circumferential arc length of each tooth. It is related to the circular pitch p_c and backlash (next page) b by

$$p_c = 2t + b$$

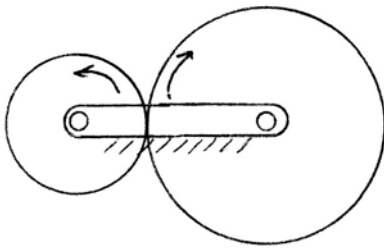
Backlash

Backlash B is the distance between mating teeth measured along the pitch circle circumference. Backlash can be thought of as circumferential clearance. All real-world gears must have some backlash in order to still function despite real-world problems of manufacturing tolerances, thermal expansion, wear, etc. However, one must minimize backlash for smooth operation. For example, robot joints must be driven both directions. Upon changing direction, nothing happens until the backlash is passed, and then an impact occurs, which is bad for gear dynamics. This is a non-linear effect in robotics. On earth gravity tends to load the backlash for predictable effects. In space however, the backlash is less predictable.



7.1.5 Planetary Gear Trains

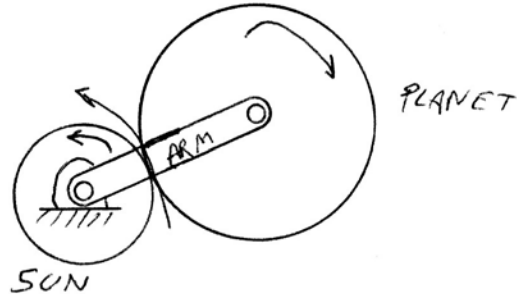
Planetary gear trains are also called epicyclic gear trains. The sun gear rotates about a fixed axis. Each planet gear rotates about its own axis and also orbits the sun gear. This happens with direct meshing of teeth, unlike celestial planetary motion. The arm link (which is a rigid body with no teeth) carries the planet(s) around the sun. The arm has a revolute joint to the sun gear on one side and another revolute joint to the planet gear(s) on the other side. Planetary gear trains have two-dof, so two inputs must be given to control the mechanism. For instance, one can drive the sun gear and the arm link with independent external motors. Alternatively, the sun gear may be fixed and the arm link driven. Using planetary gear trains, one can obtain a higher gear ratio in a smaller package, compared to non-planetary gear trains.



Conventional Gear Pair

$$M = 3(3 - 1) - 2(2) - 1(1) = 1$$

$$n = \frac{\omega_{IN}}{\omega_{OUT}} = \frac{r_{OUT}}{r_{IN}} = \frac{N_{OUT}}{N_{IN}}$$



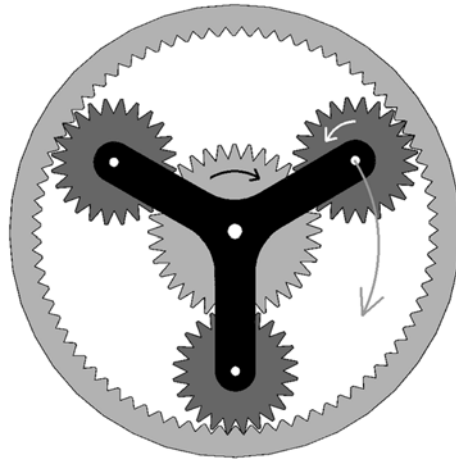
Planetary Gear Train

$$M = 3(4 - 1) - 2(3) - 1(1) = 2$$

$$n = \frac{\omega_{IN}}{\omega_{OUT}} = ?$$

We present the tabular method below to determine the gear ratio for various planetary gear trains.

Planetary Gear Train Mobility



Planetary Gear Train with Three Planets and Internally-Meshing Ring Gear (note – figure does not show the necessary ground link)

As stated and derived above, planetary gear trains have $M = 2$ dof, so they are technically classified as a robot. However, they are almost always used as mechanisms with $M = 1$ dof, by fixing to ground either the sun gear or the internally-meshing ring gear. (One cannot fix the arm, or it would no longer be a planetary gear arrangement!)

The mobility calculation using the planar Kutzbach equation is more complicated for the case shown on this page, so we will now present that. For the planetary gear train above with three planet gears and an internally-meshing ring gear, there are 7 rigid links (ground link, sun gear, three planet gears, ring gear, and non-toothed arm link). There are 6 R joints (3 between the arm and planet gears, and then a triple R-joint in the middle, connecting, the sun gear, the ring gear, and the arm to ground independently). There are 6 gear joints, between the sun and planet, and the planet and ring gears, 3 times). So we calculate the following mobility for the overall device:

$$M = 3(7 - 1) - 2(6) - 1(6) = 18 - 12 - 6 = 0 \text{ dof}$$

Clearly this is incorrect since we know this device has freedom to move and is not a statically-determinate structure. Thus, we see another example where the Kutzbach equation fails due to lack of knowledge of special geometry.

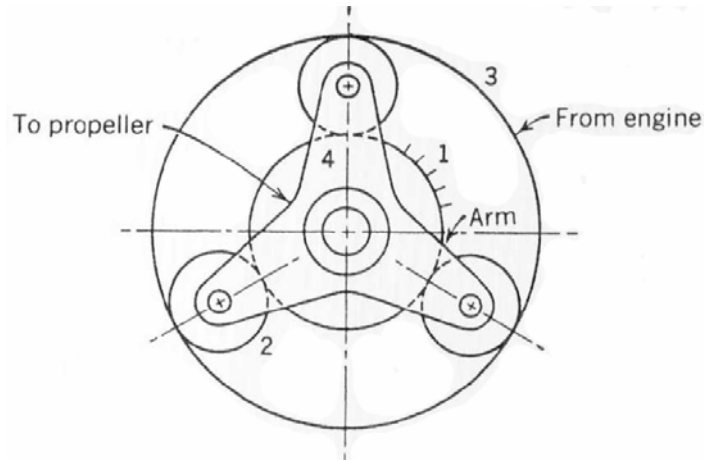
This device would function identically kinematically if there were a single-lobed arm and a single planet gear. Therefore, let us calculate the mobility with this in mind. This simplified case has 5 rigid links, 4 R joints, and 2 gear joints, yielding:

$$M = 3(5 - 1) - 2(4) - 1(2) = 12 - 8 - 2 = 2 \text{ dof}$$

as expected. As mentioned above, a practical planetary gear mechanism requires 1 dof, so we must lock either the sun gear or the ring gear to the ground link, yielding:

$$M = 3(4 - 1) - 2(3) - 1(2) = 9 - 6 - 2 = 1 \text{ dof}$$

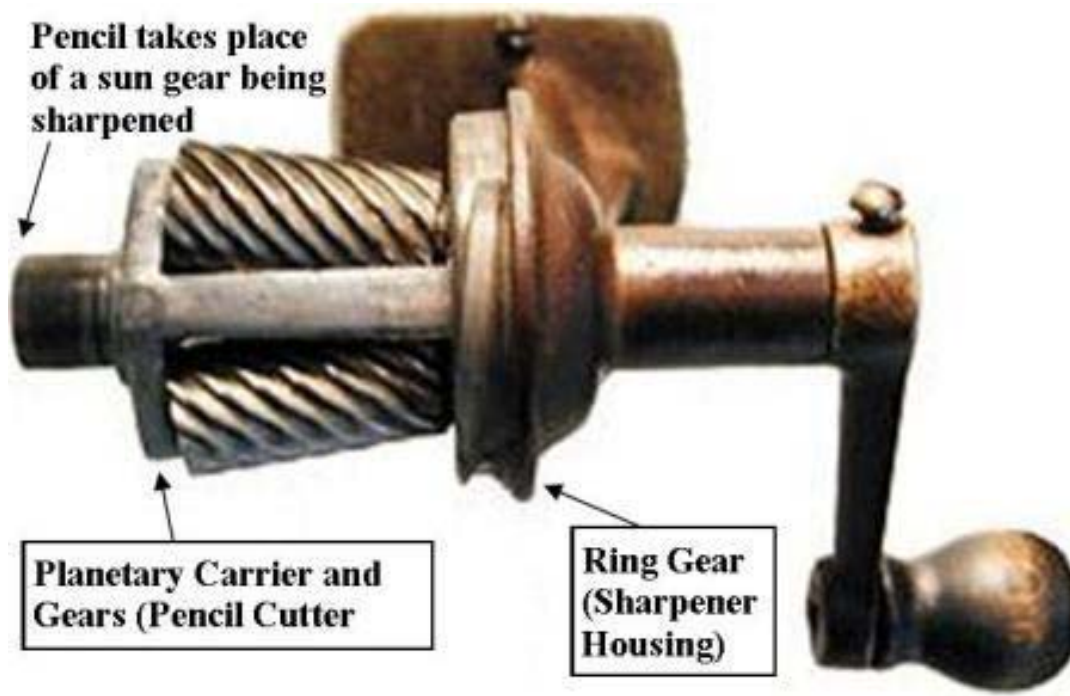
Planetary Gear Train Applications



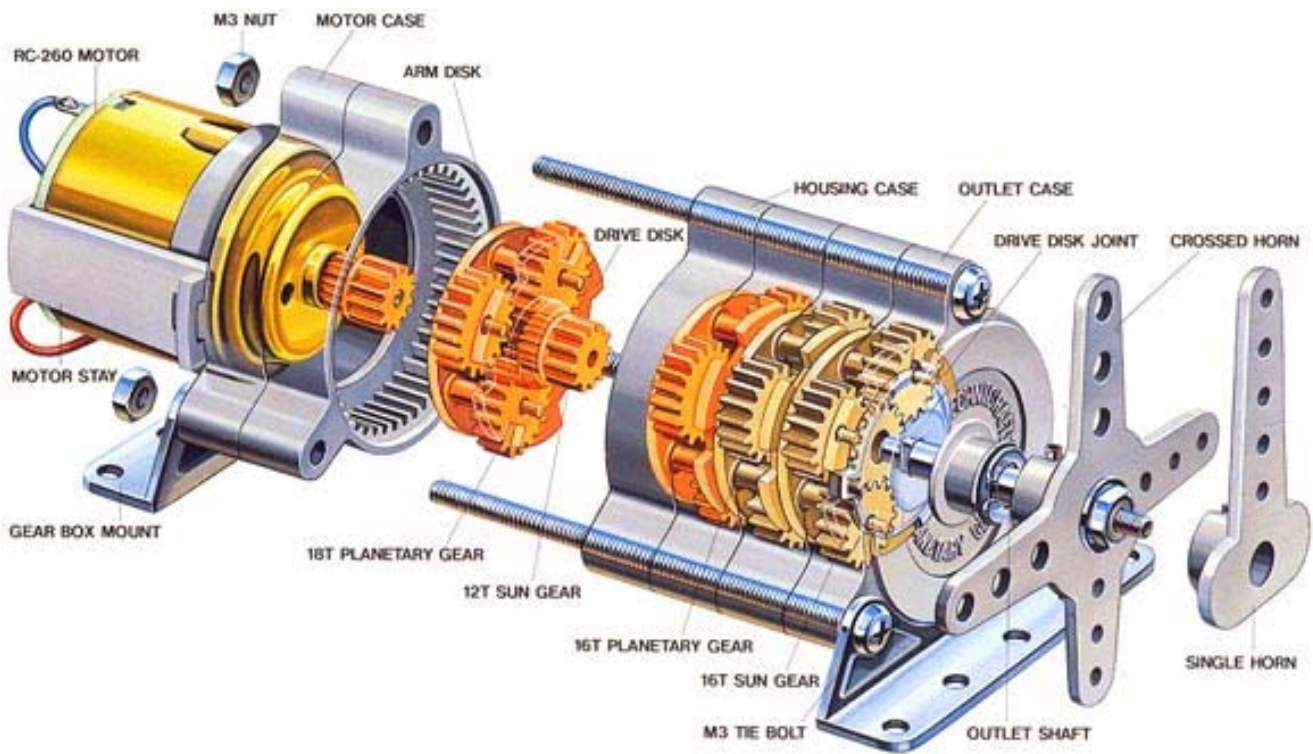
Airplane Propeller Transmission

The $M = 2$ dof from the previous page is constrained to $M = 1$ dof by fixing the sun gear to ground in the airplane propeller example above.

Planetary gear train applications include airplane propellers, some automotive transmissions and differentials, machine tools, hoists, and a hub-enclosed multi-speed bicycle transmission.



Old-Fashioned Pencil Sharpener



Planetary Gear Box in Stages

This is a commercial planetary gear set with 8 possible ratios (4:1, 5:1, 16:1, 20:1, 25:1, 80:1, 100:1, 400:1).

servocity.com

Table Method Analysis

First, consider a simplified planetary gear system with $\omega_s = 0$. With the sun gear as the fixed link, we have a 1-dof system. Given the input ω_A , calculate the absolute value of ω_P . The **Table Method** is based on the following relative velocity equation.

$$\underline{\omega}_G = \underline{\omega}_A + \underline{\omega}_{G/A}$$

This is a vector equation, but since all rotations are about the Z axis, we just use the magnitudes and + for CCW and – for CW , according to the right-hand-rule. This equation is written for each gear in the system (replace G with the appropriate index). A stands for arm. ω_G, ω_A are the absolute angular velocities of a gear and the arm link. $\omega_{G/A}$ is the relative velocity of a gear with respect to the moving arm link. Construct a table as below; each row is the relative equation written for a different gear.

G	ω_G	=	ω_A	+	$\omega_{G/A}$
S					
P					

First, fill in the given information.

G	ω_G	=	ω_A	+	$\omega_{G/A}$
S	0		ω_A		
P			ω_A		

Each row must add up according to the relative velocity equation

G	ω_G	=	ω_A	+	$\omega_{G/A}$
S	0		ω_A		$-\omega_A$
P			ω_A		

Now we can fill in down the relative column, using a simple gear ratio (relative to the arm).

$$\frac{\omega_{P/A}}{\omega_{S/A}} = -\frac{N_S}{N_P} \quad \omega_{P/A} = -\frac{N_S}{N_P} \omega_{S/A} = \frac{N_S}{N_P} \omega_A$$

G	ω_G	=	ω_A	+	$\omega_{G/A}$
S	0		ω_A		$-\omega_A$
P			ω_A		$\frac{N_S}{N_P} \omega_A$

The last row must add up according to the relative equation, to finish the table.

<i>G</i>	ω_G	=	ω_A	+	$\omega_{G/A}$
<i>S</i>	0		ω_A		$-\omega_A$
<i>P</i>	$\left(1 + \frac{N_S}{N_P}\right)\omega_A$		ω_A		$\frac{N_S}{N_P}\omega_A$

Therefore, the absolute angular velocity of the planetary gear is $\omega_p = \left(1 + \frac{N_S}{N_P}\right)\omega_A$. Since the sign is positive, it has the same direction as ω_A (CCW).

Calculate Effective Gear Ratio

$$n = \frac{\omega_{IN}}{\omega_{OUT}} = \frac{\omega_A}{\omega_p} = \frac{1}{1 + \frac{N_S}{N_P}} = \frac{N_P}{N_P + N_S}$$

Example

$$N_S = 10 \quad N_P = 40 \quad \omega_S = 0 \quad \omega_A = +100 \text{ rpm, CCW}$$

$$\omega_p = \left(1 + \frac{10}{40}\right)100 = 125 \text{ rpm, CCW}$$

$$n = \frac{N_P}{N_P + N_S} = \frac{40}{40 + 10} = 0.8$$

$$\text{Check } n = \frac{\omega_A}{\omega_p} \rightarrow \omega_p = \frac{\omega_A}{n} = \frac{100}{0.8} = 125$$

So we see that with $\omega_S = 0$, the gear ratio is not higher than the conventional gear train.

$$n = \frac{N_P}{N_S} = \frac{40}{10}$$

Let us include $\omega_S \neq 0$ next.

Table Method Analysis

Now we present a more general system with $\omega_S \neq 0$.

- 1) The given information is starred (*).
- 2) The S equation must add up; therefore $\omega_{S/A} = \omega_S - \omega_A$.
- 3) Fill down the right column using a simple gear train, relative to arm A .

$$\frac{\omega_{P/A}}{\omega_{S/A}} = -\frac{N_S}{N_P} \quad \omega_{P/A} = -\frac{N_S}{N_P} \omega_{S/A} = -\frac{N_S}{N_P} (\omega_S - \omega_A) = \frac{N_S}{N_P} (\omega_A - \omega_S)$$

- 4) The P equation must add up; therefore:

$$\omega_P = \omega_A + \frac{N_S}{N_P} (\omega_A - \omega_S) = \left(1 + \frac{N_S}{N_P}\right) \omega_A - \frac{N_S}{N_P} \omega_S$$

G	ω_G	=	ω_A	+	$\omega_{G/A}$
S	* ω_S		* ω_A		$\omega_S - \omega_A$
P	$\left(1 + \frac{N_S}{N_P}\right) \omega_A - \frac{N_S}{N_P} \omega_S$		* ω_A		$\frac{N_S}{N_P} (\omega_A - \omega_S)$

Examples

$\omega_S \neq 0$

- 1) $N_S = 10$ $N_P = 40$ $\omega_S = -100$ rpm, CW $\omega_A = +100$ rpm, CCW
 $\omega_P = \left(1 + \frac{10}{40}\right) 100 - \frac{10}{40} (-100) = 125 + 25 = +150$ rpm, CCW Still not a big ratio.

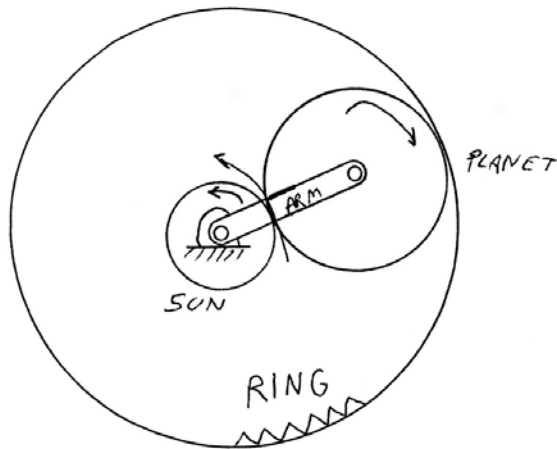
- 2) $N_S = 40$ $N_P = 10$ $\omega_S = -100$ rpm, CW $\omega_A = +100$ rpm, CCW
 $\omega_P = \left(1 + \frac{40}{10}\right) 100 - \frac{40}{10} (-100) = 500 + 400 = +900$ rpm, CCW That's a big ratio.

- 3) $N_S = 40$ $N_P = 10$ $\omega_S = +125$ rpm, CCW $\omega_A = +100$ rpm, CCW
 $\omega_P = \left(1 + \frac{40}{10}\right) 100 - \frac{40}{10} (125) = 500 - 500 = 0$

In Example 3, the *Sun* and *Arm* rotational velocities cancel so the absolute angular velocity of the *Planet* is zero.

Table Method Analysis

Now let us consider an even more general system with $\omega_s \neq 0$, also adding an internal-teeth ring gear.



- 1) The given information is starred (*).
- 2) The first two rows are identical to the case above.
- 3) Fill down the right column using a simple gear train, relative to arm A.

$$\frac{\omega_{R/A}}{\omega_{P/A}} = + \frac{N_P}{N_R} \quad \omega_{R/A} = + \frac{N_P}{N_R} \omega_{P/A} = + \frac{N_P}{N_R} \frac{N_S}{N_P} (\omega_A - \omega_S) = \frac{N_S}{N_R} (\omega_A - \omega_S)$$

- 4) The R equation must add up; therefore:

$$\omega_R = \omega_A + \frac{N_S}{N_R} (\omega_A - \omega_S) = \left(1 + \frac{N_S}{N_R} \right) \omega_A - \frac{N_S}{N_R} \omega_S$$

G	ω_G	=	ω_A	+	$\omega_{G/A}$
S	* ω_S		* ω_A		$\omega_S - \omega_A$
P	$\left(1 + \frac{N_S}{N_P} \right) \omega_A - \frac{N_S}{N_P} \omega_S$		* ω_A		$\frac{N_S}{N_P} (\omega_A - \omega_S)$
R	$\left(1 + \frac{N_S}{N_R} \right) \omega_A - \frac{N_S}{N_R} \omega_S$		* ω_A		$\frac{N_S}{N_R} (\omega_A - \omega_S)$

Examples $\omega_s \neq 0$ plus ring gear

$$1) N_S = 10 \quad N_P = 40 \quad N_R = 100 \quad \omega_s = -100 \text{ rpm, CW} \quad \omega_A = +100 \text{ rpm, CCW}$$

$$\omega_R = \left(1 + \frac{10}{100}\right) 100 - \frac{10}{100} (-100) = 110 + 10 = +120 \text{ rpm, CCW}$$

$$2) N_S = 40 \quad N_P = 20 \quad N_R = 80 \quad \omega_s = -100 \text{ rpm, CW} \quad \omega_A = -200 \text{ rpm, CW}$$

$$\omega_P = \left(1 + \frac{N_S}{N_P}\right) \omega_A - \frac{N_S}{N_P} \omega_s$$

$$\omega_P = \left(1 + \frac{40}{20}\right) (-200) - \frac{40}{20} (-100) = -600 + 200 = -400 \text{ rpm, CW}$$

$$\omega_R = \left(1 + \frac{N_S}{N_R}\right) \omega_A - \frac{N_S}{N_R} \omega_s$$

$$\omega_R = \left(1 + \frac{40}{80}\right) (-200) - \frac{40}{80} (-100) = -300 + 50 = -250 \text{ rpm, CW}$$

7.2 Cams

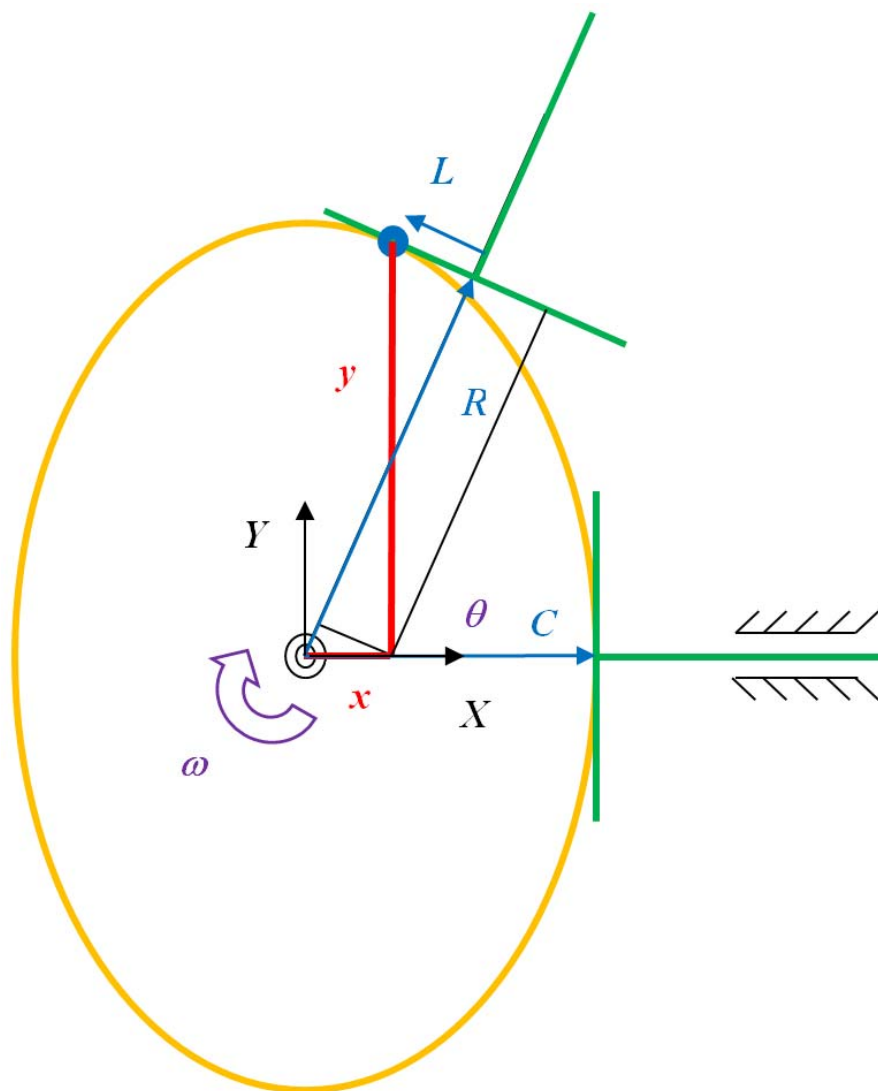
7.2.3 Analytical Cam Synthesis

Disk Cam with Radial Flat-Faced Follower

Assume a valid cam motion profile has been designed according to the **Fundamental Law of Cam Design**; i.e. we now have continuous S , V , A curves. Given the motion profile found by the engineer, now we must determine the cam contour.

Is it as simple as polar-plotting $S = f(\theta)$ vs. cam angle θ ? No – that approach would not account for the face width of the cam follower, i.e. the contact points are not along radial lines in general. We will use *kinematic inversion* to simplify the synthesis process.

DCRFFF Figure



As seen in the figure, the radius R out to the flat-faced follower (not to the point of contact x, y) is:

$$R = C + f(\theta)$$

where C is the minimum cam radius, a design variable, and $S = f(\theta)$ is the given cam motion profile. The radius R and the flat-faced follower length L can be related to the contact point x, y and the cam angle through geometry.

$$\begin{aligned} R &= x \cos \theta + y \sin \theta \\ L &= -x \sin \theta + y \cos \theta \end{aligned}$$

Notice that

$$\begin{aligned} \frac{dR}{d\theta} &= -x \sin \theta + y \cos \theta = L \\ \therefore L &= \frac{d}{d\theta}(C + f(\theta)) = \frac{df}{d\theta} \end{aligned}$$

To calculate the follower flat-face length, double the maximum of L from above. It is doubled because by symmetry the contact point will change to the other side at $\theta = 180^\circ$.

To summarize thus far:

$$R = C + f(\theta) \quad L = \frac{df}{d\theta}$$

This is sufficient to manufacture the cam since it is machined with θ, R, L coordinates. If we want to know the cam contour in Cartesian coordinates, we must solve the relationships for x, y . In matrix form:

$$\begin{bmatrix} \cos \theta & \sin \theta \\ -\sin \theta & \cos \theta \end{bmatrix} \begin{Bmatrix} x \\ y \end{Bmatrix} = \begin{Bmatrix} R \\ L \end{Bmatrix}$$

This special coefficient matrix $[A]$ is orthonormal, which means both columns and rows are perpendicular to each other and both columns and rows are unit vectors. One unique property of orthonormal matrices is $[A]^{-1} = [A]^T$. The Cartesian cam contour solution is thus:

$$\begin{Bmatrix} x \\ y \end{Bmatrix} = \begin{bmatrix} \cos \theta & -\sin \theta \\ \sin \theta & \cos \theta \end{bmatrix} \begin{Bmatrix} R \\ L \end{Bmatrix} = \begin{Bmatrix} R \cos \theta - L \sin \theta \\ R \sin \theta + L \cos \theta \end{Bmatrix}$$

$$x = (C + f(\theta)) \cos \theta - \frac{df}{d\theta} \sin \theta$$

$$y = (C + f(\theta)) \sin \theta + \frac{df}{d\theta} \cos \theta$$

Minimum Cam radius to Avoid Cusps

A cusp is when the cam becomes pointed or undercut. Clearly, this must be avoided for good cam motion. The cusp condition is that for a finite $\Delta\theta$, there is no change in x , y .

$$\frac{dx}{d\theta} = \frac{dy}{d\theta} = 0 \quad \text{will cause a cusp.}$$

$$\frac{dx}{d\theta} = -(C + f(\theta))\sin\theta + \frac{df}{d\theta}\cos\theta - \frac{df}{d\theta}\cos\theta - \frac{d^2f}{d\theta^2}\sin\theta$$

$$\frac{dy}{d\theta} = (C + f(\theta))\cos\theta + \frac{df}{d\theta}\sin\theta - \frac{df}{d\theta}\sin\theta + \frac{d^2f}{d\theta^2}\cos\theta$$

$$\frac{dx}{d\theta} = -\left(C + f(\theta) + \frac{d^2f}{d\theta^2}\right)\sin\theta$$

$$\frac{dy}{d\theta} = \left(C + f(\theta) + \frac{d^2f}{d\theta^2}\right)\cos\theta$$

$\frac{dx}{d\theta} = \frac{dy}{d\theta} = 0$ occurs simultaneously only when

$$C + f(\theta) + \frac{d^2f}{d\theta^2} = 0$$

Therefore, to avoid cusps on the entire cam contour, we must ensure that

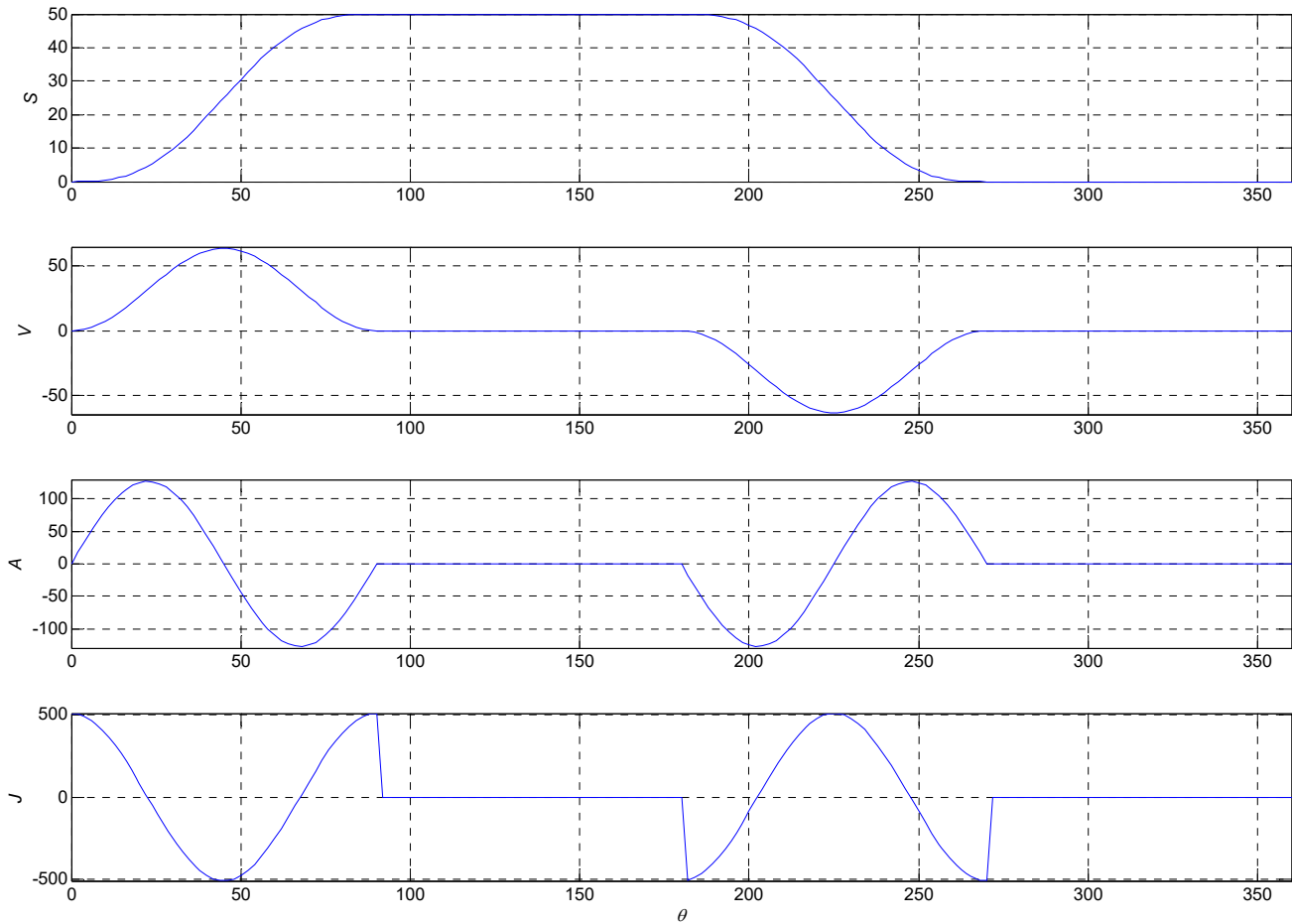
$$C + f(\theta) + \frac{d^2f}{d\theta^2} > 0$$

Note that C is always positive and $f(\theta)$ starts and ends at zero and never goes negative. So the sum of these positive terms and the sometimes-negative second derivative of the cam motion profile must always be greater than zero to avoid cusps or undercutting in the practical cam you are designing.

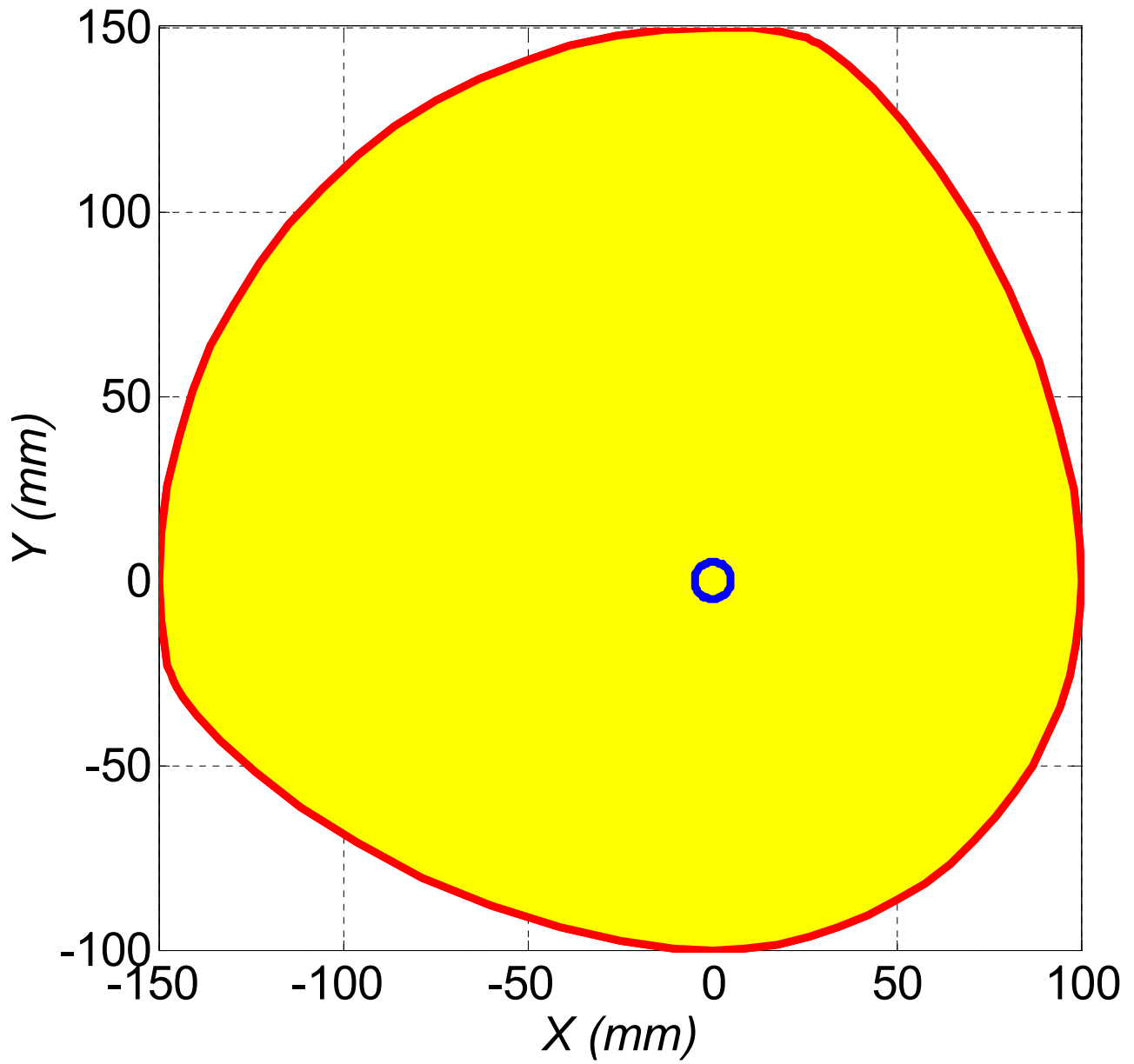
Disk Cam with Radial Flat-Faced Follower Design Example

Specify a full-cycloidal rise with a total lift of 50 mm, followed by a high dwell, a symmetric full-cycloidal return with a total fall of 50 mm, and then a low dwell. Each of these four motion steps occurs for 90° of cam shaft rotation.

The full-cycloidal rise and fall **cam motion profile** associated with this specification is shown below. Clearly, this satisfies the **Fundamental Law of Cam Design** because the position, velocity, and acceleration curves are continuous. The jerk is not continuous, but it remains finite over all cam angles.



Choosing a minimum cam radius of $C = 100 \text{ mm}$, the resulting **cam contour** is shown below.

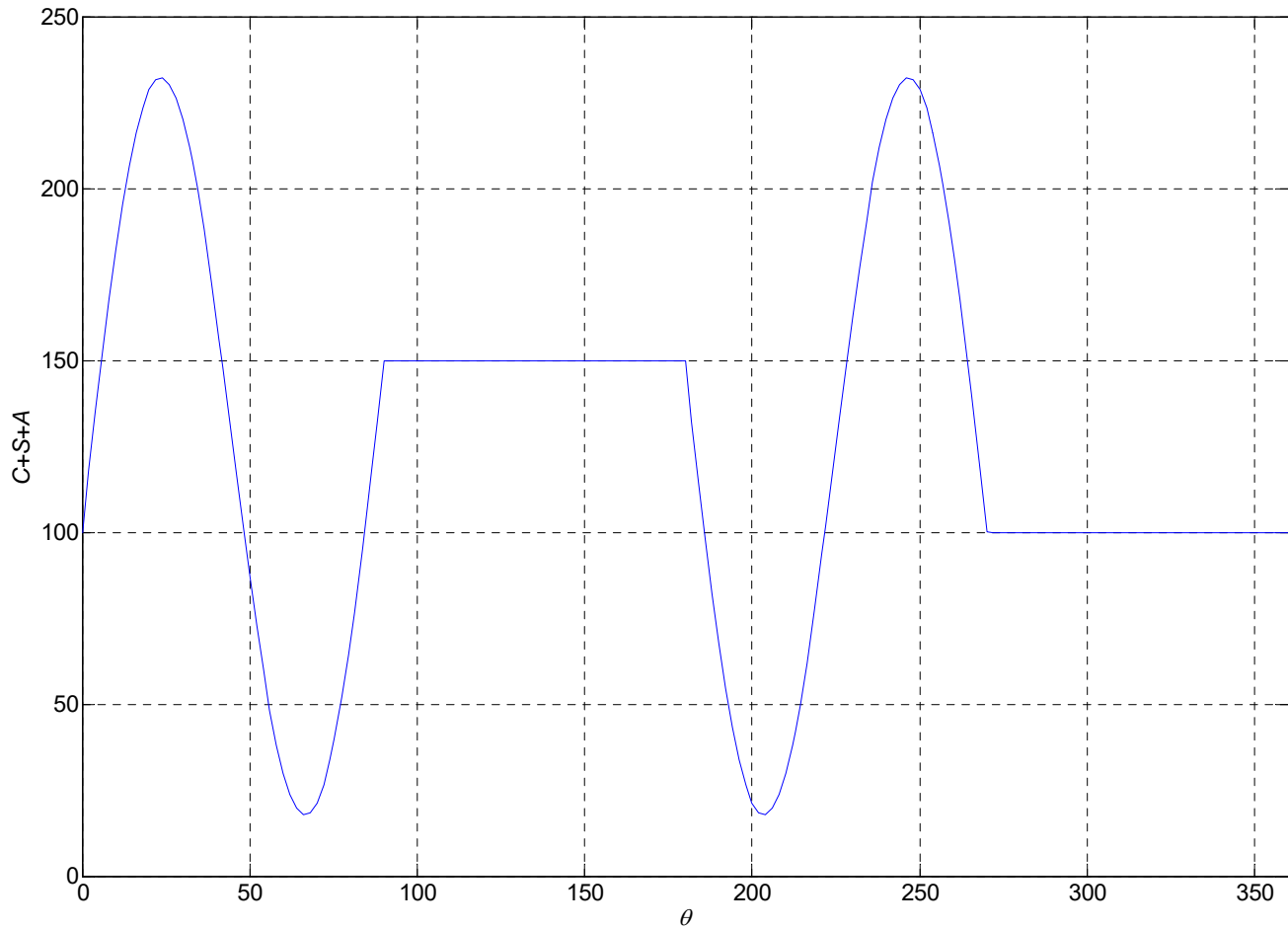


Cam Cartesian Contour

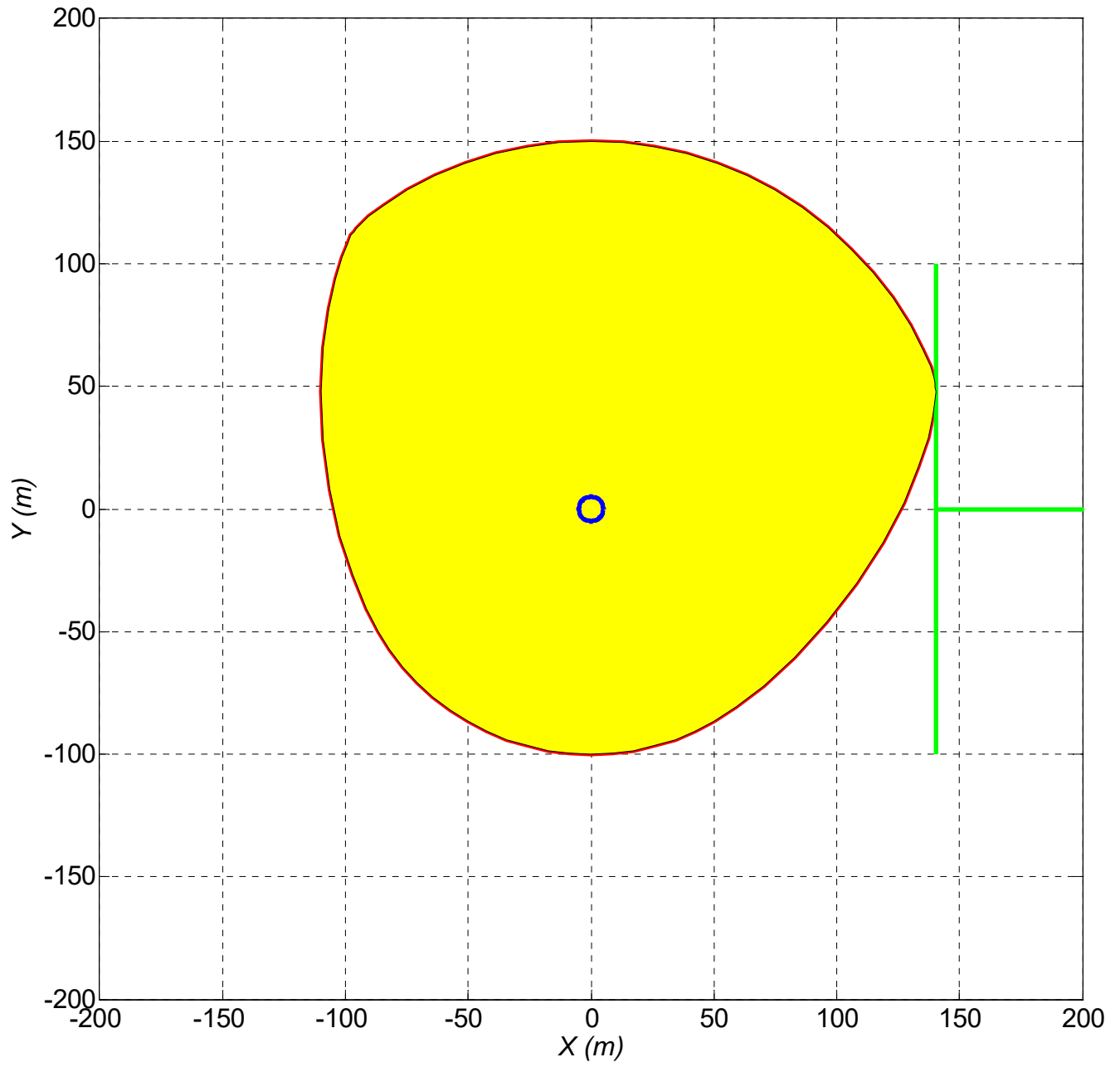
Let us check the **cuspl avoidance plot**. To avoid cusps in this cam, we require that

$$C + S(\theta) + A(\theta) = C + f(\theta) + \frac{d^2 f}{d\theta^2} > 0$$

As seen in the plot below, this inequality is satisfied for the entire range of motion, so this cam design is acceptable with respect to avoiding cusps and undercutting.



Cam Cusp Avoidance Plot



Cam/Follower Animation Snapshot for $\theta_2 = 60^\circ$ (CW)